

Report of Investigations No. 256

Groundwater Availability in the Carrizo–Wilcox Aquifer in Central Texas— Numerical Simulations of 2000 through 2050 Withdrawal Projections

by Alan R. Dutton



Bureau of Economic Geology

W. L. Fisher, Director *ad interim*

The University of Texas at Austin • Austin, Texas 78713-8924 • 1999



Report of Investigations No. 256

Groundwater Availability in the Carrizo–Wilcox Aquifer in Central Texas— Numerical Simulations of 2000 through 2050 Withdrawal Projections

by Alan R. Dutton

Sponsored by
Texas Water Development Board

Contract No. 99-483-279

Cosponsored by
San Antonio Water System
Alcoa Inc.
Aqua Water Supply Corporation

Bureau of Economic Geology

W. L. Fisher, Director *ad interim*

The University of Texas at Austin • Austin, Texas 78713-8924 • 1999



CONTENTS

Abstract	1
Introduction	1
Purpose and Objectives	1
Conceptual Hydrogeologic Model.....	4
Data Availability	4
Hydrostratigraphy	4
Flow Paths and Flow Rates	5
Recharge and Discharge	8
Model Design and Approach	9
Model Architecture	9
Aquifer Geometry	10
Aquifer Parameters	10
Boundary Conditions	14
Modeling Sequence and Calibration	19
Pumping Rates	20
Future Groundwater-Withdrawal Scenarios	20
Results	23
Baseline Historical Simulation (1951 through 1999)	23
Projected Groundwater-Withdrawal Scenarios (2000 through 2050)	27
Recommendations.....	40
Summary and Conclusions	42
Acknowledgments.....	43
References	44
Appendix A	
Observation wells used for model calibration	47
Appendix B	
Maps showing location of pumping areas used in scenarios, as well as projected 1996 through 2050 drawdown in the Simsboro for scenarios 3 and 4, the difference between scenarios 3 and 2 in simulated hydraulic head for the Simsboro in 2050, and projected 1996 through 2050 drawdown in the Carrizo for scenario 4	49

Figures

1. Study area of the Carrizo–Wilcox aquifer in Central Texas	2
2. Conceptual hydrogeologic model used for constructing the numerical model of groundwater flow	6
3. Model grid consisting of 74 columns and 42 rows	11
4. Histograms of hydraulic conductivity measured in well tests in the different formations	12

5.	Histograms of hydraulic conductivity estimated from geophysical well logs in the different formations	13
6.	Hydraulic-conductivity distribution used to represent the Simsboro Formation in cells of the model	15
7.	Hydraulic-conductivity distribution used to represent the Carrizo Formation in cells of the model	16
8.	Change in total pumping rate from the Carrizo–Wilcox aquifer in Bastrop, Burleson, Fayette, Lee, Milam, and Robertson Counties in study area between 1980 and 1996	19
9.	Location of wells to which pumping rates were specified in historical and baseline future stress periods	21
10.	Simulated potentiometric surface representing groundwater in the Simsboro Formation for the year 1996	24
11.	Southeast-northwest vertical hydrologic dip section A–A' along column 28 and southwest-northeast vertical hydrologic strike section B–B' along row 31 of the model	25
12.	Simulated historical drawdown of hydraulic head in the Simsboro Formation	26
13.	Comparison of measured and simulated hydraulic head	28
14.	Projected 1996 through 2050 drawdown in the Simsboro for scenario 1, given pumping rates of the TWDB State Water Plan	30
15.	Projected 1996 through 2050 drawdown in the Simsboro for scenario 2, superposing drawdown associated with pumping areas B and C on that for scenario 1	31
16.	Difference between scenarios 2 and 1 in simulated hydraulic head for the Simsboro Formation in the year 2050, showing incremental effects of pumping areas B and C	32
17.	Projected 1996 through 2050 drawdown in the Simsboro for scenario 5, including cumulative effects of all pumping areas superposed on the pumping rates of the TWDB State Water Plan.	33
18.	Projected 1996 through 2050 drawdown in the Carrizo for scenario 5, including cumulative effects of all pumping areas superposed on the pumping rates of the TWDB State Water Plan.	34
19.	Difference between scenarios 5 and 1 in simulated hydraulic head for the Simsboro Formation in the year 2050, showing the combined incremental effects of all pumping areas	35
20.	Difference between scenarios 5 and 1 in simulated hydraulic head for the Carrizo Formation in the year 2050, showing the combined incremental effects of simulated withdrawal of Carrizo water mainly from area D but also from area E	36
21.	Incremental drawdown of hydraulic head in the Simsboro, associated with pumping areas A and F in the year 2050	37
22.	Difference between scenarios 5 and 4 in simulated hydraulic head for the Simsboro Formation in the year 2050, showing incremental effects of pumping area E	38
23.	Difference between scenarios 5 and 3 in simulated hydraulic head for the Simsboro Formation in the year 2050, showing incremental effects of pumping area D	39

Appendix B Figures

B1.	Location of pumping areas used in scenarios modeled in this study	49
B2.	Projected 1996 through 2050 drawdown in the Simsboro for scenario 3, including cumulative effects of pumping areas A, B, C, E, and F superposed on the pumping rates of the TWDB State Water Plan	50
B3.	Difference between scenarios 3 and 2 in simulated hydraulic head for the Simsboro Formation in the year 2050, showing the combined incremental effects of pumping areas A, E, and F	51
B4.	Projected 1996 through 2050 drawdown in the Simsboro for scenario 4, including cumulative effects of pumping areas A, B, C, D, and F superposed on the pumping rates of the TWDB State Water Plan	52
B5.	Projected 1996 through 2050 drawdown in the Carrizo for scenario 4, including cumulative effects of pumping areas A, B, C, D, and F superposed on the pumping rates of the TWDB State Water Plan	53

Tables

1.	Groundwater-development scenarios modeled in this study	3
2.	Horizontal and vertical values of hydraulic conductivity assigned to property zones of Carrizo–Wilcox model by means of Visual MODFLOW	17
3.	Projected rates of groundwater withdrawal by pumping areas shown in figures 1 and B1	22
4.	Comparison of water-level differences between scenarios	27
5.	Summary of budget for groundwater in Carrizo and Simsboro Formations	29

ABSTRACT

Between 1951 and 1996, groundwater pumpage from the Carrizo–Wilcox aquifer, one of Texas' major aquifer systems, increased in the area between the Colorado and Brazos Rivers from approximately 10,600 to 37,900 acre-ft/yr, primarily as a result of mining needs. Continued (and possibly greatly accelerated) growth in groundwater demand for a variety of uses is expected through the year 2050. To assess the general availability of groundwater in the Carrizo–Wilcox aquifer between the Colorado and Brazos Rivers, five groundwater-development scenarios were simulated according to a finite-difference numerical model developed for this study. Simulated water-level change was related to the amount of groundwater withdrawal, its concentration in an area, hydrogeologic properties, and model characteristics. Actual locations and future rates of pumping of water wells, needless to say, might differ

from what were simulated. Model calibration by means of historical water-level data had a mean absolute error of 32 ft.

On the basis of the calibrated model, groundwater in the Carrizo–Wilcox aquifer in the study area is predicted to remain available to meet specified withdrawal scenarios through the year 2050 and additional demands after 2050. Except for near the centers of simulated pumping areas, the aquifer units are forecast to remain fully saturated, and simulated water-level decline reflects mainly a change in artesian or pressure head. Simulated rate of decline of hydraulic head, however, is constant through the year 2050, and continued drawdown should be expected as long as pumping remains well above historical rates. Availability of groundwater is also determined by pumping lift, drilling depth, transportation to point of use, and property access, as well as other criteria.

Keywords: aquifer, groundwater, hydrogeologic properties, numerical model

INTRODUCTION

Purpose and Objectives

The focus of this study was the Carrizo–Wilcox aquifer between the Colorado and Brazos Rivers, including parts of Bastrop, Lee, Burleson, and Milam Counties (fig. 1). The Carrizo–Wilcox aquifer, consisting of the freshwater-bearing part of the Carrizo Formation of the Claiborne Group and the underlying Wilcox Group, makes up one of Texas' major aquifer systems. Between 1951 and 1996, groundwater pumpage from the Carrizo–Wilcox aquifer in the study area increased about 250 percent, from approximately 10,600 to 37,900 acre-ft/yr, primarily as a result of mining needs. (An acre-ft of water is 43,560 ft³, or almost 326,000 gal.) Projections of additional increases in pumping by the year 2050 range from 29 to about 580 percent, reaching 48,900 to 257,700 acre-ft/yr. The projected increases in groundwater pumpage include

- ♦ water demand related to growth in population and expansion of industry within the area, according to estimates contained in the 1997 State Water Plan by the Texas Water Development Board (TWDB) (1997);
- ♦ water withdrawal from the aquifer in Bastrop, Lee, and Milam Counties for transfer under contract between Alcoa Inc. (ALCOA), San Antonio Water System (SAWS), and San Antonio's City Public Service (CPS);
- ♦ water demands in Williamson County as described in the Trans-Texas Water Program (HDR Engineering, 1998); and
- ♦ other possible demands not included in the 1997 State Water Plan.

This report assesses possible hydrologic effects of five general scenarios of groundwater withdrawal from the Carrizo–Wilcox aquifer between the Colorado and Brazos Rivers (table 1). Owing to

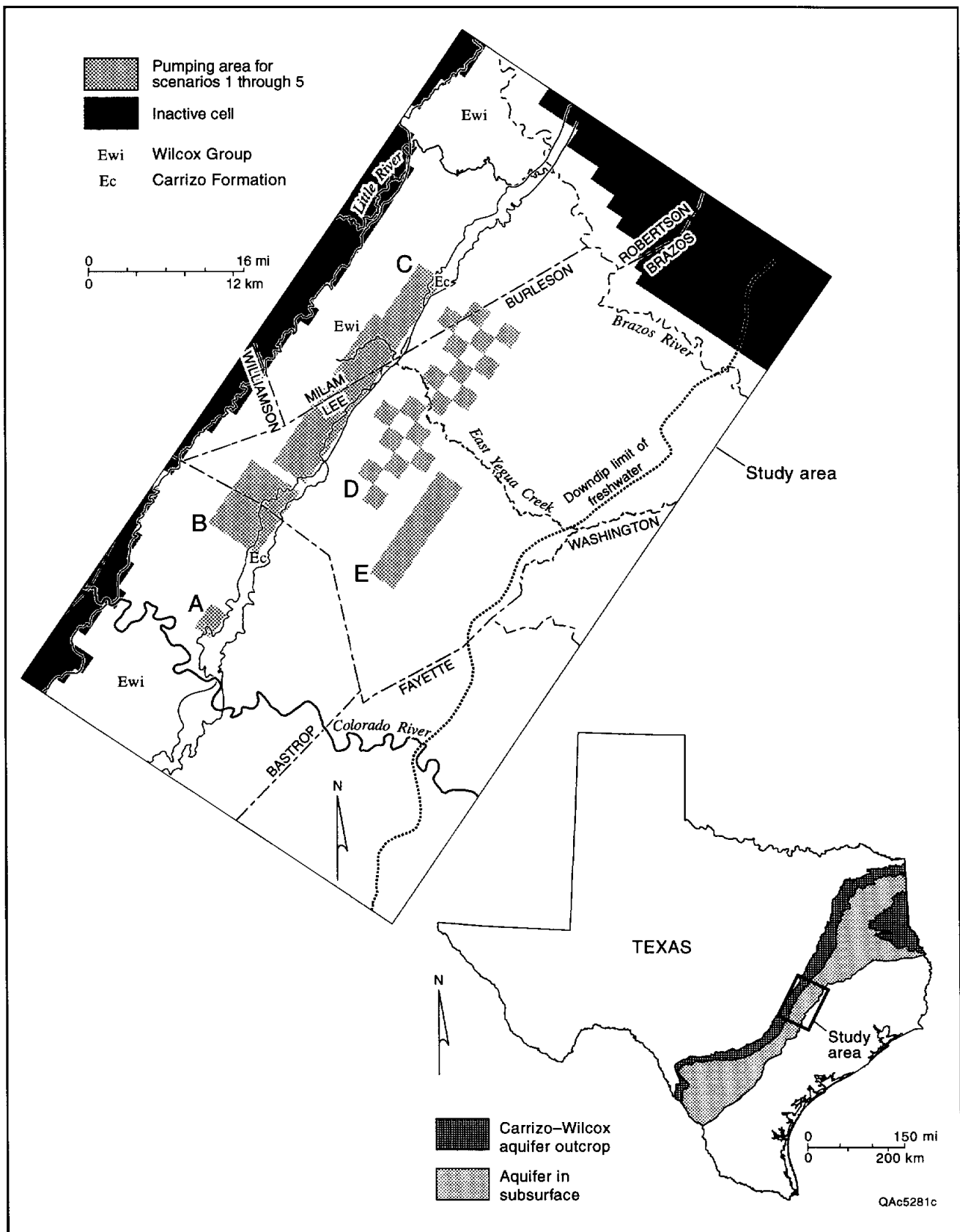


FIGURE 1. Study area of the Carrizo–Wilcox aquifer in Central Texas. The Eocene-age Wilcox Group is divided into the Hooper, Simsboro, and Calvert Bluff Formations north of the Colorado River. Extent of Carrizo–Wilcox aquifer in Texas adapted from TWDB (1997). Geologic map adapted from Proctor and others (1974). Pumping areas A through E (table 1) used in scenarios modeled in this study.

the complexity of the hydrologic system, assessing the range of hydrological effects of groundwater withdrawal requires the use of a numerical model of groundwater flow. Because no existing public-domain model covers the entire area of interest in adequate detail, however, a large part of this work consisted of building a numerical model of

the Carrizo–Wilcox aquifer before predictive simulations could be run.

Inherently models of groundwater flow are simplifications and only approximate representations of actual aquifer conditions. The goal of developing this numerical model was to make the representations of aquifer properties and

TABLE 1. Groundwater-development scenarios modeled in this study. Withdrawals projected for 2050 (except historical period). Pumping areas shown in figures 1 and B1.

Scenario	Description	Groundwater withdrawal (acre-ft/yr)				
		Total in model	Bastrop Co.	Lee Co.	Milam Co.	Burleson Co.
H	Historical period (1951–1988)	10,632	4,627	1,554	3,616	835
H	Historical period (1996)	37,896	8,847	2,043	26,165	841
H	Historical period (1999 estimate)	44,044	8,188	1,897	33,003	956
1	Projected regional groundwater production in 2050, based on TWDB (1997) State Water Plan. Includes 30,000 acre-ft/yr currently produced at ALCOA's Sandow Mine	48,873	11,959	2,178	33,429	1,307
2	Combination of scenario 1 plus 70,000 acre-ft/yr, representing full development of ALCOA and CPS contracts (areas B and C)	118,873	28,834	33,447	55,285	1,307
3	Combination of scenario 2 plus pumping areas A, E, and F	157,718	42,679	58,447	55,285	1,307
4	Combination of scenario 2 plus pumping areas A, D, and F	232,718	42,679	77,891	63,619	48,529
5	Combination of scenario 2 plus pumping areas A, D, E, and F	257,718	42,679	102,891	63,619	48,529
Pumping area						
A	Additional groundwater for LCRA related to steam–electric-power generation	7,000	7,000	0	0	0
B	Groundwater production associated with proposed mine and adjacent area	30,000	16,875	13,125	0	0
C	Groundwater production associated with Sandow Mine and adjacent area*	40,000	0	18,144	21,856	0
D	Additional groundwater withdrawal from Carrizo and Simsboro aquifers (50,000 acre-ft/yr each) to meet potential future water needs	100,000	0	44,444	8,334	47,222
E	Potential transfer of groundwater from Lee to Williamson Counties to meet increasing demand reflected in Trans-Texas Water Program (HDR Engineering, 1998)	25,000	0	25,000	0	0
F**	Incremental increase to meet Bastrop County groundwater demand not included in TWDB (1997) Water Plan	6,845	6,845	0	0	0

* Incremental increase beyond 1999 estimate

**Not shown in figure 1; applied across Bastrop Co.

withdrawal scenarios sufficiently accurate to assess the effects of the five groundwater-withdrawal scenarios on water level in wells. The model was designed as a regional model. It was not the intent of this study to target particular locations for placing water wells. Actual future location and rates of pumping of water wells undoubtedly need to be determined from detailed site considerations, although they are beyond the scope of this study.

Objectives of this study were to

- ◆ collect, compile, and synthesize hydrogeologic data and update understanding and information pertaining to the Carrizo–

Wilcox aquifer between the Colorado and Brazos Rivers;

- ◆ construct and calibrate a numerical model of groundwater flow on the basis of currently available hydrogeologic data;
- ◆ quantify groundwater supplies and describe possible future conditions of the Carrizo–Wilcox aquifer in the study area, given five specified withdrawal scenarios; and
- ◆ visualize the spatial extent of simulated drawdown in water levels in the aquifer system according to the prescribed withdrawal scenarios.

CONCEPTUAL HYDROGEOLOGIC MODEL

A conceptual model was developed on the basis of previous work to account for the occurrence and movement of water in the Carrizo–Wilcox aquifer in the study area. This conceptual model was used for constructing the numerical model to quantitatively estimate groundwater availability.

Data Availability

This study built on previous hydrogeologic investigations of the Carrizo–Wilcox aquifer. Whereas the aquifer is made up of heterogeneous packages of sand, clay, lignite, and other sediments, its geology has been characterized on a regional scale, and groundwater conditions in counties included in the study area have been documented (Cronin and Wilson, 1967; Rogers, 1967; Follett, 1970, 1974; Henry and Basciano, 1979; Henry and others, 1979; Ayers and Lewis, 1985; Dutton, 1985, 1990; Thorkildsen and others, 1989; Thorkildsen and Price, 1991). There are adequate geologic and hydrologic data with which to build a model capable of meeting the objectives of this study. The TWDB maintains an Internet data base on the Carrizo–Wilcox aquifer and other aquifers in Texas

(<ftp://rio.twdb.state.tx.us/gwdata/>). This study also used preliminary results from a data base sponsored by the TWDB on the permeability of the Carrizo–Wilcox aquifer.

The work additionally built on the insights gained from previous use of regional computer models of the Carrizo–Wilcox aquifer. These models include simulations of steady-state and transient flow of groundwater as part of an assessment of water resources on the Texas coastal plain (Ryder, 1988; Ryder and Ardis, 1991), simulations of groundwater flow in Bastrop County (Thorkildsen and others, 1989), and analyses of groundwater conditions in the Carrizo–Wilcox aquifer between the Colorado and Trinity Rivers (Thorkildsen and Price, 1991, unpublished simulations).

Hydrostratigraphy

The conceptual model of the hydrostratigraphy of the Carrizo–Wilcox aquifer in the study area includes the following hypotheses and assumptions:

- ◆ The Carrizo–Wilcox aquifer in the study area is made up of the Carrizo, Calvert Bluff, Simsboro, and Hooper Formations (fig. 2a, b).

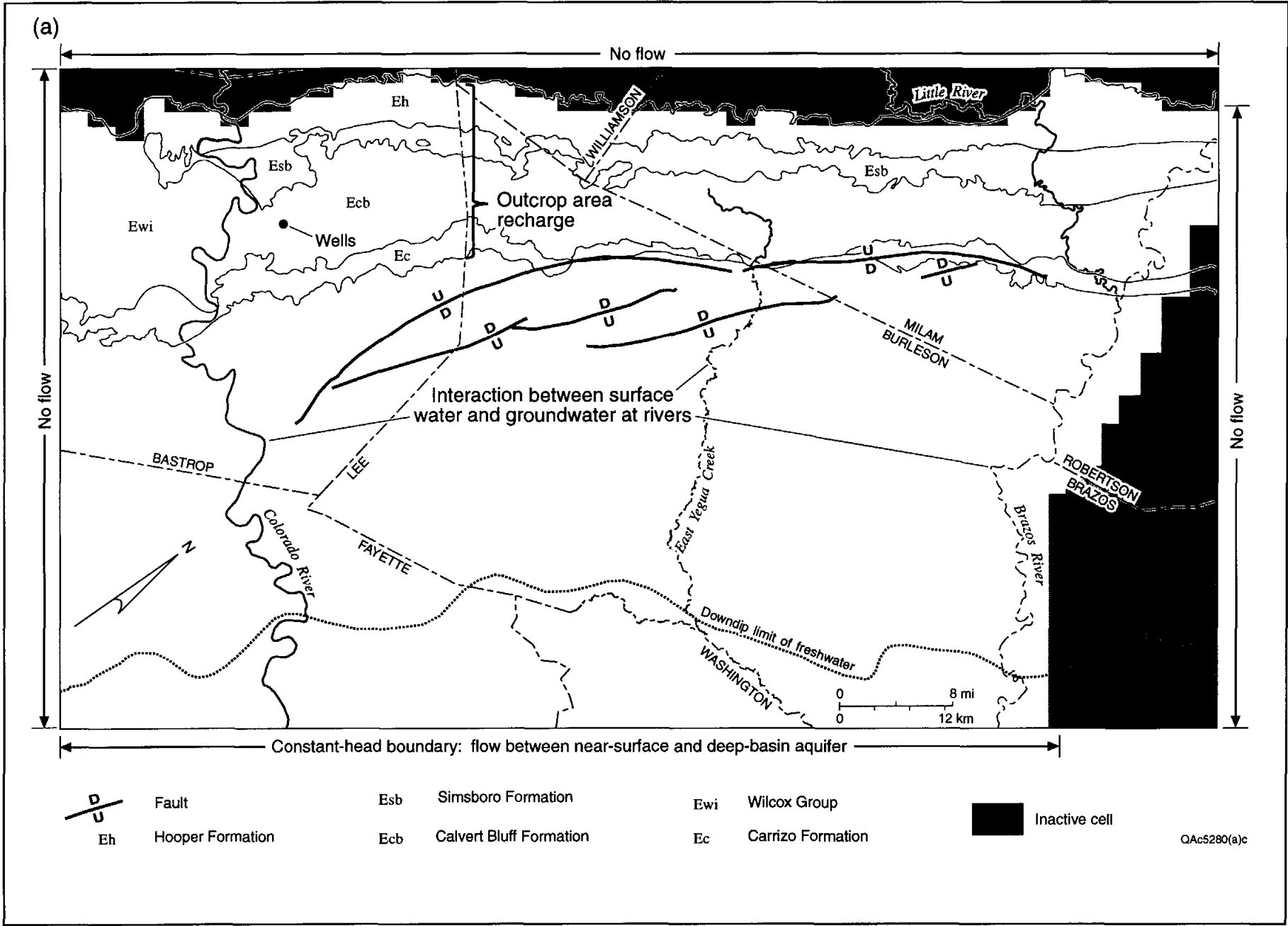
The formations dip approximately 2° southeast into the subsurface (Henry and others, 1979).

- ◆ The Carrizo and Simsboro are the main aquifer units. More than 80 percent of the Carrizo and Simsboro Formations in the study area consist of porous and permeable sandstone (Ayers and Lewis, 1985). The Simsboro in Lee and Milam Counties is composed of a multistory, multilateral sand deposit containing thick, extensive sandstone (Henry and others, 1979). To the south, the multilateral sands are less abundant. The Simsboro in Bastrop County is composed of multistory, dispersed channel-sand deposits. South of the Colorado River, Simsboro-equivalent deposits change to strike-oriented, nearshore, marine-dominated facies, which do not make up a major sand system and are not differentiated from the rest of the Wilcox Group (Proctor and others, 1974; Henry and others, 1979).
- ◆ The volume of water stored in the aquifers is large. Total volume of freshwater in the Simsboro of the study area, for example, is roughly 170 million acre-ft, given an aquifer area of more than 3,100 mi², an aquifer thickness of 50 to 920 ft, and an assumed 20-percent porosity.
- ◆ The Calvert Bluff and Hooper Formations consist mainly of low-permeability claystone and lignite deposits (Ayers and Lewis, 1985) and function like confining layers that retard the vertical movement of water within the Carrizo–Wilcox aquifer across the study area. Sandstone makes up less than 50 percent, and commonly less than 20 percent, of the Calvert Bluff and Hooper Formations. Where present in sufficient thickness, however, sandstones can yield appreciable quantities of water within these formations. The communities of Bastrop, Elgin, and Milano have had public water-supply wells in the Calvert Bluff or Hooper Formations.
- ◆ The aquifers are unconfined in the outcrop and confined in the subsurface by the Hooper, Calvert Bluff, and younger, low-permeability formations. A narrow transition area lies downdip of the outcrop where degree of aquifer confinement rapidly increases.
- ◆ The sediments that make up the Carrizo–Wilcox aquifer were deposited in fluvial and deltaic environments. The hydrogeologic properties of such sediments are typically heterogeneous on local and regional scales. Generally, water resources may be considered greater in areas where thick sandstones have high hydraulic conductivity. Other factors besides hydrogeologic properties, however, also determine where to site well fields.
- ◆ On a regional scale, both aquifers and confining layers have different hydraulic conductivity vertically and laterally. This directional difference, referred to as vertical anisotropy, is attributed to the presence of sedimentary structures, bedding, and interbedded low-permeability layers. Vertical anisotropy is poorly quantified and is generally estimated during model calibration (Anderson and Woessner, 1992).
- ◆ Faults bounding a graben structure (fig. 2a, b) in Bastrop, Lee, Burleson, and Milam Counties affect movement of water from the outcrop into the deeper subsurface. Formations within the graben are dropped down to a lower elevation relative to their position on the other side of the bounding faults. Faults may also affect the spread of drawdown resulting from groundwater withdrawal located on either side of the faults.

Flow Paths and Flow Rates

The conceptual model of flow in the Carrizo–Wilcox aquifer includes the following:

- ◆ Groundwater flows primarily from outcrop recharge areas, especially where sandy soils developed on the Carrizo and Simsboro Formations (Henry and Basciano, 1979), to discharge areas in river bottomlands, at wells, and to deeper regional flow paths.
- ◆ Some flow paths that are relatively short remain in the unconfined part of the aquifer, following the outcrop from upland areas toward discharge zones within the river



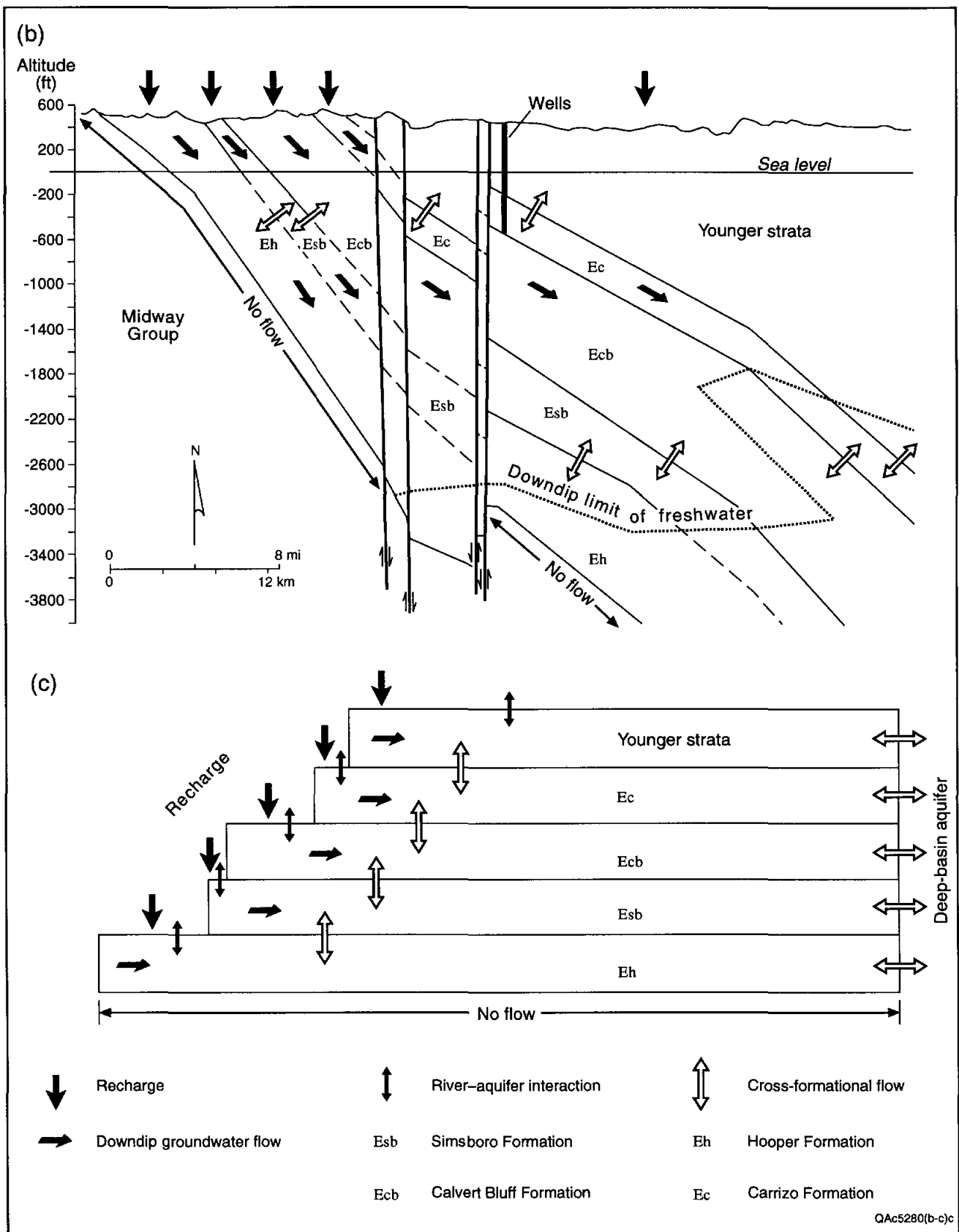


FIGURE 2. Conceptual hydrogeologic model used for constructing the numerical model of groundwater flow. (a) Boundary conditions include no-flow, constant-head, and river boundaries. (b) Generalized hydrogeologic cross section showing conceptual model of movement of groundwater (adapted from Thorkildsen and Price, 1991). (c) Representation of how the conceptual hydrogeologic model is translated into a computer model.

bottomlands. Other flow paths pass deeper into the confined part of the aquifer (fig. 2b, c).

- ◆ The proportion of recharge that reaches the confined aquifer changes with increased pumping.
- ◆ Eventually most groundwater that reaches the confined part of the aquifer follows arcuate paths curving toward the areas beneath river bottomlands, passing upward into overlying formations or into the alluvium underlying river valleys.
- ◆ Cross-formational flow of groundwater within the Carrizo–Wilcox aquifer is probably directed mostly downward beneath the upland areas that cross surface-water divides and mostly upward beneath low-lying river bottomlands, although this pattern may change with groundwater withdrawal from wells.
- ◆ Some amount of water passes into the deeper part of the basin beyond the zone of freshwater.
- ◆ On the basis of the interpreted ^{14}C ages of groundwater in Bastrop County (Kreitler and Senger, 1991), flow rates in the Simsboro are estimated to be roughly 0.0002 to 0.0008 mi/yr (0.00033 to 0.0013 km/yr).
- ◆ Flow rates within highly permeable sandstone can be large.
- ◆ Whereas cross-formational flow might not be detectable at a local scale (given the low vertical hydraulic conductivity of the Hooper and Calvert Bluff Formations), on a regional scale, vertical flow may account for an appreciable part of the water budget of an aquifer. Site-specific and regional data on vertical hydraulic conductivity are absent, and hydrogeology of rocks of low hydraulic conductivity is a long-standing technical issue (International Association of Hydrogeologists, 1985).

and an even smaller amount reaches the water table as recharge. This regional model did not take runoff, evapotranspiration, or interflow into account; their net effect is assumed to be reflected in the simulated recharge rate.

- ◆ Estimates of recharge from infiltrating rainwater across upland areas of the formation outcrops range from an average rate of 1 inch/yr (Thorkildsen and Price, 1991) to as much as 2 to 4 inches/yr (Ryder, 1988; Ryder and Ardis, 1991). Recharge rates are undoubtedly higher for the Carrizo and Simsboro than for the Calvert Bluff and Hooper Formations.
- ◆ River bottomlands can be groundwater-discharge areas. Groundwater discharge may provide varying amounts of base flow to the Colorado and Brazos Rivers.
- ◆ Flow in smaller streams such as Yegua Creek can be highly variable, with seasonal changes in the inflow and outflow relationships between surface water and groundwater. Surface-water flow in Yegua Creek has been augmented by runoff of groundwater pumped from the Simsboro aquifer as part of operations at the Sandow Mine in Milam County.
- ◆ Hydrographs of water levels in wells in the study area show no long-term trends for the period of record before 1988, although annual or short-term cycles can be seen. The lack of a trend suggests that recharge and discharge for the whole aquifer system were near equilibrium (pseudo-steady state) during much of the period from 1951 through 1988. The lack of a long-term trend also suggests that groundwater withdrawal was a small percentage of the water budget of the aquifer during this period.

Recharge and Discharge

The conceptual model of recharge and discharge includes the following assumptions:

- ◆ Of all the precipitation that strikes the ground surface, only a fraction infiltrates into the soil,

MODEL DESIGN AND APPROACH

Models represent approximations and simplifications of a natural system. Assumptions and compromises owing to the conceptual model, objectives, input data, software capabilities, and schedule and budget for developing a model influence the results, accuracy, and applicability of a model. Five general categories of information and decision making needed for model construction are (1) model architecture, (2) aquifer geometry, (3) aquifer parameters, (4) boundary conditions, and (5) aquifer stresses, such as pumping. Different combinations of input data can result in different model predictions. Model design and calibration are attempts at constraining possible results.

Model Architecture

Model architecture refers to the code, size of blocks, and number of layers used in the model. The choice of code is necessary to ensure that important processes in the aquifer are modeled accurately.

The governing equation for regional flow of groundwater derives from a water-balance equation:

$$\text{inflow} - \text{outflow} = -\text{div } q - R^* = S_s \partial h / \partial t, \quad (1)$$

where $\text{div } q$ represents the divergence or difference between the rates of specific discharge of water (q , volumetric flow of fluid per unit time per unit volume) flowing into and out of a unit volume of an aquifer, R^* represents the volumetric flux of various sources and sinks of water such as recharge (source) and extraction wells (sinks) per unit volume of an aquifer, S_s is specific storage, and $\partial h / \partial t$ expresses the rate of change of hydraulic head. Any imbalance in the left-hand side of equation 1 results in a change of hydraulic head, h . Specific storage is a proportionality factor between the divergence or difference in water inflow and outflow rates and the rate of change of hydraulic head. It measures the volume of water released as a result of expansion of water and compression of the porous media per unit volume

and unit decline in hydraulic head. Specific storage \times aquifer thickness = the storativity of the aquifer, which is equal to the volume of water released from a vertical column of the aquifer per unit surface area of the aquifer and unit decline in hydraulic head.

Flow rates (q) are generally unknown or not directly measured. Equation 1 is typically solved by factoring in the expression of Darcy's law describing the flow of groundwater:

$$q = -K \text{ grad } h, \quad (2)$$

where K is hydraulic conductivity, which expresses the ease with which water moves through a porous medium, and $\text{grad } h$ is the gradient of hydraulic head (h) in horizontal and vertical directions. Hydraulic conductivity \times aquifer thickness = the transmissivity of the aquifer, which is the rate of flow of groundwater under a unit hydraulic gradient and through a unit width of a column of an aquifer.

Combining equations 1 and 2 yields the general form of the governing equation for groundwater flow:

$$-\text{div}(-K \text{ grad } h) - R^* = S_s \partial h / \partial t, \text{ and} \quad (3a)$$

$$\frac{\partial}{\partial x} \left(K_x \frac{\partial h}{\partial x} \right) + \frac{\partial}{\partial y} \left(K_y \frac{\partial h}{\partial y} \right) + \frac{\partial}{\partial z} \left(K_z \frac{\partial h}{\partial z} \right) - R^* = S_s \frac{\partial h}{\partial t}, \quad (3b)$$

where x , y , and z are Cartesian coordinates of the system and K_x , K_y , and K_z are the directional components of hydraulic conductivity.

Solving equation 3 for the distribution of head in time and space also requires specified values of initial and lateral boundary conditions. A numerical model represents an approximate solution to the flow equation, given a particular set of boundary conditions. Constructing a numerical model involves specifying all of the parameters in equation 3b and in the initial and boundary conditions. This study used MODFLOW (McDonald and Harbaugh, 1988) to solve the flow equation according to the

finite-difference method (Anderson and Woessner, 1992). MODFLOW is a widely tested and used groundwater-modeling software package. Visual MODFLOW (version 2.72, Guiguer and Franz, 1998) was used as the modeling interface to help load and package data into the formats needed for running simulations in MODFLOW and for looking at simulation results.

The model grid for the finite-difference model consists of 74 columns, 42 rows, and 5 layers (figs. 2c, 3). The four units of the Carrizo–Wilcox aquifer were distinguished from younger, overlying formations; the latter were included in layer 1 (fig. 2b, c). Rows were aligned parallel to the strike of the Wilcox outcrop. Most cells or blocks of the model cover 1 mi², although block area increased to as much as 4 mi² at the edges of the model away from the main area of interest between the Colorado and Brazos Rivers (fig. 3). Block size impacts modeling because of the smoothing or averaging of input parameters that must be made and the detail at which the model is useful. The models by Ryder (Ryder, 1988; Ryder and Ardis, 1991) have model blocks that represent an area of 25 mi². The models of the Carrizo–Wilcox aquifer by Thorkildsen and others (1989) and Thorkildsen and Price (1991; unpublished simulations) have model blocks that represent areas of 4 and 16 mi², respectively.

Model calibration was evaluated by comparing simulated hydraulic heads with hydrographs for 45 water wells (fig. 3). Wells in the Carrizo–Wilcox aquifer having the longest period of record in the study area were chosen from the data base on the TWDB Internet site for use in calibration.

Aquifer Geometry

Geometry of the aquifer system consists of the physical dimensions of the aquifer and confining layers: the six surfaces describing the elevations of the tops and bottoms and the position of the sides of the model layers. Of all the input data, aquifer-system geometry is probably the best characterized. Structure of the top and bottom of the aquifer is defined by numerous wells, topography of the land surface is mapped, water levels are repeatedly measured to define the top of the aquifer in the

outcrop zone, and geologic maps show the lateral extent of formation outcrops. Although formation thickness was not defined exactly at every point in the aquifer, the uncertainty is acceptable and generally does not greatly impact results of a model.

The bottom of the Hooper Formation was taken from a contoured structure map by Ayers and Lewis (1985). As part of their study, Ayers and Lewis (1985) also marked on geophysical logs the position of the interpreted bases of the Simsboro, Calvert Bluff, and Carrizo Formations and the top of the Newby Member of the Reklaw Formation. This information for more than 600 wells was entered into a data base, posted on maps, and contoured by hand. The contoured structure surfaces were scanned, digitized, and gridded for input into the model. A digital elevation model of ground surface was downloaded from the U.S. Geological Survey Internet site, and ground-surface elevations were interpolated to model cell centers by geographic information system (GIS) software.

Aquifer Parameters

Horizontal hydraulic conductivity must be assigned in models used for steady-state and transient simulations; specific storage is also needed for transient simulations. Robust estimates of horizontal hydraulic conductivity (K_x , K_y) are important for calibrating other, less well known parameters such as recharge and vertical hydraulic conductivity (K_z). Parameter values for large areas of the model are estimated or extrapolated from measured values.

Three data sets on hydraulic properties were used. One data set included interpreted results of field tests conducted near the Sandow Mine in Milam County according to standard hydrological techniques. Most of the tests in the Simsboro Formation were in wells that penetrate only about the upper half to two-thirds of the formation. This is the zone from which most of the groundwater has been withdrawn for pressure reduction (Bob Harden, R. W. Harden and Associates, Inc., personal communication, February 1999). It was assumed that these test results were representative of the whole Simsboro section. This assumption appears to be justified, judging from the blocky appearance

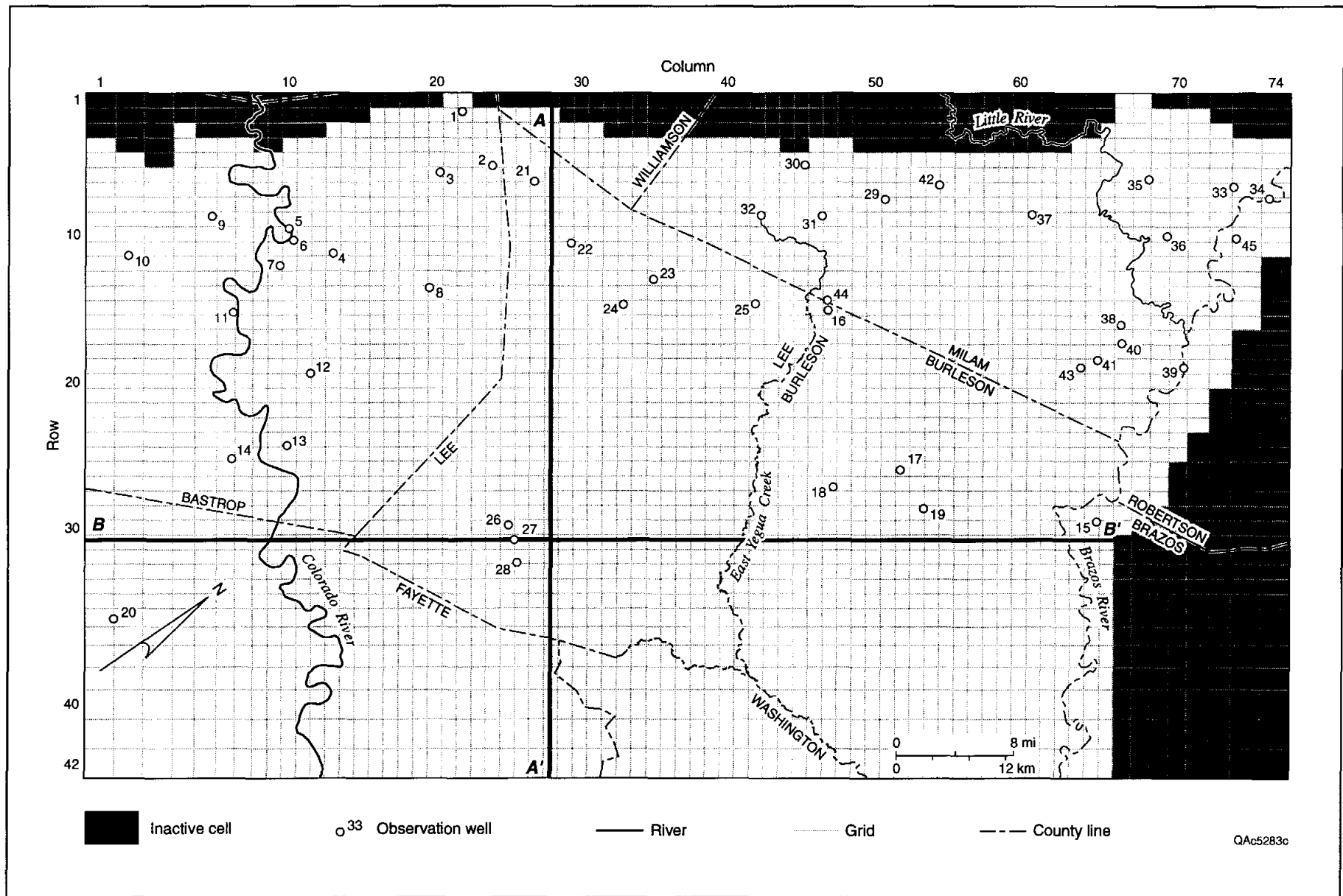


FIGURE 3. Model grid consisting of 74 columns and 42 rows. Observation wells completed in various layers. To relate map numbers to observation well numbers, see appendix A. The same grid applies to all five layers. The no-flow area lies updip of the formation outcrop in each layer. Cross sections A–A' and B–B' shown in figure 11.

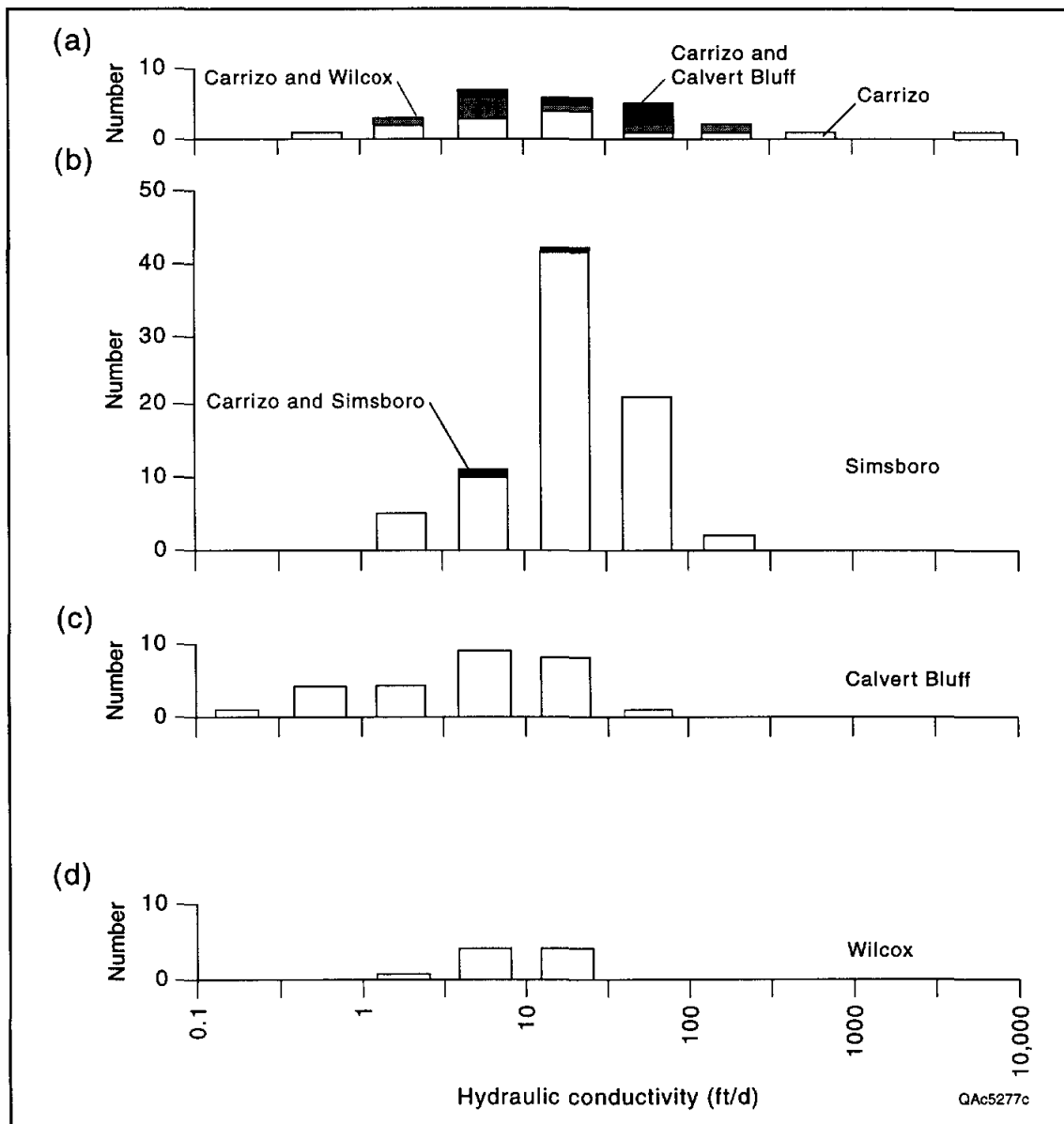


FIGURE 4. Histograms of hydraulic conductivity measured in well tests in the different formations. Combination of data sets from tests near Sandow Mine in Milam County and tests reported in literature.

of resistivity logs through the Simsboro, which show a general absence of upward-fining trends.

A second set of field-test results was compiled from literature and the TWDB Internet site. Literature sources include Guyton (1942), Follett (1970), Gaylord and others (1985), Thorkildsen and Price (1991), Fisher and others (1996), and Kier and Larkin (1998). The two data sets that had made use of field tests were combined. The statistical distribution of hydraulic conductivity appears to follow a log-normal distribution (fig. 4). Mean hydraulic conductivity of sandstones appears slightly lower for the Calvert Bluff than for the

Carrizo and Simsboro Formations. Hydraulic conductivity in the Carrizo aquifer in this data set appears to have the greatest variance, contrary to what was noted by Thorkildsen and others (1989). The literature values, which range from 2.6 to 59 ft/d, fall within the range of the other field-test data.

The third data set (fig. 5), provided by Mr. David Thorkildsen, was used in his previous model of the Carrizo–Wilcox aquifer. These data were based on interpretation of resistivity well logs. Mean hydraulic conductivity of sandstones does not differ significantly in a comparison between aquifer-test and well log data, and the mean values of the Carrizo

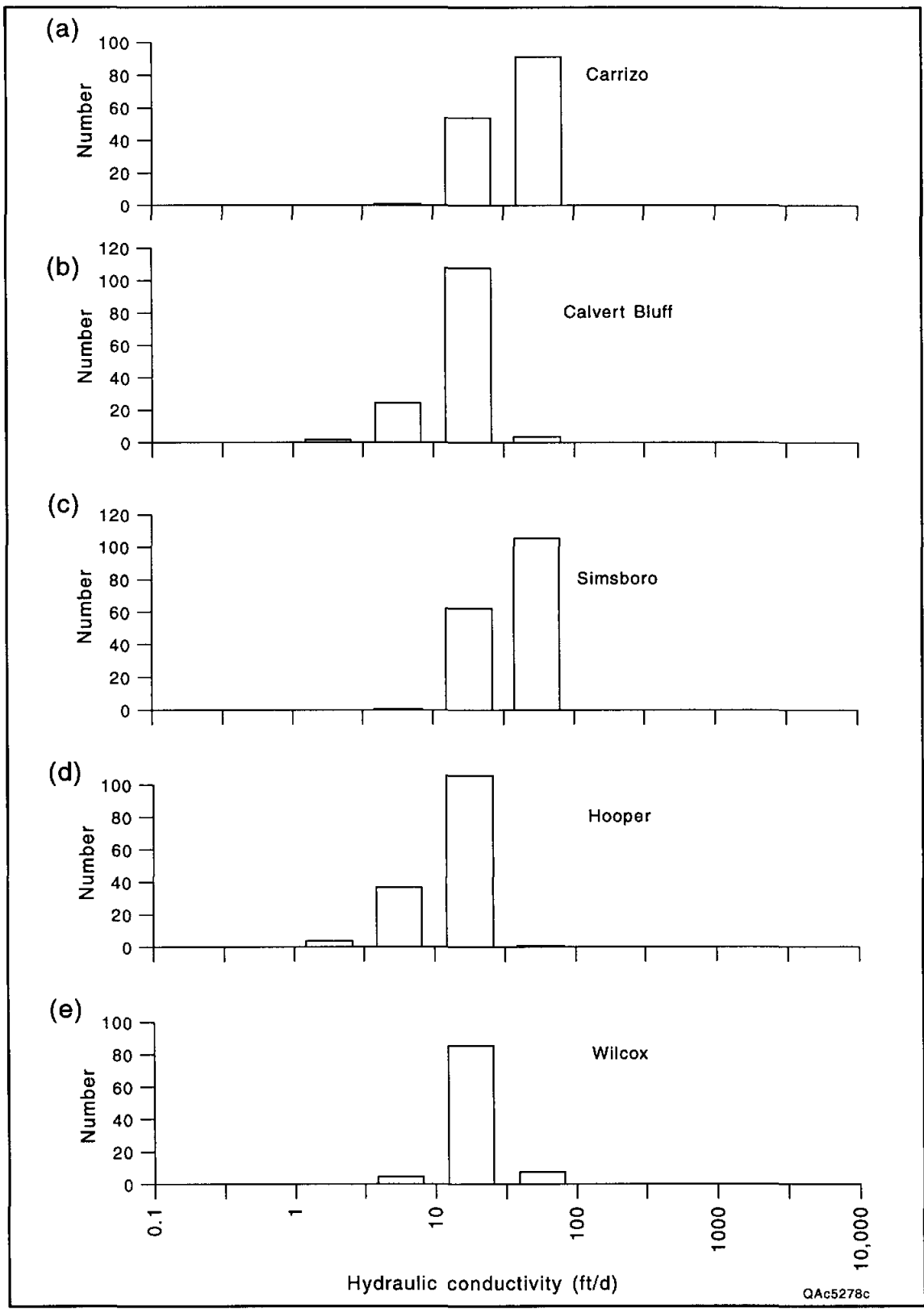


FIGURE 5. Histograms of hydraulic conductivity estimated from geophysical well logs in the different formations.

and Simsboro are slightly higher than those of the Calvert Bluff and Hooper. Accordingly, all data on hydraulic conductivity were pooled together.

Horizontal hydraulic conductivity was assumed to be locally isotropic, that is, the same in x and y directions ($K_x = K_y$). Vertical anisotropy (K_z/K_x)

within each aquifer was assumed to be 0.01; that is, hydraulic conductivity was assumed to be 100 times less in the vertical than in the horizontal direction (Anderson and Woessner, 1992, p. 70). It was also assumed that the Carrizo–Wilcox aquifer is made up of consolidated materials and that no compaction occurs with change in storage.

Test data for the Calvert Bluff and Hooper Formations, reflecting the horizontal hydraulic conductivity of sandstones, do not take into account the abundance of claystone that makes up these confining layers. Horizontal hydraulic conductivity of the entire thickness of the Calvert Bluff and Hooper Formations was averaged by using the pooled test data for sandstones and an assumed horizontal hydraulic conductivity of claystone of $10^{-3.5}$ ft/d. Sandstone was assumed to make up 20 percent of the Calvert Bluff and 10 percent of the Hooper. The vertical hydraulic conductivity of these confining layers was calculated as a harmonic mean, which gives most weight to the thick, low-permeability claystones. The vertical hydraulic conductivity of claystone was assumed to be $10^{-5.5}$ ft/d. Formation thickness was taken from the structural data.

To represent the natural heterogeneity of the formations, hydraulic conductivity was mapped for each layer and contoured on the basis of the trends in major-sand thickness in the formations (Ayers and Lewis, 1985). The posted values of measured or estimated hydraulic conductivity were overlain on the maps of major sand thickness, and contours of equal hydraulic conductivity were drawn following a subjective correlation between hydraulic conductivity and sand thickness. The contours were digitized and loaded into Visual MODFLOW as digital exchange files (DXF). These DXF overlays were then traced in order to assign hydraulic conductivity to cells of the model. Figures 6 and 7 show the inferred maps of horizontal hydraulic conductivity for the Simsboro and Carrizo aquifers. Table 2 lists hydrologic properties assigned in the model to various zones.

Ayers and Lewis (1985) mapped an ancient fault-bounded graben that strikes northeast and extends across the study area. The northwest-bounding fault intersects the outcrop of the Carrizo Formation (fig. 2a), and the amount of offset

across the fault reaches as high as 1,100 ft. To represent the hydrological effects of the graben in the model, we used Hydrologic Barrier (Hsieh and Freckleton, 1993)—a MODFLOW module included in Visual MODFLOW—to represent the decrease in lateral connectivity due to the presence of low-permeability formations downdropped into juxtaposition with the Carrizo and Simsboro Formations along the trend of the northeast-bounding fault. The hydrologic barrier was also placed in the Calvert Bluff and Hooper Formations along the southeast-bounding fault to represent a transition back into these low-permeability formations downdip from the graben. The hydrologic barrier was simulated by a thickness of 3.28 ft and a hydraulic conductivity that decreased from 0.003 to 0.00003 ft/d with increased fault throw. The resulting reduction in hydraulic conductivity across the fault was as much as 10^{-6} .

In the outcrop of the aquifer units, specific storage was set to range from 0.003 to 0.001 ft^{-1} . When multiplied by saturated thickness, these values give a storativity for the Simsboro aquifer outcrop that averages 0.29. Specific storage was assigned to vary in the subsurface as a function of degree of confinement. A steep transition zone between the unconfined and confined values of specific storage was set just downdip of the outcrop. Specific storage in the subsurface was as low as $10^{-7.2}$ ft^{-1} . Storativity assigned in the model averaged $10^{-4.0}$ for the Simsboro and $10^{-3.6}$ for the Carrizo. For comparison, the average of 19 measured values of storativity in the Carrizo–Wilcox aquifer is $10^{-3.6}$.

Boundary Conditions

Numerical models solve the general equation of groundwater flow with specified initial and spatial boundary conditions. Initial conditions are discussed in the section on modeling sequence and calibration (p. 19). Spatial boundary conditions include the six sides or edges of a modeled aquifer, although internal boundaries such as rivers can also be applied. Lateral boundaries can be placed at three locations: (1) physical boundaries, such as the updip edge of the formation; (2) hydraulic

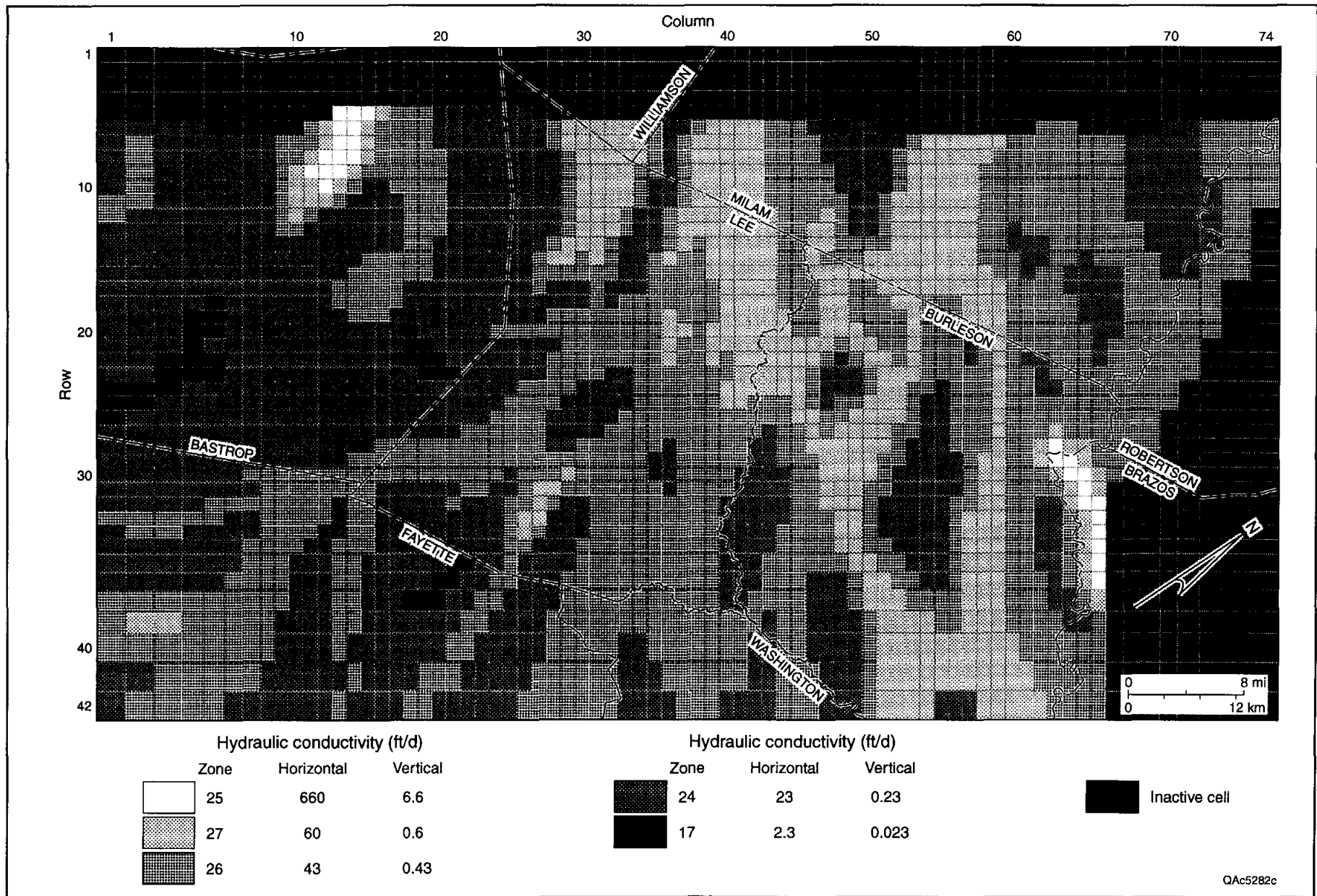


FIGURE 6. Hydraulic-conductivity distribution used to represent the Simsboro Formation in cells of the model.

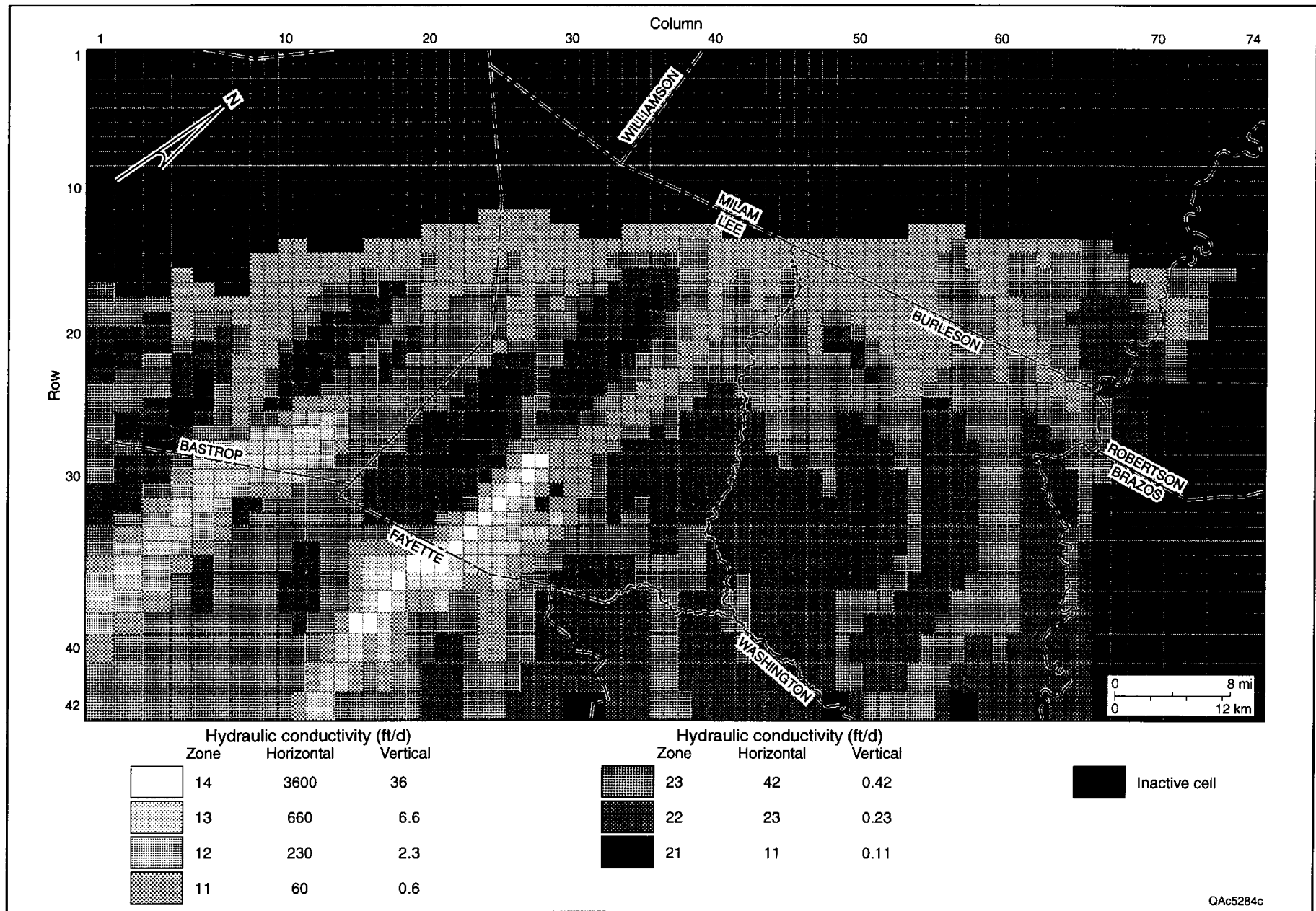


FIGURE 7. Hydraulic-conductivity distribution used to represent the Carrizo Formation in cells of the model.

TABLE 2. Horizontal (K_x) and vertical (K_z) values of hydraulic conductivity (ft/d) assigned to property zones of Carrizo–Wilcox model by means of Visual MODFLOW. Assigned K_x and K_z weighted for presence of low-permeability claystone in Calvert Bluff and Hooper Formations.

Property zone	Formation	Average test data K_x	Assigned K_x	Assigned K_z
21	Carrizo	11	11	1.1 E-01
22	Carrizo	23	23	2.3 E-01
23	Carrizo	42	42	4.3 E-01
11	Carrizo	60	60	6.0 E-01
12	Carrizo	230	230	2.3 E+00
13	Carrizo	660	660	6.6 E+00
14	Carrizo	3,600	3,600	3.6 E+01
7	Calvert Bluff	7	0.07	7.5 E-06
8	Calvert Bluff	11	0.11	1.1 E-05
9	Calvert Bluff	23	0.23	2.3 E-05
16	Calvert Bluff	26	0.26	2.6 E-05
10	Calvert Bluff	43	0.43	4.3 E-05
17	Simsboro	2.3	2.3	2.3 E-02
26	Simsboro	23	23	2.3 E-01
24	Simsboro	43	43	4.3 E-01
27	Simsboro	60	60	6.0 E-01
25	Simsboro	660	660	6.6 E+00
18	Hooper	7	0.07	6.6 E-05
19	Hooper	11	0.11	1.1 E-04
20	Hooper	20	0.20	2.0 E-04

boundaries, such as groundwater divides and streamlines; and (3) artificial boundaries, which are placed away from the area of interest. Physical boundaries can be represented by a number of different boundary conditions, depending on the nature of the boundary. Hydraulic boundaries are represented by no-flow boundaries, and artificial boundaries are generally represented by constant-head or constant-flux boundaries.

Of the three types, physical and hydraulic boundaries are preferable because they more accurately represent actual boundaries in the natural system. Artificial boundaries are generally used to limit the upstream or downstream extent of a model to the area of interest and are most appropriate for steady-state models. They are appropriate in transient models if the variation of water levels at the boundary is minimal over time and the area of interest is a sufficient distance away from the boundary.

The limited amount of water that flows across the bottom of the aquifer between the Midway Group and the Hooper Formation was assumed to be negligible in comparison with the overall water budget. The lower boundary of the aquifer, therefore, was defined as a no-flow boundary.

The top of the model was treated as a specified flux boundary to represent a constant rate of recharge into the aquifer. Recharge rates for upland areas of the Simsboro and Carrizo (2 to 4 inches/yr) were consistent with those used by Ryder (Ryder, 1988; Ryder and Ardis, 1991). Recharge was set to zero in the bottomlands of the Colorado and Brazos Rivers. The average recharge applied to the model matched the average recharge (1 inch/yr) used by Thorkildsen (Thorkildsen and Price, 1991; unpublished model). Recharge was assumed constant for all stress periods.

Recharge rates were adjusted during model calibration to improve the match between simulated

and observed hydraulic head in the outcrop, as expressed by the mean absolute error between simulated and measured water levels. Model results were particularly sensitive to the assigned values of recharge and vertical hydraulic conductivity of the confining layers. Decreasing vertical hydraulic conductivity of the confining layers required a compensating increase in recharge to the aquifers to maintain the same calibration error.

To evaluate the sensitivity of model results to the recharge rate and hydraulic properties assigned to layer 1 (representing younger formations), modified simulations were run replacing layer 1 with MODFLOW's general-head boundary module. The bounding head was set approximately equal to ground surface. Vertical conductance was estimated on the basis of the average thickness of the overburden and the hydraulic conductivity of clay. Results indicated that as long as there were similar volumes of water moving in and out of layer 2 (Carrizo), model results were insensitive to how the uppermost boundary of the model was set.

The updip (northwest) limit of each model layer was bounded by a no-flow boundary. Cells that were in rows lying beyond the updip limit of each aquifer layer were set as "inactive" cells in the model.

The downdip (southeast) limit of the model was set approximately 4 to 9 mi downdip of the limit of freshwater in the aquifer. The boundary was set this far away to minimize the effect of the boundary on simulation results for the area of interest. The downdip boundary was prescribed as a constant-head boundary. The vertical gradient of head versus depth was iteratively adjusted to yield overall distributions of hydraulic head and flow path consistent with the conceptual model (Fogg and others, 1983). A steep vertical increase in hydraulic head, as much as 1.05 ft/ft, was found to result in simulated heads in the deeper aquifers being greater than heads at their outcrop, implying that groundwater flows toward the recharge zone, contrary to what is described in the conceptual model. Even at a vertical gradient averaging as little as 1.01 ft/ft, a slight updip flow potential resulted near the constant-head boundary. A better match between simulated and observed hydraulic head was obtained with a downward vertical gradient in hydraulic head of 0.98 ft/ft, where the upland areas cross the boundary, and an upward-directed

gradient of 1.01 ft/ft beneath the river bottomlands. The fact that the gradient was near 1.0 indicates that some water passes deeper into the basin beyond the limit of freshwater.

The Brazos and Colorado Rivers are thought to be natural hydrologic boundaries within parts of the model that can function as either a source or sink of water for the regional aquifer system, as stated in the conceptual model. The actual northeast and southwest sides of the model were defined as no-flow boundaries north of the Brazos River and south of the Colorado River. This boundary definition allowed interaction of groundwater and surface water to be considered within the model and moved the artificial lateral boundaries farther from the main area of interest, which lies between the Colorado and Brazos Rivers. Given the rates of pumping included in the model, however, the area of simulated drawdown reaches the model boundaries. The area of inactive cells northeast of the Brazos River (fig. 3) was defined to exclude well fields near Bryan and College Station. The no-flow boundary was set approximately 2 to 3 mi northeast of the Brazos River.

Few flow-gauging data exist for reaches of the Colorado and Brazos Rivers and Yegua Creek within the study area. The model includes the river-boundary package of MODFLOW to simulate exchange of surface water and groundwater from a water-balance perspective. The model does not take surface-water flow or fluctuations in stage height into account. For the purpose of the model, river-stage height was assigned on the basis of topographic elevation of the river, as read from 7.5-minute U.S. Geological Survey topographic maps. Thickness (45 ft) and hydraulic conductance ($\sim 48,000 \text{ ft}^2/\text{d}$; vertical hydraulic conductivity \times length of river reach in cell \div thickness of alluvium) of Colorado and Brazos River alluvium were assumed to be the same and were based on Cronin and Wilson (1967). The hydraulic conductance of alluvium flooring Yegua Creek was assumed to be 10 times less than that along the Colorado and Brazos Rivers. The river module was turned off for Yegua Creek after 2000 for scenarios 2 through 5, assuming that surface-water flow would no longer be augmented by runoff of pumped groundwater.

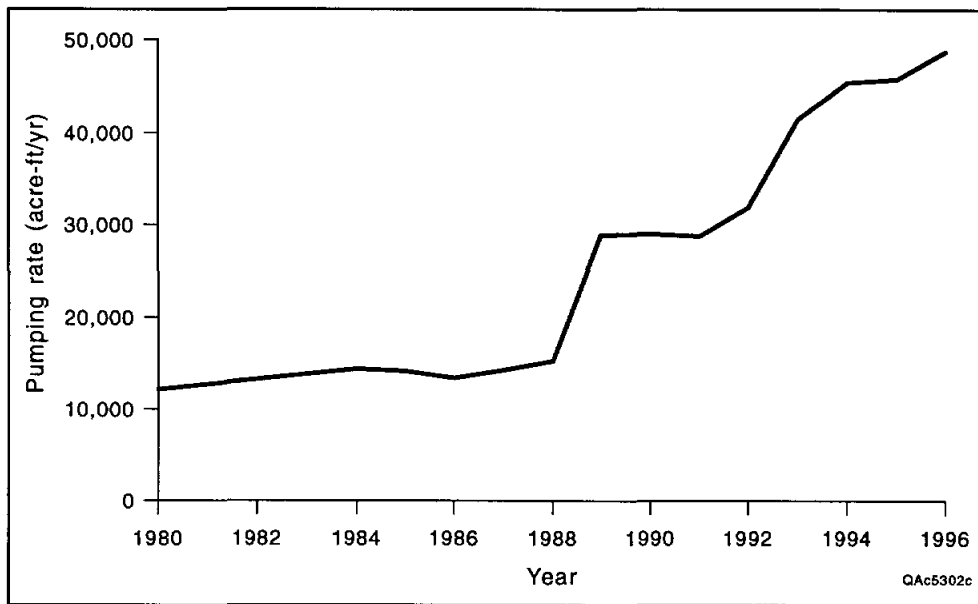


FIGURE 8. Change in total pumping rate from the Carrizo–Wilcox aquifer in Bastrop, Burleson, Fayette, Lee, Milam, and Robertson Counties in study area between 1980 and 1996. Not all of this withdrawal was included because parts of the counties lie outside the modeled area.

Modeling Sequence and Calibration

The modeling sequence included first running the model to get an estimate of the steady-state distribution of hydraulic head and then using these head values as the initial boundary condition for simulating transient flow for all scenarios. The transient simulations included a baseline historical period (1951 through 1999) and five scenarios predicting future (2000 through 2050) groundwater withdrawal and associated water-level change.

The absence of long-term trends in water levels before 1988 (Thorkildsen and Price, 1991) suggests that recharge and discharge in the whole aquifer system were near equilibrium (pseudo-steady state) and that groundwater withdrawal was a small percentage of recharge during this period. The steady state was simulated by substituting the uniform hydraulic heads suggested by Visual MODFLOW for initial heads and including the pumping rates assigned to the first “stress” period (January 1951 through April 1988). A stress period is a time interval in a model during which all inflow and outflow, properties, and boundary conditions are constant. Horizontal hydraulic conductivity was assumed to be the best-known information and was not changed during either steady-state or transient calibration. The distribution of hydraulic head

assigned to the downdip, constant-head boundary, as previously described, was adjusted in successive steady-state runs.

Transient simulations began at January 1951, initial values of hydraulic head being determined from the steady-state simulation. The simulation divided 1951 through 1999 into six stress periods having constant pumping rates (fig. 8):

- (1) January 1951 through April 1988,
- (2) May 1988 through December 1992,
- (3) January 1993 through December 1993,
- (4) January 1994 through December 1995,
- (5) January 1996 through December 1996, and
- (6) January 1997 through December 1999.

Groundwater pumpage for 1997 through 1999 (stress period 6) was estimated as the average of 1996 and the year-2000 projection. Hydraulic heads calculated for the end of stress period 6 (December 1999) were used as starting values of hydraulic head for each 2000 through 2050 scenario, which was divided into six stress periods as well. Stress period 7 was a 1-yr period representing 2000, and stress periods 8 through 12 (2001 through 2050) were each 10 yr long.

Three criteria were used for evaluating the quality of the calibration. First, mean absolute error was calculated for the end of the first and fifth stress periods (April 1988 and December 1996,

respectively). Mean absolute error is the mean of the absolute value of the differences in measured and simulated heads (Anderson and Woessner, 1992). Second, simulated drawdown and estimated cumulative drawdown as of 1996 were qualitatively compared near the Sandow Mine in Milam County (Bob Harden, R. W. Harden and Associates, personal communication, 1999). Third, simulated and published potentiometric surfaces were qualitatively compared and flow paths were compared with those of the conceptual model.

Recharge rate, vertical hydraulic conductivity of the Calvert Bluff and Hooper Formations, and hydraulic conductivity of the barrier wall (fault) were adjusted during model calibration. Specific storage was adjusted very little during transient-model calibration; corrections were made as needed to make storativity uniform across the outcrop of the Simsboro and Carrizo aquifers.

Pumping Rates

Accurate estimates of water withdrawals by pumping have been found to be key to modeling, especially for prediction of drawdown (Konikow, 1986). Pumping affects the calibration of the model and predictions of water levels in the future. Because there are no direct measures of historical pumping, it is generally estimated indirectly, making it a possibly large source of calibration error in this and other numerical models.

Historical pumpage rate tables were constructed by compiling and reconciling data on wells from the TWDB Internet site, TWDB archived data used for developing the Thorkildsen (unpublished) model, the TWDB pumpage summary for the 1980 through 1996 period, and the TWDB summary of 1996 pumpage allocation by user. For 1980 total pumpage from the study area was allocated among approximately 130 water wells located according to municipal, industrial, and irrigation uses, following the Thorkildsen data set. A representative pumpage history was then reconstructed by prorating the amount of pumpage per well according to how much total pumpage had changed in each stress period, relative to the 1980 rates, in each use category. Pumpage per well was adjusted as needed to match the category totals listed in the

TWDB pumpage summary. Pumpage of groundwater from the Carrizo–Wilcox aquifer for domestic use in rural parts of the counties was calculated by applying the ratio of domestic pumpage versus total pumpage for 1996. The combined estimate for domestic and stock-water use was prorated for the amount of each county within the model area, which ranged from 20 percent for Robertson County to 100 percent for Lee County, and distributed across all blocks within each county. Rural pumpage for domestic and stock uses added less than 6 acre-ft/yr to each block of the model.

The pumping-rate schedules and well locations (fig. 9) were imported into Visual MODFLOW. The aquifer assignment for each well was adjusted by the Visual MODFLOW screen editor to set the pumpage for the layer (for example, Simsboro, Carrizo, Calvert Bluff, or Hooper) identified for each well in the TWDB Internet data base. Several of the wells were designated to be screened in two flow units (for example, Carrizo and Calvert Bluff, Carrizo and Simsboro), and the Visual MODFLOW screen editor was used to assign pumpage to these two zones. Visual MODFLOW allocates total pumping between multiple layers on the basis of screen length and hydraulic conductivity of the aquifer.

Future Groundwater-Withdrawal Scenarios

Baseline pumping rates for the 2000 through 2050 scenarios were allocated across the same sets of wells as had been used for the historical period. Additional pumping was added to model cells for specific scenario elements (fig. 1). Actual locations and future rates of pumping should be determined on the basis of detailed site considerations that are beyond the scope of this study.

Scenario 1

Projected pumpage from 2000 through 2050 as described in the 1997 State Water Plan is included in scenario 1 (table 3). This scenario includes 30,000 acre-ft/yr of water currently being produced

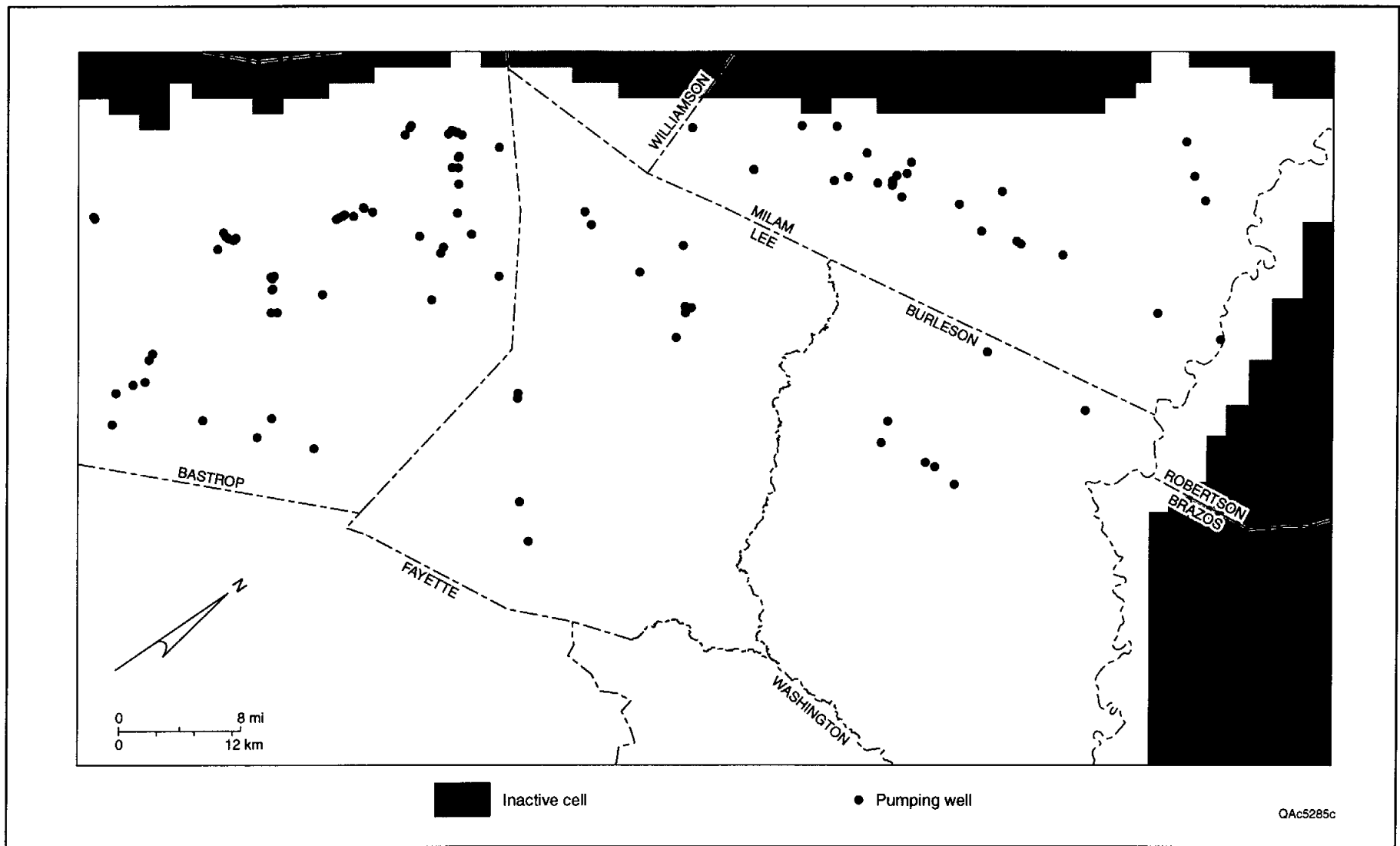


FIGURE 9. Location of wells to which pumping rates were specified in historical and baseline future stress periods.

TABLE 3. Projected rates of groundwater withdrawal by pumping areas shown in figures 1 and B1.

Pumping area	Scenario	Aquifer	Amount (acre-ft/yr)	County
A	3, 4, 5	Simsboro	7,000	Bastrop
B	2, 3, 4, 5	Simsboro	30,000	Bastrop, Lee
C	2, 3, 4, 5	Simsboro	70,000	Lee, Milam
D	4, 5	Carrizo	50,000	Lee, Milam, Burleson
D	4, 5	Simsboro	50,000	Lee, Milam, Burleson
E	3, 5	Carrizo	6,667	Lee
E	3, 5	Simsboro	18,333	Lee
F	3, 4, 5	Carrizo–Wilcox	930 to 6,845*	Bastrop
Water plan projection**	1, 2, 3, 4, 5	Carrizo–Wilcox	5,765 to 10,888*	Bastrop, Burleson, Lee, and Milam

*Range for 2000 through 2050

**Increment in addition to 1999 estimated rate

for aquifer-pressure reduction at the Sandow Mine in Lee and Milam Counties. By 2050, the pumping rate for the entire model area was increased by 10,977 acre-ft/yr, relative to the estimated 1996 rate.

Scenario 2

Scenario 2 includes projected pumpage from 2000 through 2050, as in scenario 1, plus an incremental increase of 70,000 acre-ft/yr in groundwater production to the maximum rate contracted by ALCOA, SAWS, and CPS (tables 1, 3). The maximum rate was assumed to begin in 2000 and was held constant through 2050. Pumping was assigned to cells in areas B and C of figure 1. As previously stated, these locations were used only for purposes of modeling possible-withdrawal scenarios, whereas actual locations should be chosen on the basis of criteria that are beyond the scope of this study to consider.

Scenario 3

Scenario 3 includes projected pumpage from 2000 through 2050, as in scenario 2, plus additional pumpage (table 1): (a) 7,000 acre-ft/yr from near Lake Bastrop to meet demand for additional water related to steam-electric power generation (area A, fig. 1); (b) 930 to 6,845 acre-ft/yr,

increasing during the 2000 through 2050 period, throughout Bastrop County for “county-other” uses; and (c) 25,000 acre-ft/yr (area E, fig. 1) to help meet Williamson County water demand as described in the Trans-Texas Water Program (HDR Engineering, 1998). The 25,000 acre-ft/yr was split between the Simsboro and Carrizo layers of the model (table 3).

Scenario 4

Scenario 4 includes projected pumpage from 2000 through 2050, as in scenario 2, plus additional pumpage (table 1): (a) 7,000 acre-ft/yr from near Lake Bastrop to meet demand for additional water related to steam-electric power generation (area A, fig. 1); (b) 930 to 6,845 acre-ft/yr, increasing during the 2000 through 2050 period, throughout Bastrop County for “county-other” uses; and (c) 50,000 acre-ft/yr from the Simsboro and 50,000 acre-ft/yr from the Carrizo from area D (fig. 1).

Scenario 5

Scenario 5 includes projected pumpage from 2000 through 2050, as in scenario 3, and an additional 50,000 acre-ft/yr from the Simsboro and 50,000 acre-ft/yr from the Carrizo from area D (fig. 1). Scenario 5 has the greatest amount of simulated groundwater withdrawal considered in this study.

RESULTS

Baseline Historical Simulation (1951 through 1999)

Groundwater pumpage, fairly constant between 1951 and 1988, increased to approximately 37,900 acre-ft/yr by 1996 in the model area (table 1; fig. 8). Groundwater withdrawal from the Simsboro increased in 1988 and 1993 as a part of mining operations in Milam County. The simulated potentiometric surface for groundwater in the Simsboro Formation (fig. 10) bears the main features of the potentiometric surface shown by Thorkildsen and Price (1991). The latter includes data from all units of the Carrizo–Wilcox aquifer and from a wide window of time. The simulated equipotential contours (lines of equal hydraulic head) bend upstream across the valleys of the Colorado, Brazos, and Little Rivers, indicating discharge of groundwater from the regional aquifers in those river bottomlands, which is consistent with that of the conceptual model. Model results also show that the horizontal gradient is steeper near the outcrop than in the subsurface (fig. 10).

Simulated hydraulic head decreases with depth beneath the upland area (fig. 11a, b), although it is simulated as increasing with depth beneath the major river valleys, reflecting the potential for upward discharge of groundwater to the river bottomlands (fig. 11b). The equipotential contours on the vertical cross sections suggest that the horizontal component of flow is greater in the Simsboro and Carrizo aquifer than in the Calvert Bluff and Hooper, which act like confining layers having predominantly vertical flow. Groundwater in the Simsboro and Carrizo appears to derive from recharge in their outcrops, as well as from cross-formational leakage from the confining layers (fig. 11a, b).

The estimate of historical drawdown shown in figure 12 compares simulated potentiometric surfaces of groundwater in the Simsboro Formation for 1951 and 1996. Simulated drawdown between 1951 and 1996 averaged 9 ft and was as much as

80 ft (table 4). This simulation underestimates the maximum measured drawdown (~119 ft) near the Sandow Mine in Milam County by about 30 percent. The discrepancy in drawdown may exist partly because wells at the mine produce from the upper part of the Simsboro (Bob Harden, R. W. Harden and Associates, Inc., personal communication, 1999). Model results, however, average the effect of groundwater withdrawal over the whole thickness of the formation. The incremental drawdown reflects a change in the artesian or pressure head and not the draining or dewatering of pore space.

For stress periods 1 through 5 (1951 through 1996), the mean absolute error between simulated and observed hydraulic head in all formations was approximately 32 ft (fig. 13), meaning that simulated hydraulic head on average was 32 ft greater or less than observed hydraulic head. The fact that there are more points beneath than above the line in figure 13 suggests that the model has a bias toward underestimating true hydraulic head.

Under present conditions, water from precipitation that recharges the unconfined part of the aquifers discharges either by (a) evapotranspiration or flow to rivers or (b) movement deeper into the subsurface, which recharges the confined part of the aquifer (table 5). Recharge was held constant, as previously explained. Model measurements of net discharge to rivers and streams in 1996 are calculated as approximately 12,800 acre-ft/yr for the Carrizo and 9,700 acre-ft/yr for the Simsboro. Given the assumed values of river stage and simulated hydraulic head for 1996, there is a net loss of water (~300 acre-ft/yr) from the Colorado River across the outcrop of the Simsboro, whereas there is a net gain in water (~10,000 acre-ft/yr) in the Brazos River. Simulated discharge rate also depends on the assumed value of riverbed conductance used in the model, as previously discussed. Additional work is needed to calibrate river–aquifer interaction. Flow from the outcrop into the confined part of the aquifer and net inflow from adjacent confining layers are balanced by flow deeper into the basin (out of the model) and by discharge to wells.

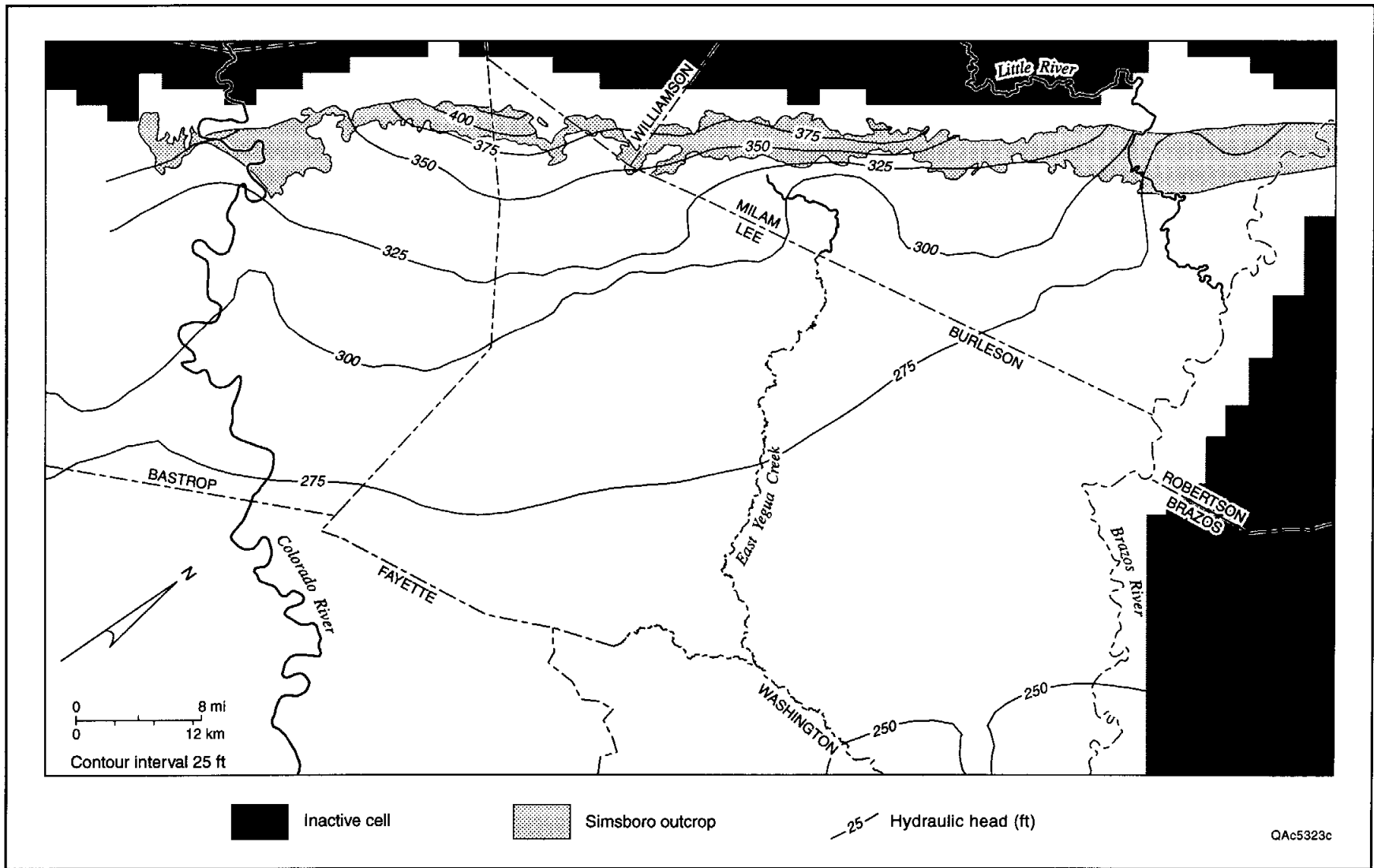


FIGURE 10. Simulated potentiometric surface representing groundwater in the Simsboro Formation for the year 1996. Mean absolute error of simulation is 32 ft.

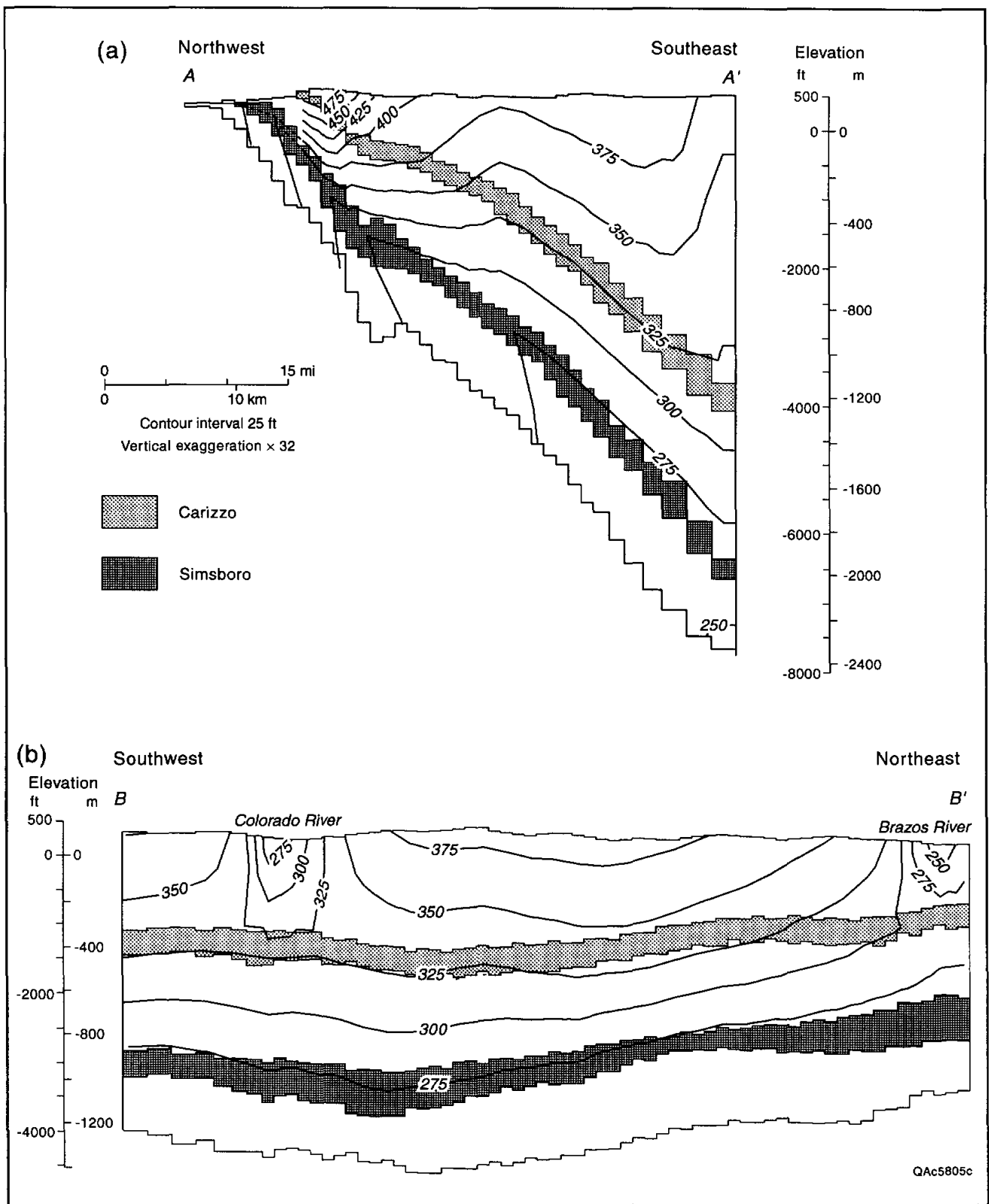


FIGURE 11. (a) Southeast-northwest vertical hydrologic dip section A–A' along column 28 and (b) Southwest-northeast vertical hydrologic strike section B–B' along row 31 of the model. Both sections show the simulated decrease in head with depth beneath upland areas and increase in head with depth beneath rivers for 1996. Lines of sections shown in figure 3.

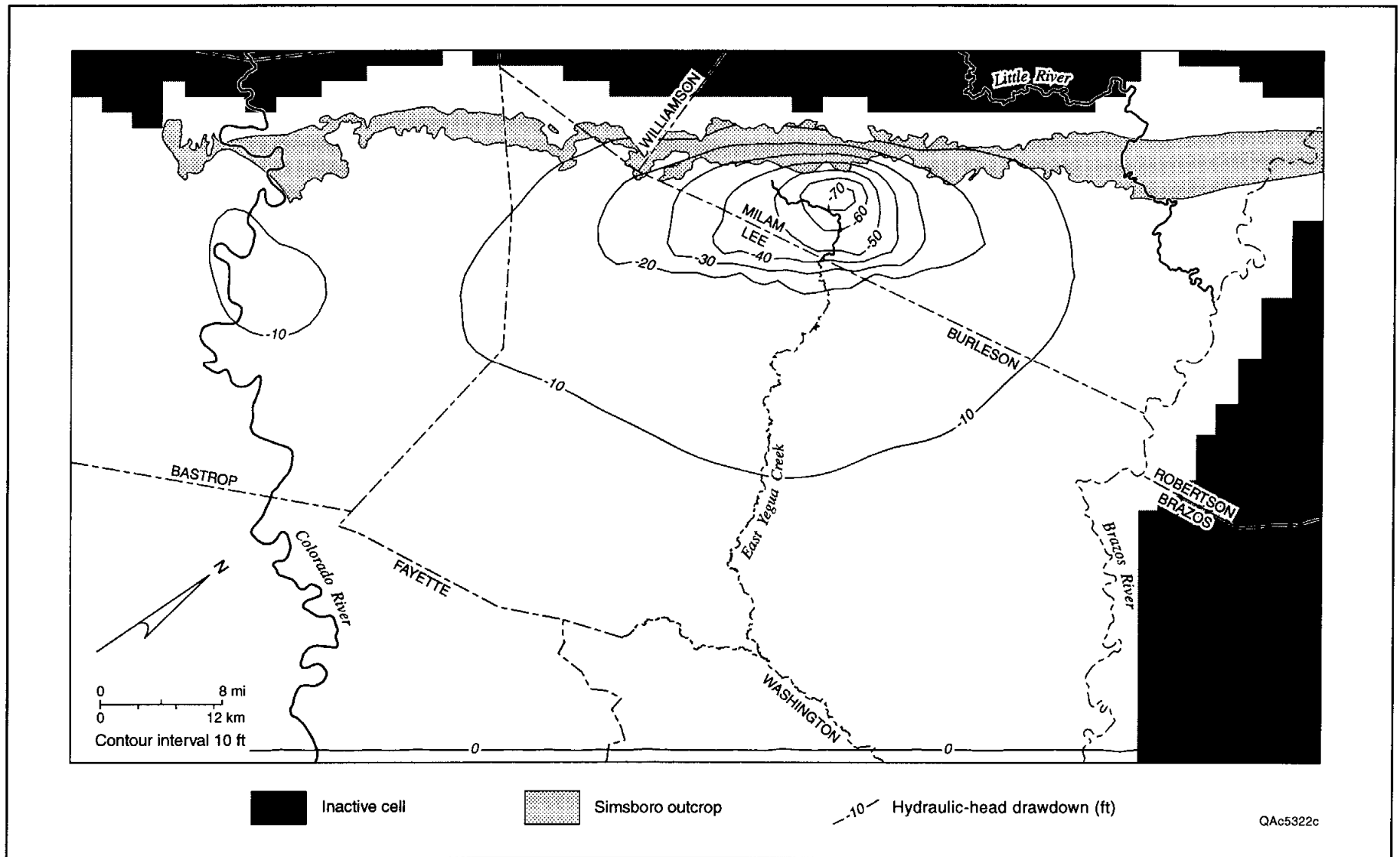


FIGURE 12. Simulated historical (1951 through 1996) drawdown of hydraulic head in the Simsboro Formation. Northwest-bounding fault (fig. 2a) restricts propagation of drawdown down-dip.

TABLE 4. Comparison of water-level differences between scenarios. Cumulative drawdowns given as comparisons with simulations for 1951 or 1996. Incremental drawdowns given as comparisons between scenarios for 2050. Mean absolute error in model calibration was 32 ft. Pumping areas shown in figures 1 and B1 and described in table 1.

Scenario	Compared with scenario	Model layer	Figure no.	Average (ft)	Maximum (ft)	Pumping area evaluated
H (1996)	H (1951)	Simsboro	12	-9	-81	Regional
1 (2050)	H (1996)	Simsboro	14	-21	-98	Regional
2 (2050)	H (1996)	Simsboro	15	-76	-320	Regional, B, C
2 (2050)	1 (2050)	Simsboro	16	-42	-263	B, C
3 (2050)	H (1996)	Simsboro	B2	-104	-353	Regional, A, B, C, E, F
3 (2050)	2 (2050)	Simsboro	B3	-22	-91	A, E, F
4 (2050)	H (1996)	Simsboro	B4	-123	-391	Regional, A, B, C, D, F
4 (2050)	H (1996)	Carrizo	B5	-32	-112	Regional, A, B, C, D, F
4 (2050)	1 (2050)	Simsboro	—	-103	-324	A, B, C, D, F
4 (2050)	1 (2050)	Carrizo	—	-31	-110	A, B, C, D, F
5 (2050)	H (1996)	Simsboro	17	-143	-419	Regional, A, B, C, D, E, F
5 (2050)	1 (2050)	Simsboro	19	-121	-348	A, B, C, D, E, F
5 (2050)	3 (2050)	Simsboro	23	-40	-146	D
5 (2050)	4 (2050)	Simsboro	22	-21	-87	E
5 (2050)	H (1996)	Carrizo	18	-33	-118	Regional, A, B, C, D, E, F
5 (2050)	1 (2050)	Carrizo	20	-32	-116	A, B, C, D, E, F
3X (2050)*	1 (2050)	Simsboro	21	-5	-55	A, F

H = Simulation for historical period, including steady state (1951) and stress period 5 (1996)
 * = To evaluate areas A and F, pumping areas B, C, and E removed from scenario 3

Projected Groundwater-Withdrawal Scenarios (2000 through 2050)

Evaluation of groundwater availability focused on the Simsboro Formation; it is the best-characterized part of the Carrizo–Wilcox aquifer and, along with the Carrizo Formation, comprises the main water-yielding zones. Scenarios were evaluated in two ways: (a) comparing 2050 to 1996 simulation results and (b) comparing 2050 simulation results between scenarios (table 4). The former shows the total predicted change in water

level, given the location and amount of groundwater withdrawal for each scenario and the combined effect of model assumptions. The latter has had the effects of common scenario elements and model assumptions subtracted out, allowing for an assessment of incremental drawdown associated with individual scenario elements. For example, subtracting scenario 2 from scenario 1 removes the common effect of the baseline increase in pumping predicted by the TWDB (1997) State Water Plan, allowing evaluation of the drawdown predicted for only pumping areas B and C (fig. 1). As another example, subtracting scenario 5 from 3 removes all effects except for the drawdown predicted for area D (fig. 1).

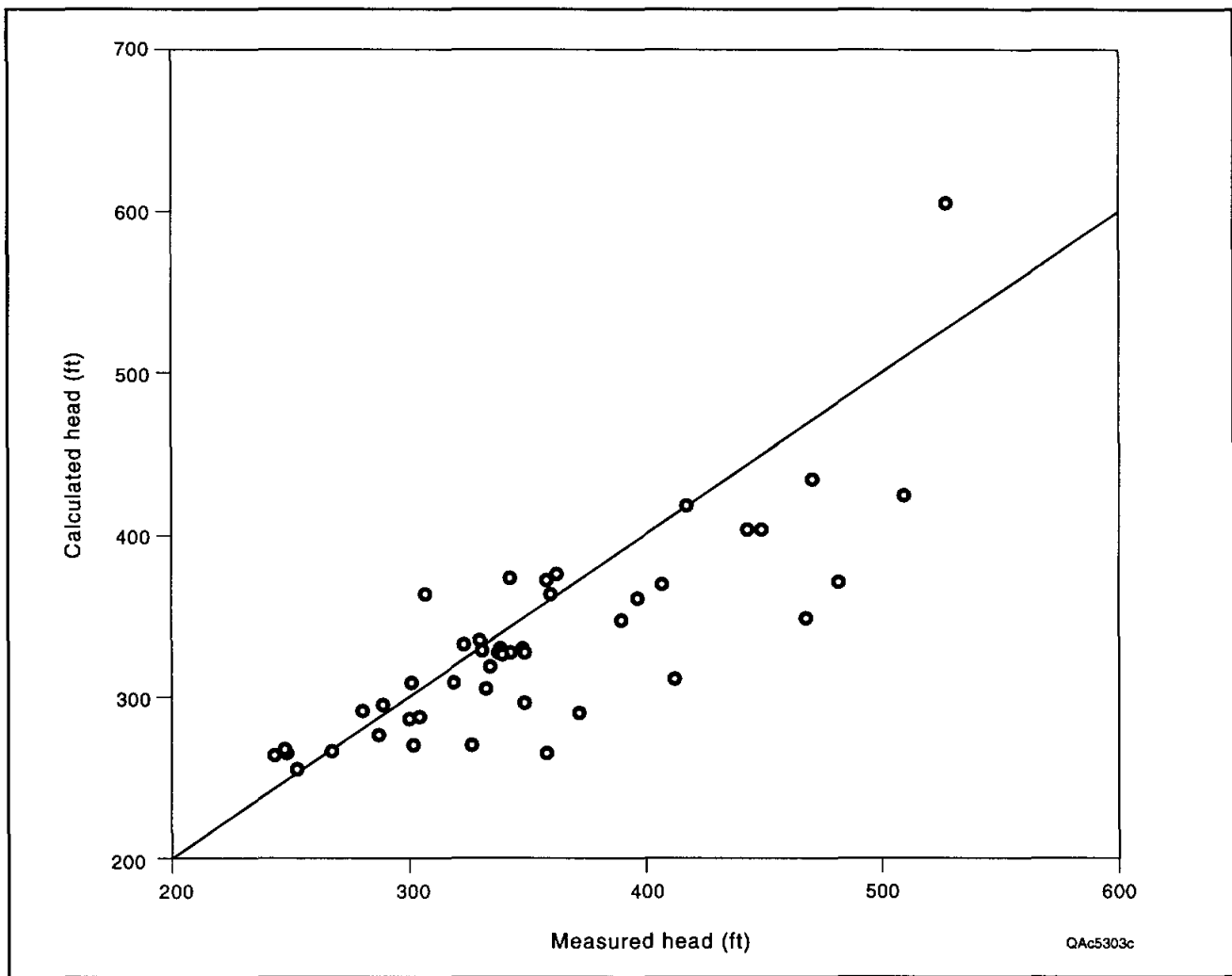


FIGURE 13. Comparison of measured and simulated hydraulic head. Mean absolute error of 32 ft reflects uncertainties in the conceptual model, parameter values, and location and rate of pumping assigned to the 1951 through 1996 calibration period.

The 18-percent increase in pumping between 1996 and 2050 described in scenario 1 is predicted to add on average another 21 ft of drawdown (table 4; fig. 14) to the cumulative drawdown as of 1996 (fig. 12). In comparison, the 180-percent increase described in scenario 2 is predicted to add an average 76 ft of drawdown (fig. 15) to the 1996 drawdown. Figure 16 shows the difference in hydraulic head between scenarios 2 and 1 for groundwater in the Simsboro Formation as of 2050. The map in figure 16 subtracts the effect of rates of groundwater withdrawal described in the TWDB (1997) State Water Plan (scenario 1) and quantifies the incremental drawdown attributable to increasing withdrawal from pumping areas B and C (fig. 1; tables 1, 3). Model results suggest that in-

cremental drawdown averages about 40 ft in the Simsboro (table 4). The maximum additional drawdown by 2050 is approximately 260 ft. The drawdown is elongate parallel to the outcrop not only because the combined pumping areas of B and C (fig. 1) are similarly elongate but also because the effect of the graben is taken into account (fig. 2a).

Simulated drawdown for scenario 2 and the other scenarios occurs primarily as a pressure reduction in the aquifer. Some dewatering in the Simsboro occurs in the center of pumping areas, but additional water resources remain through 2050. Parallel but smaller changes in hydraulic head in the adjacent confining layers are also predicted. The calculated amount of

TABLE 5. Summary of budget for groundwater in Carrizo and Simsboro Formations (1,000 acre-ft/yr). Budgets for scenarios 3 and 4 lie between those of scenarios 1 and 5. Water budget equation: $R-D+C-M-W=S$. Flow to confined aquifer occurs within aquifer and is not part of the water-budget equation.

	Recharge to outcrop (R)	Discharge to river at outcrop (D)	Flow to confined aquifer (F)	Cross- formational flow (C)	Movement to deep basin (M)	Discharge to wells (W)	Increase in storage (S)
Carrizo							
1996	31.6	12.8	18.5	16.5	29.2	4.2	2.2
2050 (Scenario 1)	31.6	12.8	19.3	16.9	29.1	5.2	1.6
2050 (Scenario 2)	31.6	12.8	19.3	16.8	29.0	5.2	1.6
2050 (Scenario 5)	31.6	10.4	35.0	21.1	5.4	53.0	-15.8
Simsboro							
1996	30.4	9.7	34.6	4.4	11.1	31.8	-17.4
2050 (Scenario 1)	30.4	3.0	28.7	5.5	2.8	41.7	-11.5
2050 (Scenario 2)	30.4	-11.1	33.1	8.6	-19.9	105.7	-36.5
2050 (Scenario 5)	30.4	-28.3	39.2	11.2	-74.7	188.7	-45.2

communication of pressure between the Simsboro and Calvert Bluff, however, is affected by the assumed value of vertical hydraulic conductivity (table 2).

Figures 17 and 18 show the cumulative effect of the maximum amount of groundwater withdrawal simulated in this study, given the assumptions of scenario 5, which includes all the pumping areas (table 4). Compared with 1996 water levels, those in scenario 5 result in an average drawdown of about 140 ft in the Simsboro and 30 ft in the Carrizo (figs. 17, 18). Maximum simulated drawdown relative to 1996 levels is predicted to be about 420 ft in the Simsboro and 120 ft in the Carrizo (figs. 17, 18). Subtracting scenario 5 from 1 removes the effect of baseline rates of groundwater withdrawal given in the TWDB (1997) State Water Plan. This incremental drawdown, as opposed to cumulative drawdown since 1996, averages about 120 ft in the Simsboro and 30 ft in the Carrizo (table 4; figs. 19, 20). Maximum incremental drawdown in 2050 is simulated to be approximately 350 ft in the Simsboro and 115 ft in the Carrizo (figs. 19, 20). The effects of pumping areas B, C, and D (fig. 1) on drawdown in the Simsboro are most obvious partly because they account for the most withdrawal (fig. 19). Their incremental effect on the Carrizo (fig. 20) is less mainly because less water is withdrawn from the Carrizo in the simulation (table 3). The center of the area of

incremental drawdown for the Carrizo mainly reflects the assumed location of pumping area D (figs. 1, 20), from which the most Carrizo water is withdrawn. Different actual locations and rates of pumping would result in a different distribution of drawdown. Note that the area of simulated drawdown for scenario 5 reaches all three artificial model boundaries. Additional work is needed to evaluate how alternative boundary conditions affect the calculated drawdown.

Figure 21 shows the incremental drawdown associated with pumping from area A (fig. 1) and area F (projected "county-other" demand for Bastrop County [table 1]). The incremental drawdown associated with withdrawing 25,000 acre-ft/yr from area E, drawn on the basis of the Trans-Texas Water Program (HDR Engineering, 1998), is illustrated in figure 22. Incremental drawdown in the Simsboro for area E, averaging about 20 ft, has a maximum of about 85 ft (table 4; fig. 22).

Figure 23 shows the projected effect of withdrawal of 50,000 acre-ft/yr of groundwater from the Simsboro in pumping area D (tables 3, 4). Drawdown due to other pumping is factored out by subtracting the hydraulic heads of scenario 3 from those of scenario 5. Pumping area D was simulated to encompass a large withdrawal of groundwater beyond that predicted by the TWDB (1997) State Water Plan. Rather than distribute

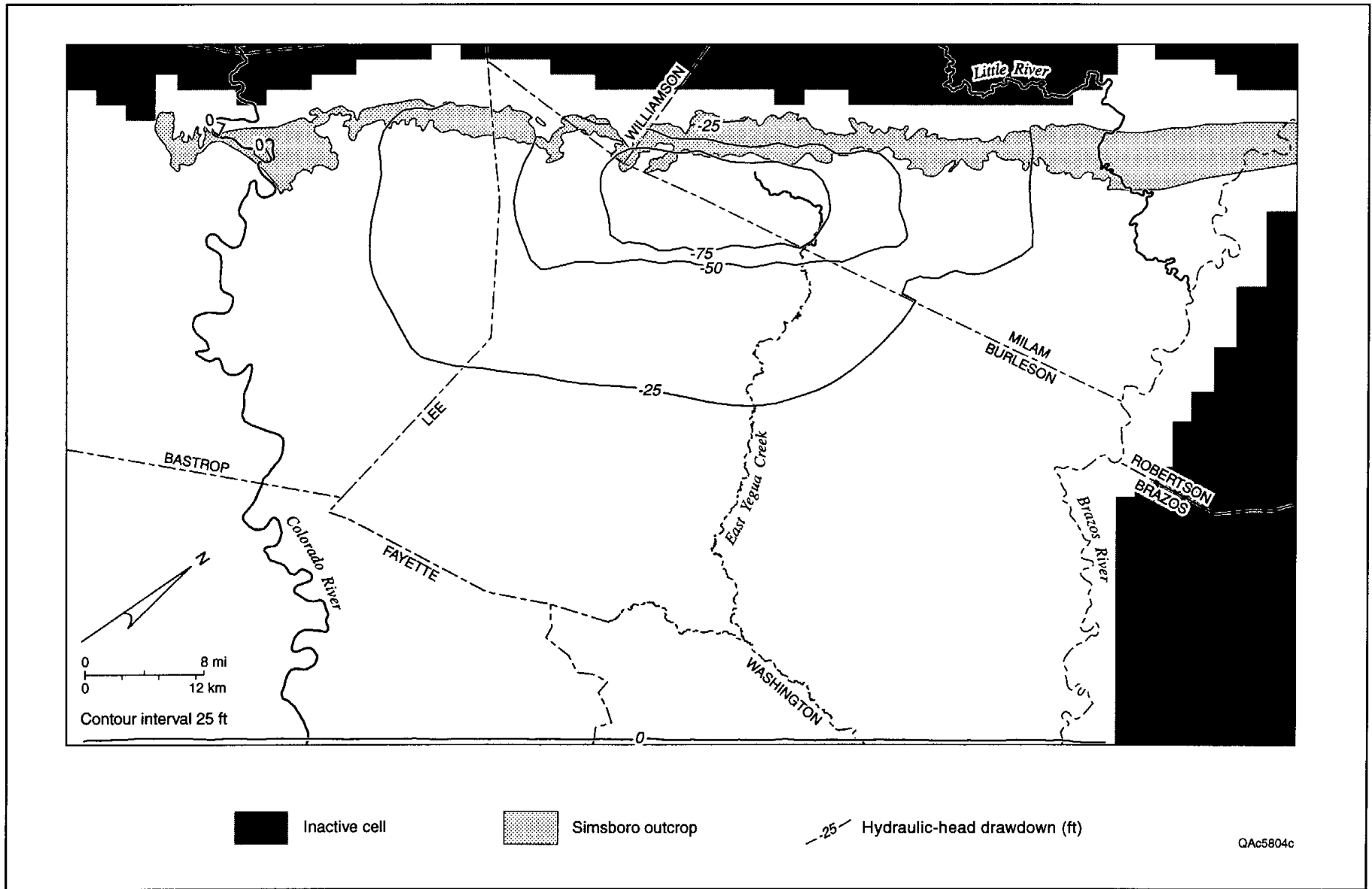


FIGURE 14. Projected 1996 through 2050 drawdown in the Simsboro for scenario 1, given pumping rates of the TWDB (1997) State Water Plan.

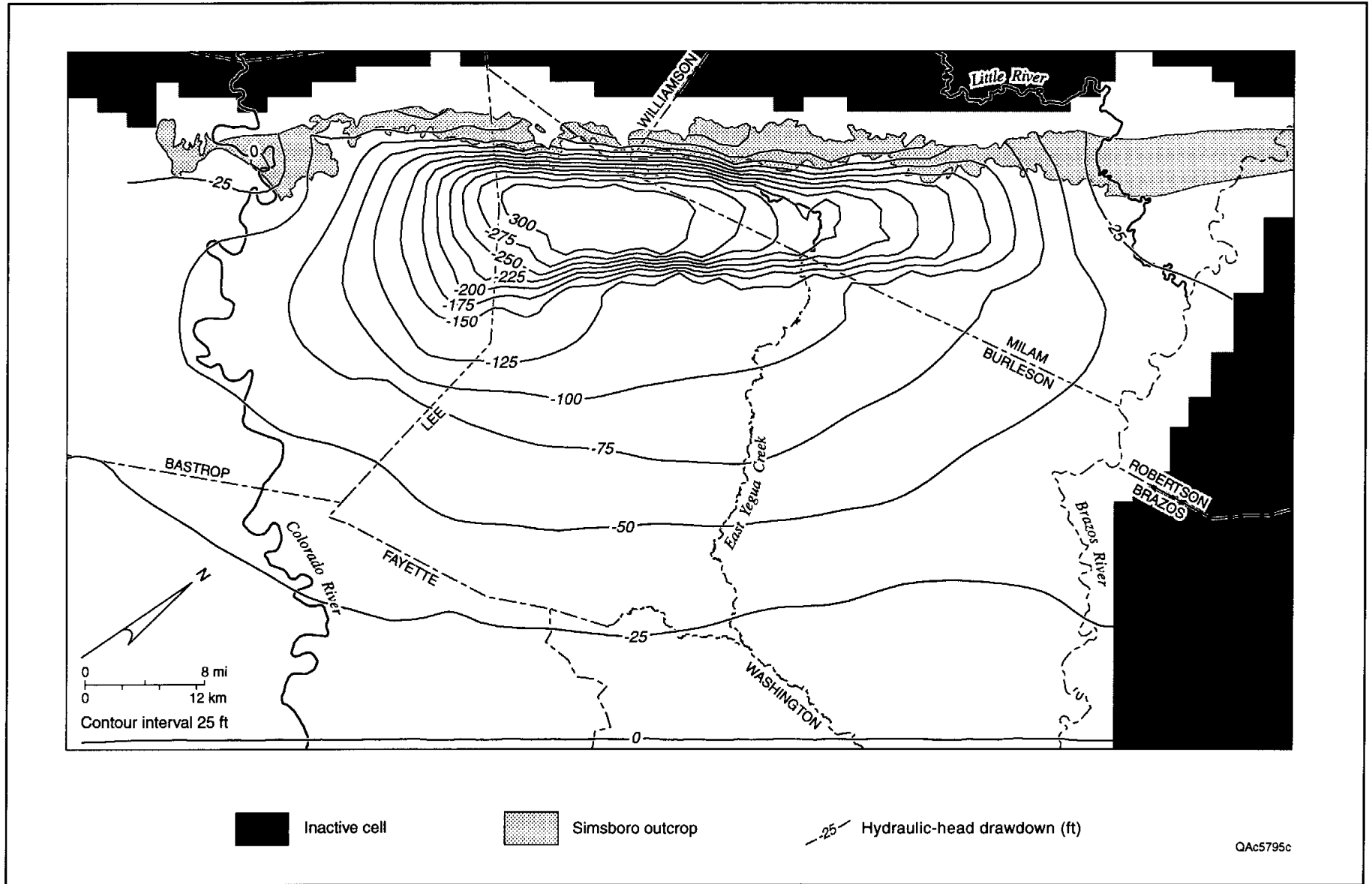


FIGURE 15. Projected 1996 through 2050 drawdown in the Simsboro for scenario 2, superposing drawdown associated with pumping areas B and C (fig. 1) on that for scenario 1 (fig. 14).

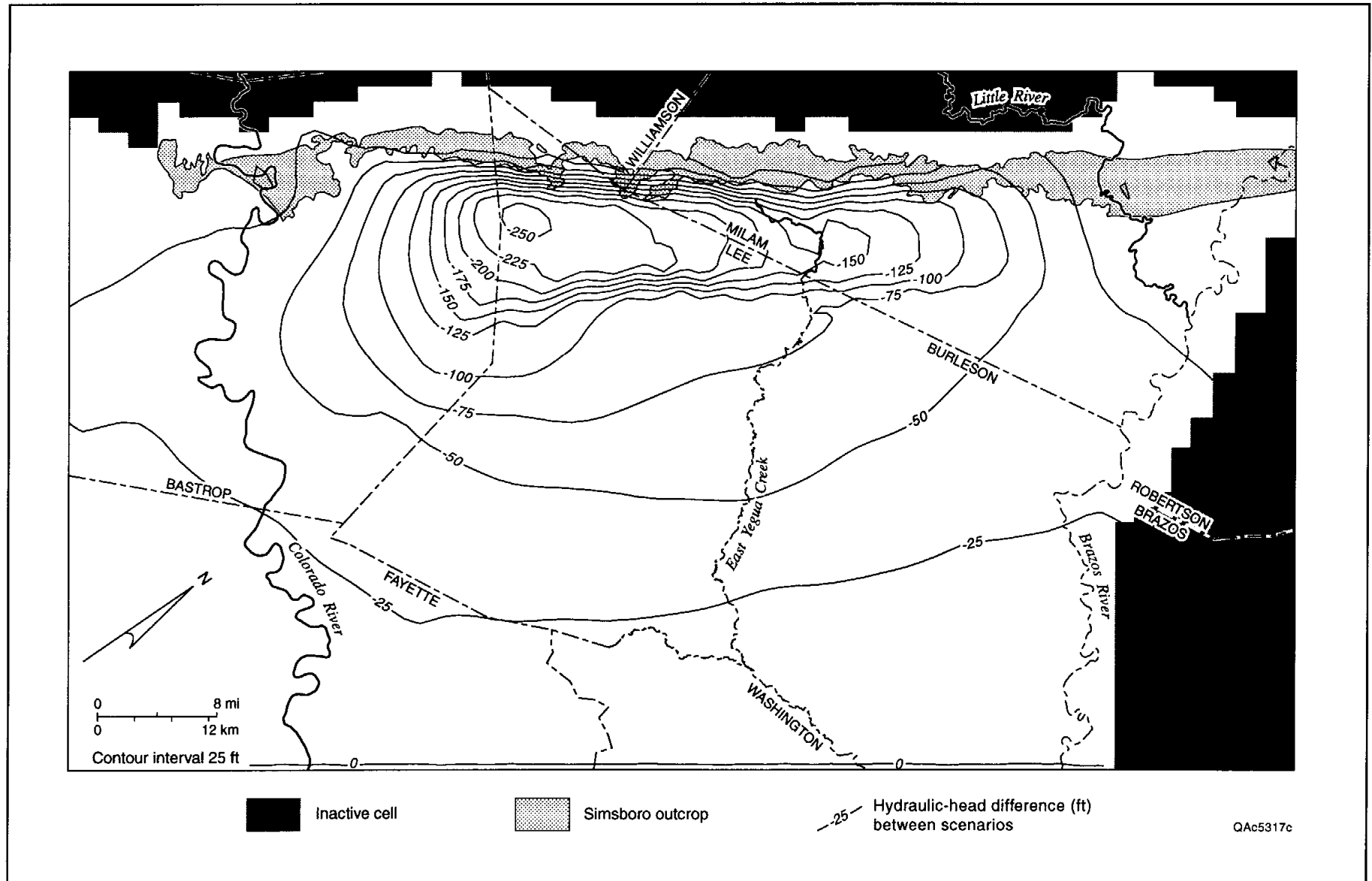


FIGURE 16. Difference between scenarios 2 and 1 in simulated hydraulic head for the Simsboro Formation in the year 2050, showing incremental effects of pumping areas B and C (fig. 1).

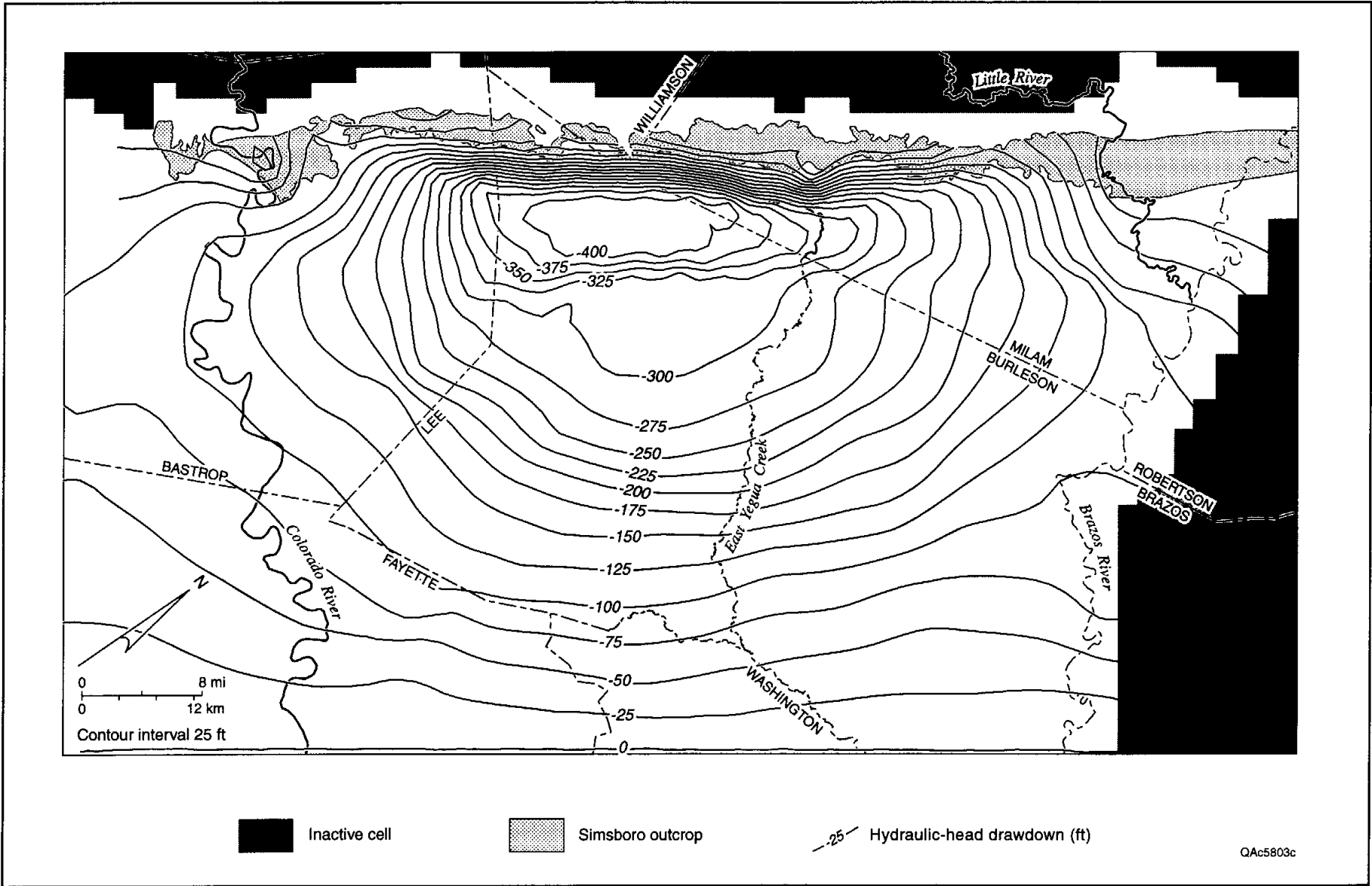


FIGURE 17. Projected 1996 through 2050 drawdown in the Simsboro for scenario 5, including cumulative effects of all pumping areas (A through F, table 1) superposed on the pumping rates of the TWDB (1997) State Water Plan.

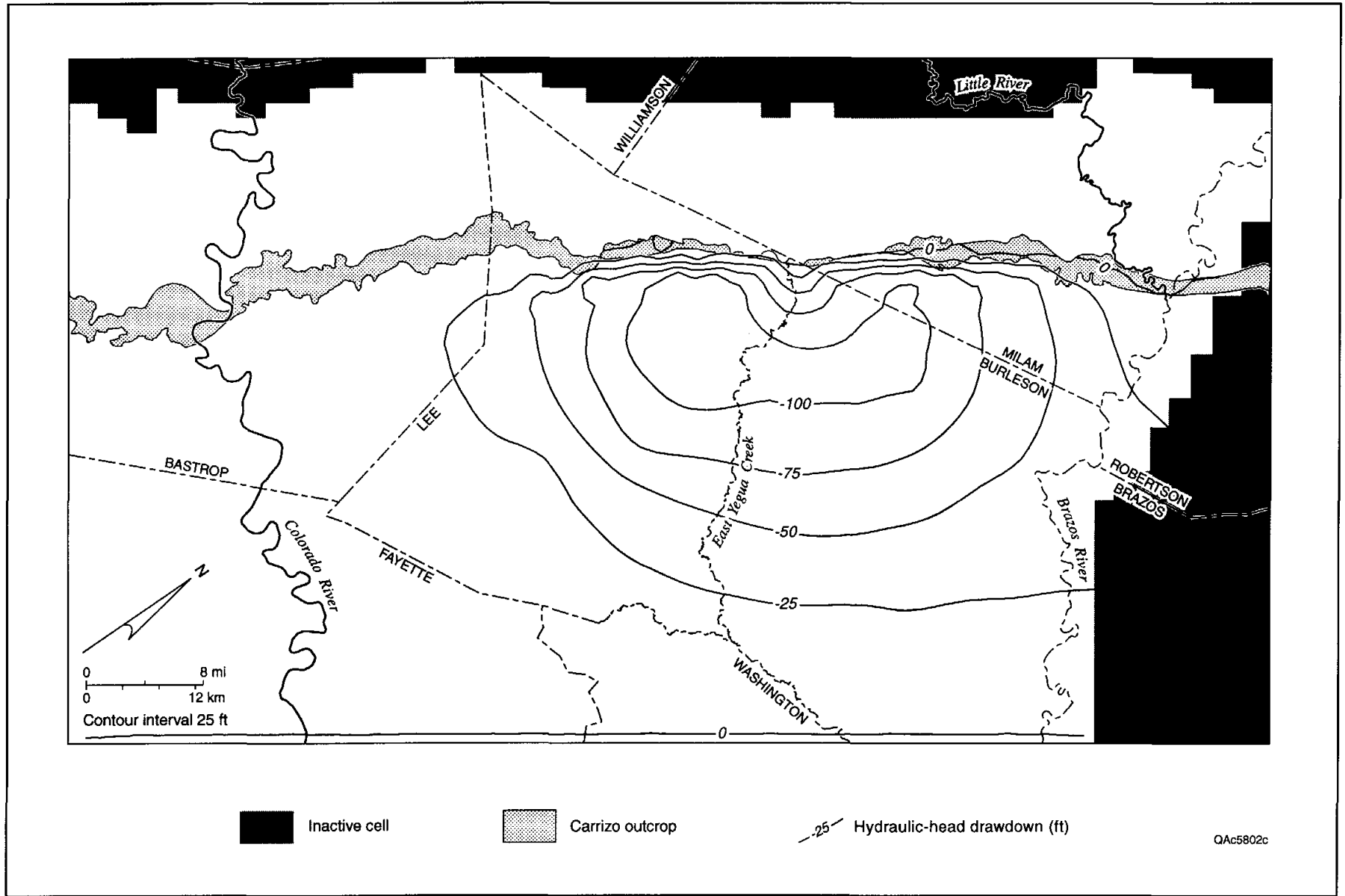


FIGURE 18. Projected 1996 through 2050 drawdown in the Carrizo for scenario 5, including cumulative effects of all pumping areas (A through E, table 1) superposed on the pumping rates of the TWDB (1997) State Water Plan. Only pumping areas D and E (fig. 1) include pumping from the Carrizo.

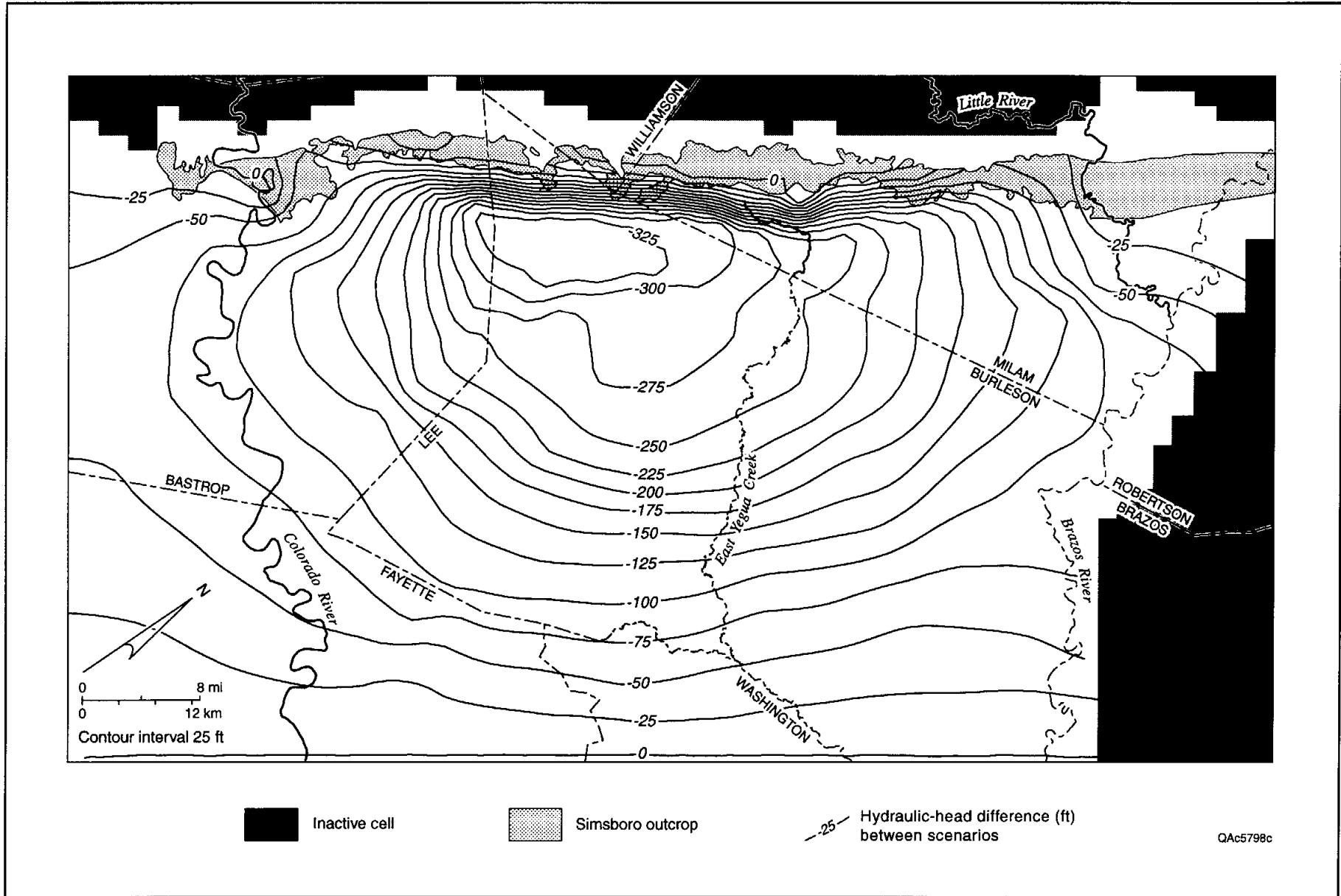


FIGURE 19. Difference between scenarios 5 and 1 in simulated hydraulic head for the Simsboro Formation in the year 2050, showing the combined incremental effects of all pumping areas (fig. 1).

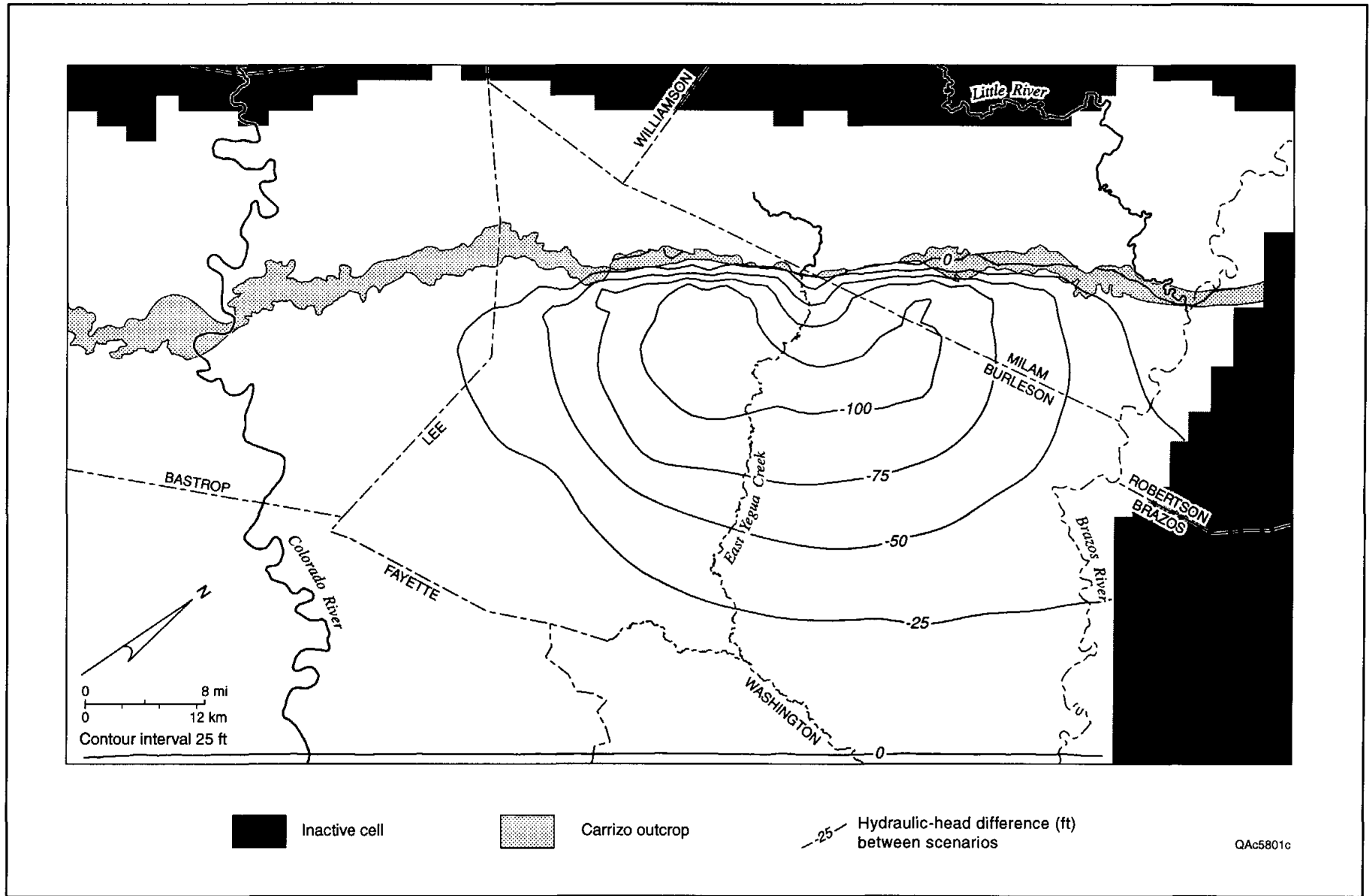


FIGURE 20. Difference between scenarios 5 and 1 in simulated hydraulic head for the Carrizo Formation in the year 2050, showing the combined incremental effects of simulated withdrawal of Carrizo water mainly from area D but also from area E (fig. 1).

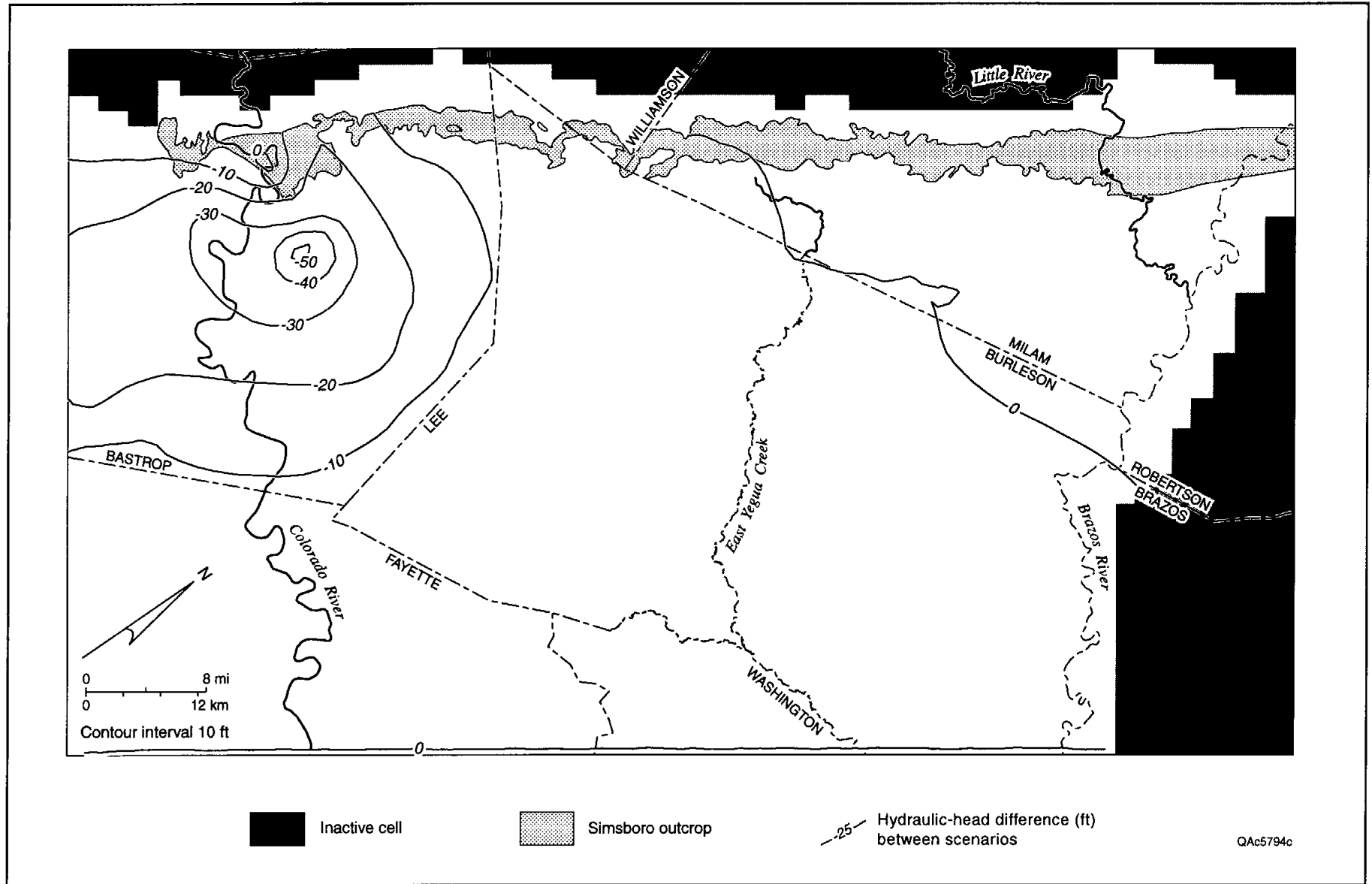


FIGURE 21. Incremental drawdown of hydraulic head in the Simsboro, associated with pumping areas A and F (table 1, fig. 1) in the year 2050.

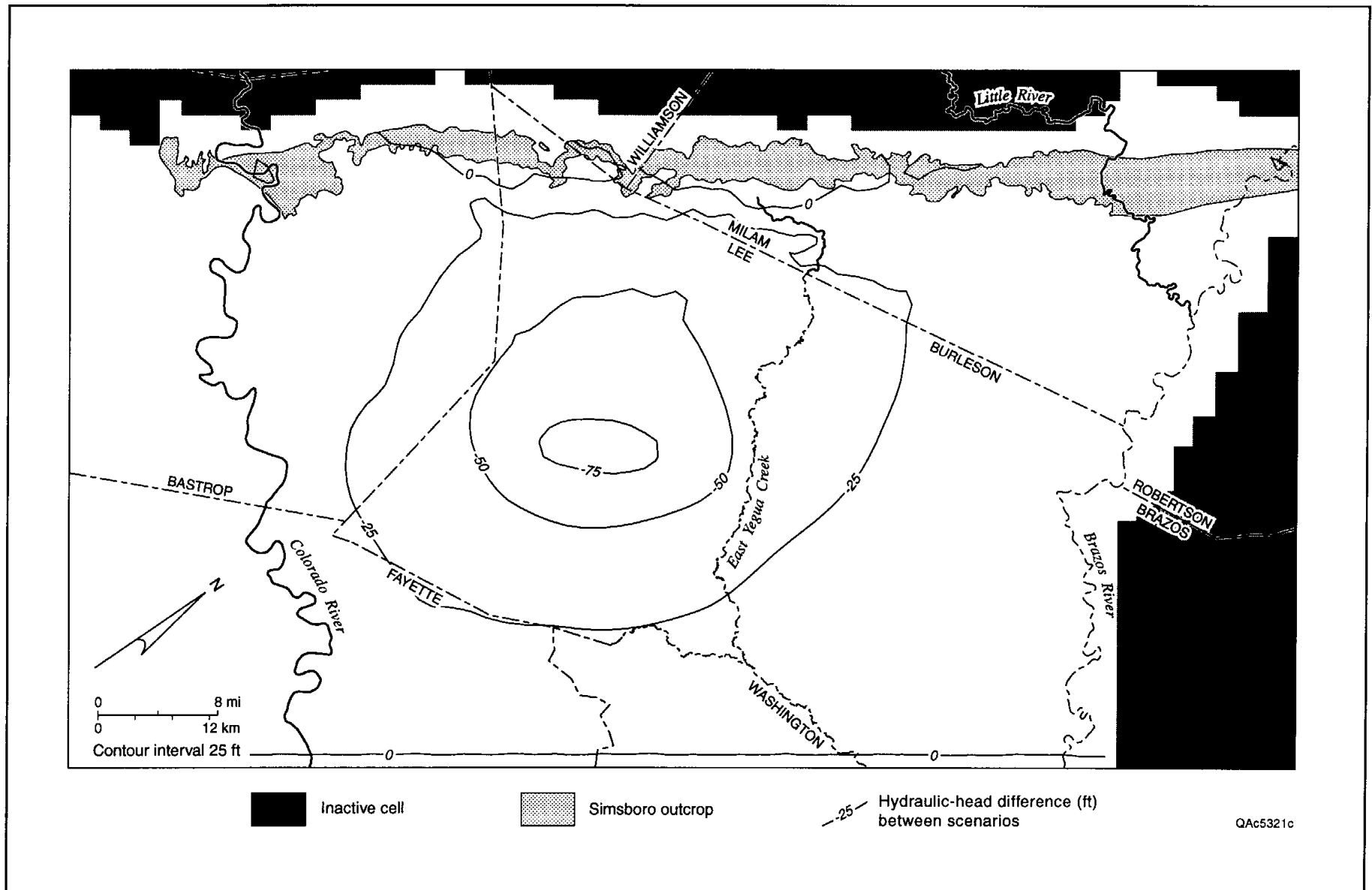


FIGURE 22. Difference between scenarios 5 and 4 in simulated hydraulic head for the Simsboro Formation in the year 2050, showing incremental effects of pumping area E (fig. 1).

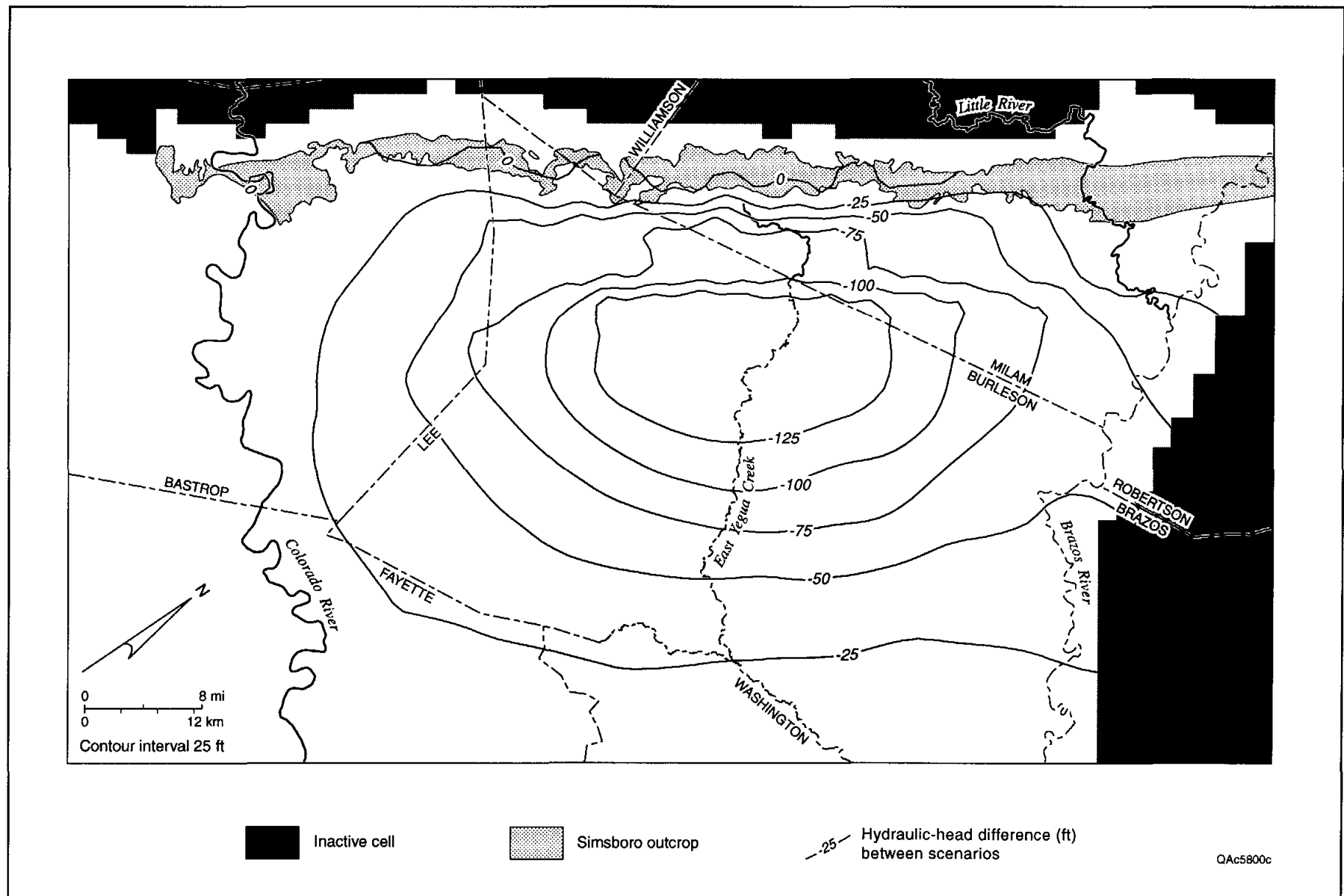


FIGURE 23. Difference between scenarios 5 and 3 in simulated hydraulic head for the Simsboro Formation in the year 2050, showing incremental effects of pumping area D (fig. 1)

the pumping uniformly or randomly around the model area to meet this assumed need, the model used the arbitrary configuration of pumping area D. The concentration of pumping from the Simsboro in this region results in an incremental drawdown that reaches about 145 ft and averages about 40 ft (table 4; fig. 23).

For scenario 1, the projected change in total pumping by 2050 does not much change other parts of the water budget (table 5). The greater withdrawal of groundwater associated with scenario 5, needless to say, results in more changes. With a simulated decline in artesian pressure, more groundwater is induced to flow from the unconfined to the confined parts of the aquifers, and cross-formational flow into the aquifers is increased. The simulation predicts that the Colorado will continue to have a losing reach over the Simsboro outcrop, with a net loss of ~17,000 acre-ft/yr by 2050, given the rest of the assumptions of scenario 5. The Brazos River will possibly change from a gaining reach to a losing reach over the Simsboro outcrop, with a net loss of ~11,000 acre-ft/yr by 2050. The model

takes neither surface-water flow nor near-surface hydrologic processes into account, however, and additional calibration of model parameters is needed to evaluate the significance of the simulated amount of exchange of groundwater and surface water in Yegua Creek and the Colorado and Brazos Rivers.

Withdrawal of groundwater from the confined part of the Simsboro is simulated to have the effect of increasing cross-formational flow into the Simsboro. Whereas cross-formational flow might be undetectable at a local scale, given the low vertical hydraulic conductivity of the Hooper and Calvert Bluff Formations, on a regional scale, vertical flow can be an appreciable part of the water budget of an aquifer. The change in sign of flow to the deep basin reflects the fact that the simulated area of drawdown has reached the downdip model boundary. The distance downdip that the hydraulic-head gradient is reversed is not accurately simulated once drawdown reaches the boundary.

RECOMMENDATIONS

This numerical model was developed with the goal of making representations of aquifer properties and withdrawal scenarios sufficiently accurate to assess the effects of the five groundwater-withdrawal scenarios within the schedule constraints of the study. Additional work on hydrogeologic properties and other model characteristics beyond the scope of the preliminary assessment may further improve the accuracy and completeness of model predictions. Such additional work includes

- ◆ evaluating alternate lateral boundary conditions,
- ◆ analyzing prediction results' sensitivity to storativity and other model properties and possibly making minor changes in assigned property values,
- ◆ reexamining and adjusting hydrologic properties governing river–aquifer interaction,

- ◆ evaluating how recharge rates might vary by also simulating evapotranspiration,
- ◆ assessing possible changes in water quality,
- ◆ making a continued investment in monitoring of water levels, and
- ◆ auditing model performance and revising the model as needed within about 10 yr.

The model's side boundaries were set as “no-flow” boundaries, which ended up exaggerating simulated drawdown because the area of influence could not expand farther and draw water from a larger area. On the other hand, the downdip boundary was set as a “constant-head” boundary to represent a likely vertical gradient in hydraulic head. This constant-head boundary ended up in an underestimation of simulated drawdown because no matter how much water was withdrawn, head at the downdip side of the model remained constant. These issues arose because the area influenced by

pumping was larger than expected and drawdown intersected the lateral and downdip boundaries. Additional model adjustment is needed to select and incorporate alternate lateral boundary conditions and evaluate the effect of these alternates on simulation results.

The approach to calibrating model parameters involved (1) accepting mapped values of horizontal hydraulic conductivity as “known,” (2) spreading out values of specific storage and storativity between an assumed unconfined value in the outcrop and confined values that varied with depth of aquifer burial in the subsurface, and (3) inversely varying vertical hydraulic conductivity and recharge to minimize calibration error and match previous estimates of recharge rate. Because model results appeared more sensitive to vertical hydraulic conductivity and recharge than to specific storage, the latter was not adjusted to improve calibration error. Additional minor changes in specific storage distribution are needed, along with an analysis of the effect of these changes on simulation results.

Interaction of surface water and groundwater was simulated for segments of the Brazos and Colorado Rivers. The model predicts that segments will change from gaining to losing because of drawdown in groundwater levels. The amount of simulated flow loss, however, seems unreasonably high, probably owing to the value of riverbed conductance used in the model. Accurate calibration of the riverbed conductance term was beyond the scope of the original study. Additional work is needed to reexamine hydrologic properties that are used for governing river–aquifer interaction in the model before the significance of the simulated amount of surface-water loss can be evaluated.

Recharge rates were assigned in conjunction with calibrating vertical hydraulic conductivity. Recharge rates were consistent with those of previous models but were held constant rather than having them vary with time and drawdown. It is possible that recharge rate might increase as the water table is lowered in response to pumping.

For example, evapotranspiration (ET) removes water when the water table is within a certain range of ground surface but becomes ineffective when the water table falls. Additional work is needed to further evaluate how recharge rates might be assigned along with evapotranspiration in the model and to assess how incorporating evapotranspiration might change simulation results.

Assessing possible changes in water quality was beyond the scope of this study. Current information indicates that water quality in the Carrizo–Wilcox aquifer will not limit future development. Some naturally occurring, poorer quality water exists, however, in the Calvert Bluff (Henry and others 1979; Dutton, 1985), and some cross-formational flow occurs and would be increased as a result of groundwater withdrawal. A potential therefore exists for some gradual change in water quality to occur in the Simsboro owing to current and future pumpage. Whereas present information indicates that the water-quality change would be small and have negligible consequences, additional work could be conducted to quantify possible changes.

Hydraulic-head data are critical in calibrating a model. As more groundwater is withdrawn from Texas aquifers, the rate of change of water level is expected to increase. A greater investment in monitoring of water levels in observation wells will be needed not only to maintain, but also to improve, the adequacy of hydraulic-head data for model calibration.

This model was calibrated by using hydraulic-head data from a period of about 35 yr, but the projected simulation period extends more than 50 yr. Given the uncertainty in locations and rates of pumping, aquifer parameters, and model calibration, periodic “postaudits” of the groundwater model should be made. A postaudit, key to determining the accuracy with which a given groundwater model is predicting the future (Anderson and Woessner, 1992), can help improve continued assessment of groundwater availability.

SUMMARY AND CONCLUSIONS

Groundwater pumpage from the Carrizo–Wilcox aquifer, one of Texas' major aquifer systems, increased in the area between the Colorado and Brazos Rivers from approximately 10,600 to more than 37,900 acre-ft/yr during the second half of the 20th century. Continued and possibly accelerated growth in demand for groundwater is expected in the first half of the 21st century. To assess the availability of groundwater from the Carrizo–Wilcox aquifer to meet future demand, five 2000 through 2050 groundwater-development scenarios were simulated by means of a computer model developed for this study (table 1). Simulation of the historical period (1951 through 1999) included as much as 30,000 acre-ft/yr of water currently withdrawn for aquifer-pressure reduction at the Sandow Mine in Lee and Milam Counties. A model calibration (mean absolute) error of 32 ft was estimated by means of historical water-level data. Additional prediction errors will result from differences in the locations and rates of withdrawal between the simulated cases and what eventually occurs.

The five scenarios are

- (1) Projected groundwater withdrawal, with increases of 10,977 acre-ft/yr relative to the estimated 1996 rate, in accordance with pumpage projections in the TWDB (1997) State Water Plan. This scenario assumes that the 30,000 acre-ft/yr of Simsboro water currently being produced for aquifer-pressure reduction at the Sandow Mine in Milam County will continue through 2050.
- (2) Projected 2000 through 2050 pumpage, as in scenario 1, plus an incremental increase of 70,000 acre-ft/yr in groundwater production from the Simsboro, representing full development of contracts between ALCOA, SAWS, and CPS. The maximum rate was assumed to begin in 2000 and to be held constant through 2050.
- (3) Scenario 2 plus additional pumpage: (a) 7,000 acre-ft/yr from near Lake Bastrop to meet demand for additional water related to steam-electric power generation; (b) as much as 930 to 6,845 acre-ft/yr, increasing during the 2000 through 2050 period, throughout Bastrop County for "county-other" uses; and (c) 25,000 acre-ft/yr to help meet Williamson County water demand as described in the Trans-Texas Water Program (HDR Engineering, 1998).
- (4) Projected 2000 through 2050 pumpage, as in scenario 2, plus additional pumpage: (a) 7,000 acre-ft/yr from near Lake Bastrop to meet demand for additional water related to steam-electric power generation; (b) 930 to 6,845 acre-ft/yr, increasing during the 2000 through 2050 period, throughout Bastrop County for "county-other" uses; and (c) 100,000 acre-ft/yr split between the Simsboro and Carrizo Formations to help meet potential water demand.
- (5) Projected 2000 through 2050 pumpage, as in scenario 3, plus 100,000 acre-ft/yr split between the Simsboro and Carrizo Formations to help meet potential water demand. This scenario includes the greatest amount of simulated withdrawal considered in the study.

The incremental withdrawal of 70,000 acre-ft/yr under contract between ALCOA, SAWS, and CPS (scenario 2) is estimated to result in an average of about 40 ft of additional drawdown in hydraulic head in the Simsboro Formation by 2050 and as much as about 260 ft of additional drawdown near the main water-withdrawal areas. Maximum drawdown resulting from a well field can be reduced by spreading out the wells, but to do so increases the area that is affected. The incremental effect of all pumping areas simulated in this study (scenario 5) is an average drawdown of approximately 120 ft and a maximum water-level decline of approximately 350 ft by the year 2050, in addition to the drawdown associated with the water demand projected by the TWDB (1997) State Water Plan. The incremental effects of scenarios 3 and 4 fall between the results of scenarios 2 and 5.

On the basis of the calibrated model, groundwater in the Carrizo–Wilcox aquifer in the study area is predicted to remain available to meet the specified withdrawal scenarios through the year 2050 and additional demands after 2050. Except near the centers of simulated pumping areas, the aquifer units are forecast to remain fully saturated, and simulated water-level decline mainly reflects a change in artesian or pressure head. Simulated rate of decline of hydraulic head, however, is constant through the year 2050, and continued drawdown should be expected as long as pumping remains well above historic rates. Availability of groundwater is also determined by pumping lift, drilling depth, transportation to point of use, property access, and other criteria not considered in this regional study.

The simulated water budget for the Simsboro and Carrizo Formations estimates a recharge rate of approximately 61,200 acre-ft/yr, which is greater than the total groundwater withdrawal in the study area as of 1996. Of this amount, about 86 percent apparently flows downdip to the confined part of the aquifer, the rest of which is discharged to wells and rivers in the outcropping, unconfined part of the aquifer. Drawdown of water levels in the confined part of the aquifer can induce more cross-

formational leakage of water and less discharge of groundwater to rivers. Additionally, the relationship between groundwater and surface water may change; model results predict that Colorado and Brazos Rivers may begin to lose water to the aquifer by the year 2050. Discharge from the water table in the outcrop by evapotranspiration, however, was not taken into account in the model. Additional study is needed to evaluate the effect of groundwater withdrawal on surface-water resources.

Actual effects of groundwater withdrawal will depend on the locations and rates of pumping, which must be determined from detailed site considerations beyond the scope of this study. It should be noted that, as required by law, the surface-mining authorization granted by the Railroad Commission of Texas (RRC) for operation of the Sandow Mine in Lee and Milam Counties requires the mining company to mitigate effects to public and domestic water-supply wells caused by pumpage associated with the mining operations. Also, ALCOA and SAWS agreed in their water-supply contract to mitigate effects to public and private water-supply wells, including stock and irrigation wells, related to pumpage even from wells not covered under the surface-mining authorization.

ACKNOWLEDGMENTS

The work described in this report, performed during a 12-week period between January and April 1999, was sponsored by the Texas Water Development Board (TWDB). SAWS, ALCOA, and Aqua Water Supply Corporation (Aqua) also contributed funds to the study. In order to share the knowledge and expertise of individuals who have worked on the hydrogeology of the Carrizo–Wilcox aquifer, the TWDB set up an Advisory Group and Technical Oversight Subgroup. The Advisory Group comprised Mr. Dick Burns and Mr. James Kowis, representing ALCOA; Ms. Susan Butler, representing SAWS; Mr. John Burke, representing Aqua and Regional Planning Group K; Dr. Jobaid Kabir, representing Lower Colorado River Authority

(LCRA); Ms. Cindy Loeffler, representing Texas Parks and Wildlife Department (TPWD); Mr. Denis Qualls, representing the Brazos River Authority and Regional Planning Group G; Mr. Mike Mahoney, representing Regional Planning Group I; Mr. Larry Land, consulting for the Regional Planning Group G and SAWS; Mr. Ridge Kaiser and Mr. Bob Harden, consulting for ALCOA; Dr. Robert S. Kier, consulting for Aqua; Mr. William F. Mullican III (Director, TWDB Water Resources Planning); and Mr. Jorge Arroyo (Project Manager) and Mr. Harald Petrini (Contract Manager) for the TWDB. The Advisory Group, in coordination with the TWDB, developed the withdrawal scenarios for model simulation of the period from 2000 through 2050 and provided

review comments on the draft version of this report.

The Technical Oversight Subgroup included Mr. Ridge Kaiser and Mr. Bob Harden of R. W. Harden and Associates, Dr. Robert S. Kier of Robert S. Kier Consulting, Mr. Larry Land of HDR Engineering, Dr. Jobaid Kabir, Mr. William F. Mullican III, Mr. Harald Petrini, and Mr. Jorge Arroyo. These individuals helped this study by taking part in discussions on the modeling of hydrogeology of the Carrizo–Wilcox aquifer and by providing data.

In addition to the Advisory Group members, the following provided review comments on the report draft: Ms. Ann Mesrobian, representing the Bastrop County Environmental Network; Mr. Travis Brown, representing Neighbors For Neighbors; and Mr. George Rice, a private citizen. All comments provided by the TWDB, including those of the Advisory Group and the public, that were within the scope of work were addressed within the body of this report.

Dr. Bridget Scanlon and Ms. Rebecca Smyth at the Bureau of Economic Geology assisted with

numerical simulations. Ms. Robin Nava, Mr. Greg Jeffers, Mr. Tom Tremblay, Mr. Jeff Beckage, and Ms. Susan Palachek assisted in GIS mapping and data reduction. Dr. Robert Mace made data on hydrologic properties available, which were being compiled as part of a study of the Carrizo–Wilcox aquifer separately sponsored by the TWDB, and helped review the modeling. Dr. Robert Mace and Dr. Bridget Scanlon also reviewed a draft of this report. Report illustrations were prepared by Ms. Jamie H. Coggin, Ms. Kerza A. Prewitt, and Mr. David M. Stephens, under the direction of Mr. Joel L. Lardon, Graphics Manager. Ms. Coggin also designed the cover and layout. Word processing was done by Ms. Susan Lloyd, and Ms. Lana Dieterich edited the report.

The views and conclusions contained in this document are those of the author and should not be interpreted as necessarily representing the official policies, either expressed or implied, of TWDB, SAWS, ALCOA, or Aqua Water Supply Corporation.

REFERENCES

- Anderson, M. P., and Woessner, W. W., 1992, Applied groundwater modeling, simulation of flow and advective transport: New York, Academic Press, 381 p.
- Ayers, W. B., Jr., and Lewis, A. H., 1985, The Wilcox Group and Carrizo Sand (Paleogene) in East-Central Texas: depositional systems and deep-basin lignite: The University of Texas at Austin, Bureau of Economic Geology, 19 p. + 30 pl.
- Cronin, J. G., and Wilson, C. A., 1967, Ground water in the flood-plain alluvium of the Brazos River, Whitney Dam to vicinity of Richmond, Texas: Texas Water Development Board, Report 41, 206 p.
- Dutton, A. R., 1985, Brackish water in unsaturated confining beds at a Texas lignite mine: *Ground Water*, v. 23, no. 1, p. 42–51.
- _____ 1990, Vadose-zone recharge and weathering in an Eocene sand deposit, East Texas, U.S.A.: *Journal of Hydrology*, v. 114, p. 93–108.
- Fisher, R. S., Mace, R. E., and Boghici, Erika, 1996, Ground-water and surface-water hydrology of Camp Swift, Bastrop County, Texas: The University of Texas at Austin, Bureau of Economic Geology, final report prepared for the Adjutant General's Department of Texas, Texas Army National Guard and the Nature Conservancy of Texas under contract no. Texas THCB-95-1-05-01, 48 p. + 4 apps.
- Fogg, G. E., Seni, S. J., and Kreidler, C. W., 1983, Three-dimensional ground-water modeling in depositional systems, Wilcox Group, Oakwood salt dome area, East Texas: The University of Texas at Austin, Bureau of Economic Geology Report of Investigations No. 133, 55 p.
- Follett, C. R., 1970, Ground-water resources of Bastrop County, Texas: Texas Water Development Board, Report 109, 138 p.
- _____ 1974, Ground-water resources of Brazos and Burleson Counties, Texas: Texas Water Development Board, Report 185, 194 p.
- Gaylord, J. L., Slade, R. M., Jr., Ruiz, L. M., Welborn, C. T., and Baker, E. T., Jr., 1985, Water-resources appraisal of the Camp Swift lignite area, Central Texas: U.S. Geological Survey, Water-Resources Investigations Report 84-4333, 164 p.

- Guiguer, N., and Franz, T., 1998, User's manual for Visual MODFLOW: Waterloo, Ontario, Waterloo Hydrogeologic, 315 p.
- Guyton, W. E., 1942, Results of pump tests in wells at Camp Swift, Texas: U.S. Geological Survey, Open-File Report, 27 p.
- HDR Engineering, 1998, Trans-Texas Water Program, North Central Study Area, Phase II report, volume 1, integrated water supply plans: variously paginated.
- Henry, C. D., and Basciano, J. M., 1979, Environmental geology of the Wilcox Group lignite belt, East Texas: The University of Texas at Austin, Bureau of Economic Geology Report of Investigations No. 98, 28 p.
- Henry, C. D., Basciano, J. M., and Duex, T. W., 1979, Hydrology and water quality of the Eocene Wilcox Group: significance for the lignite development in East Texas: Gulf Coast Association of Geological Societies Transactions, v. 29, p. 127–135.
- Hsieh, P. A., and Freckleton, J. R., 1993, Documentation of a computer program to simulate horizontal-flow barriers using the U.S. Geological Survey's modular three-dimensional finite-difference ground-water flow model: U.S. Geological Survey Open-File Report 92-477, 32 p.
- International Association of Hydrogeologists, 1985, Hydrogeology of rocks of low permeability: Tucson, Arizona, Memoirs of the 17th International Congress of the International Association of Hydrogeologists (January 7–11), no. 17, pts. 1–2.
- Kier, R. S., and Larkin, R. G., 1998, Hydrogeology of the Carrizo–Wilcox aquifer system—Bastrop, Caldwell, Fayette, Lee, Travis, and Williamson Counties: Robert S. Kier Consulting, preliminary report prepared for the Aqua Water Supply Company, Bastrop, Texas, variously paginated.
- Konikow, L. F., 1986, Predictive accuracy of a ground-water model—lessons from a postaudit: *Ground Water*, v. 24, no. 2, p. 173–184.
- Kreitler, C. W., and Senger, R. K., 1991, Appendix 1, comparison of wellhead protection areas, two examples, *in* Wellhead protection strategies for confined-aquifer settings: The University of Texas at Austin, Bureau of Economic Geology, prepared for U.S. Environmental Protection Agency, Office of Ground Water and Drinking Water, Ground-Water Protection Division, under cooperative agreement no. CX-815385-01-0, contract report no. EPA 57019-91-008, p. 111–130.
- McDonald, M. G., and Harbaugh, A. W., 1988, A modular three-dimensional finite-difference ground-water flow model: U.S. Geological Survey, Techniques of Water-Resources Investigations, book 6, chapter A1, variously paginated.
- Proctor, C. V., Jr., Brown, T. E., McGowen, J. H., and Waechter, N. B., 1974, Austin sheet: The University of Texas at Austin, Bureau of Economic Geology, Geologic Atlas of Texas, scale 1:250,000.
- Rogers, L. T., 1967, Availability and quality of ground water in Fayette County, Texas: Texas Water Development Board Report 56, 134 p.
- Ryder, P. D., 1988, Hydrogeology and predevelopment flow in the Texas Gulf Coast aquifer systems: U.S. Geological Survey, Water-Resources Investigations Report 87-4248, 109 p.
- Ryder, P. D., and Ardis, A. F., 1991, Hydrology of the Texas Gulf Coast aquifer systems: U.S. Geological Survey Open-File Report 91-64, 147 p.
- Texas Water Development Board (TWDB), 1997, Water for Texas—a consensus-based update to the State Water Plan: Austin, Texas, v. 2, variously paginated.
- Thorkildsen, D., and Price, R. D., 1991, Ground-water resources of the Carrizo–Wilcox aquifer in the Central Texas region: Texas Water Development Board, Report LP-208, 46 p.
- Thorkildsen, D., Quincy, R., and Preston, R., 1989, A digital model of the Carrizo–Wilcox aquifer within the Colorado River Basin of Texas: Texas Water Development Board, Report 332, 59 p.

APPENDIX A

Observation wells used for model calibration. Data source TWDB Internet site.

Map no.	Well ID	Formation*	Easting (UTM zone 15)	Northing (UTM zone 15)	Well depth (ft)	County
1	5846102	HOOP	81228.225	3367785.554	76	BASTROP
2	5846301	SMBR	87865.319	3367038.574	63	BASTROP
3	5846503	SMBR	85074.664	3361958.431	51	BASTROP
4	5854507	SMBR	85135.365	3347324.428	672	BASTROP
5	5854706	HOOP	80111.345	3344985.447	440	BASTROP
6	5854707	SMBR	81438.947	3344625.745	277	BASTROP
7	5854801	SMBR	82725.878	3341798.562	360	BASTROP
8	5855103	CABF	94408.508	3353705.906	618	BASTROP
9	5861201	CABF	74025.119	3338859.805	14	BASTROP
10	5861801	CABF	71974.234	3328906.921	32	BASTROP
11	5862506	CABF	83797.201	3334658.267	290	BASTROP
12	5863103	CRRZ	94245.371	3337693.459	120	BASTROP
13	5863606	CRRZ	99018.352	3330975.668	868	BASTROP
14	6707204	CRRZ	96577.043	3325170.866	765	BASTROP
15	5920559	CRRZ	158301.134	3398183.965	900	BRAZOS
16	5925502	CZCB	122224.484	3387728.181	614	BURLESON
17	5927706	CRRZ	141003.205	3384002.229	900	BURLESON
18	5927810	CZCB	145902.975	3383594.039	1,290	BURLESON
19	5934303	WLCX	138150.316	3376939.964	806	BURLESON
20	6716404	CRRZ	102927.949	3304450.206	2,000	FAYETTE
21	5839706	HOOP	92038.947	3369843.578	326	LEE
22	5839905	CABF	99748.950	3369217.930	248	LEE
23	5840509	CABF	108223.415	3374217.130	680	LEE
24	5840808	CZWX	108496.887	3369947.944	578	LEE
25	5925711	CABF	116937.432	3381711.627	734	LEE
26	5949509	CRRZ	120438.283	3345643.369	2,018	LEE
27	5949512	CRRZ	122112.254	3345215.653	2,020	LEE
28	5949604	CRRZ	124268.828	3343999.750	2,160	LEE
29	5824610	HOOP	116274.388	3399848.804	392	MILAM
30	5832101	HOOP	108062.290	3394836.880	60	MILAM
31	5832302	SMBR	113608.501	3393186.670	224	MILAM
32	5832501	SMBR	109595.891	3387806.579	182	MILAM
33	5902307	WLCX	137837.443	3431647.022	450	MILAM
34	5902309	SMBR	141110.316	3434097.005	417	MILAM
35	5902706	WLCX	131717.679	3424607.738	315	MILAM
36	5902901	WLCX	137796.097	3422640.051	318	MILAM
37	5909901	SMBR	127151.579	3411961.721	169	MILAM
38	5911402	CABF	142630.763	3412852.778	323	MILAM
39	5911621	CRRZ	150422.607	3415772.233	297	MILAM
40	5911703	SMBR	144271.824	3411748.624	992	MILAM
41	5911706	CABF	144164.316	3408513.926	450	MILAM
42	5917103	HOOP	118558.590	3405568.349	410	MILAM
43	5919103	CABF	143726.059	3406553.991	522	MILAM
44	5925508	CABF	121310.73	3388315.59	490	MILAM
45	5903437	SMBR	142466.553	3428590.493	460	ROBERTSON

* CABF=Calvert Bluff, CRRZ=Carrizo, CZCB=Carrizo and Calvert Bluff, CZWX=Carrizo and Wilcox, HOOP=Hooper, SMBR=Simsboro, WLCX=Wilcox

APPENDIX B

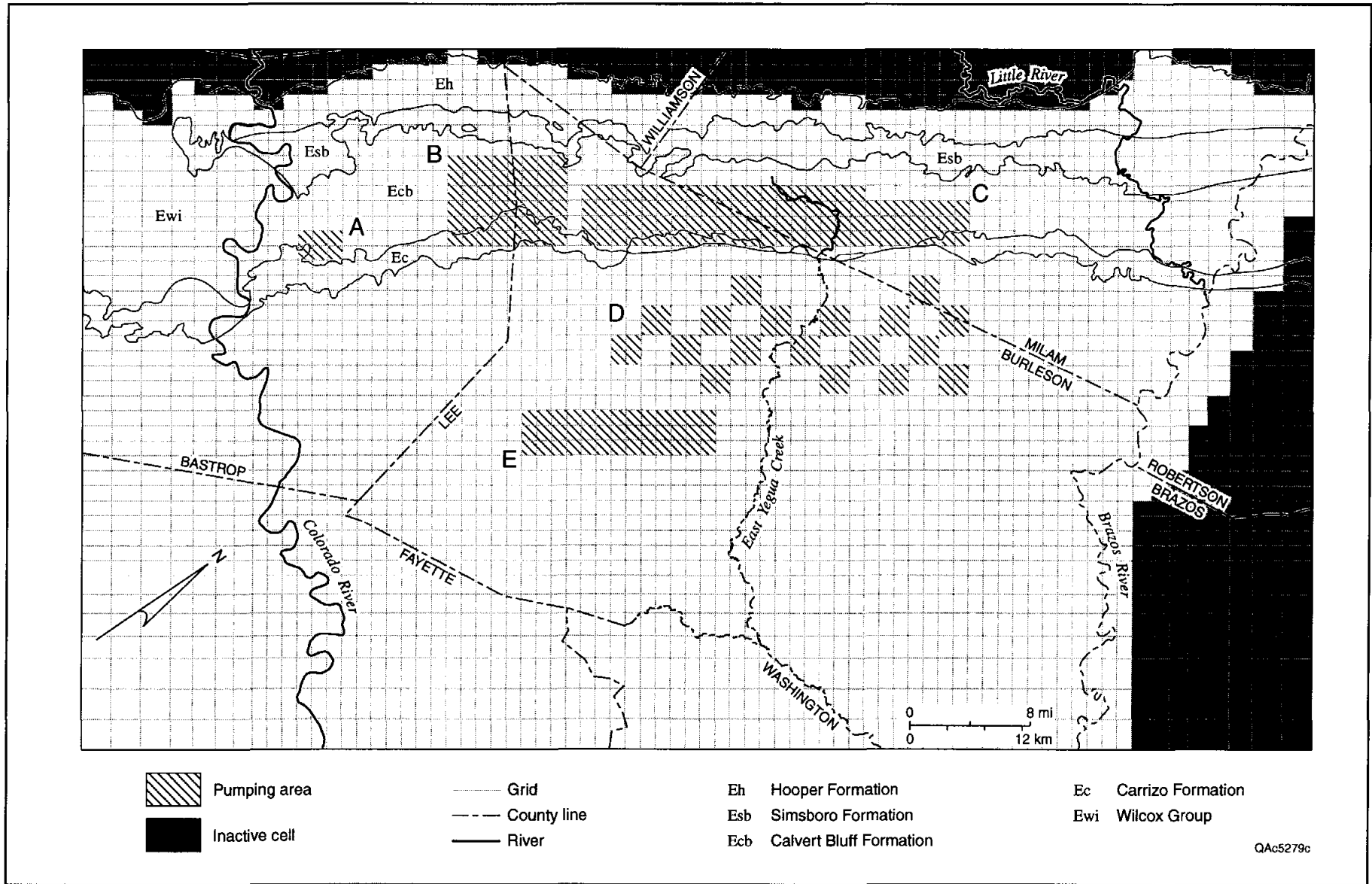


FIGURE B1. Location of pumping areas used in scenarios modeled in this study. Areas A through E explained in table 1.

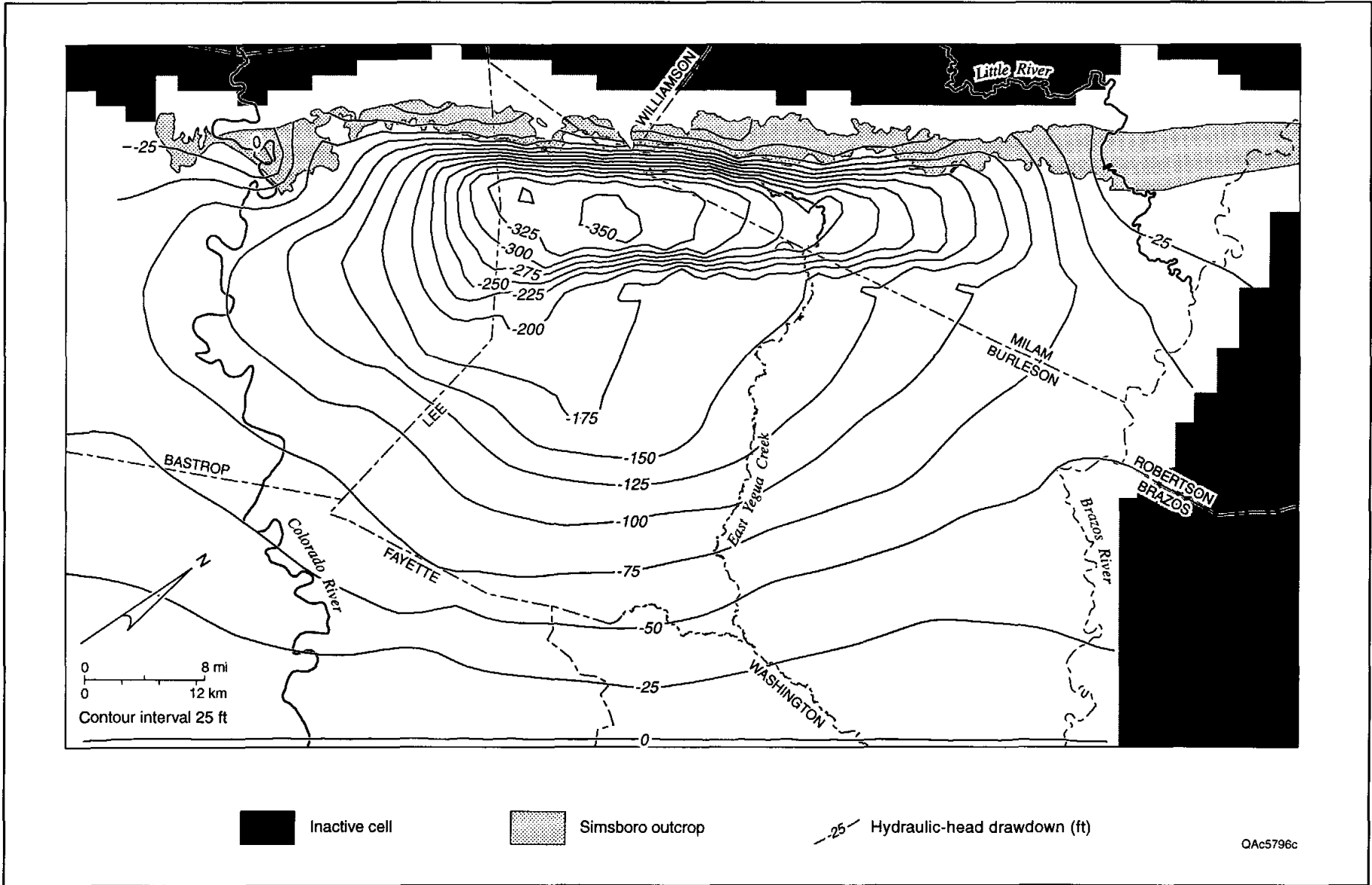


FIGURE B2. Projected 1996 through 2050 drawdown in the Simsboro for scenario 3, including cumulative effects of pumping areas A, B, C, E, and F (table 1, fig. B1) superposed on the pumping rates of the TWDB (1997) State Water Plan.

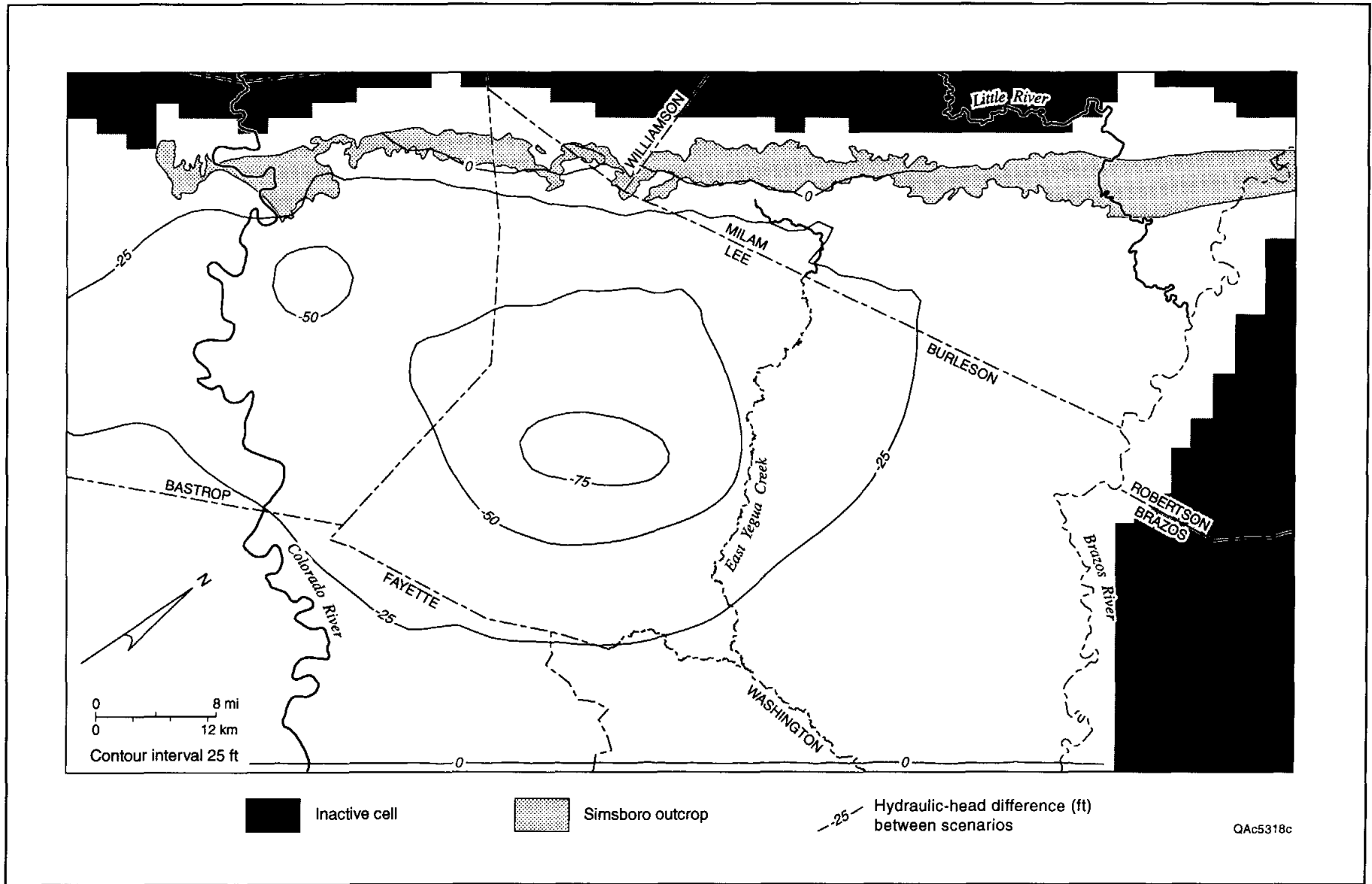


FIGURE B3. Difference between scenarios 3 and 2 in simulated hydraulic head for the Simsboro Formation in the year 2050, showing the combined incremental effects of pumping areas A, E, and F (table 1, fig. B1).

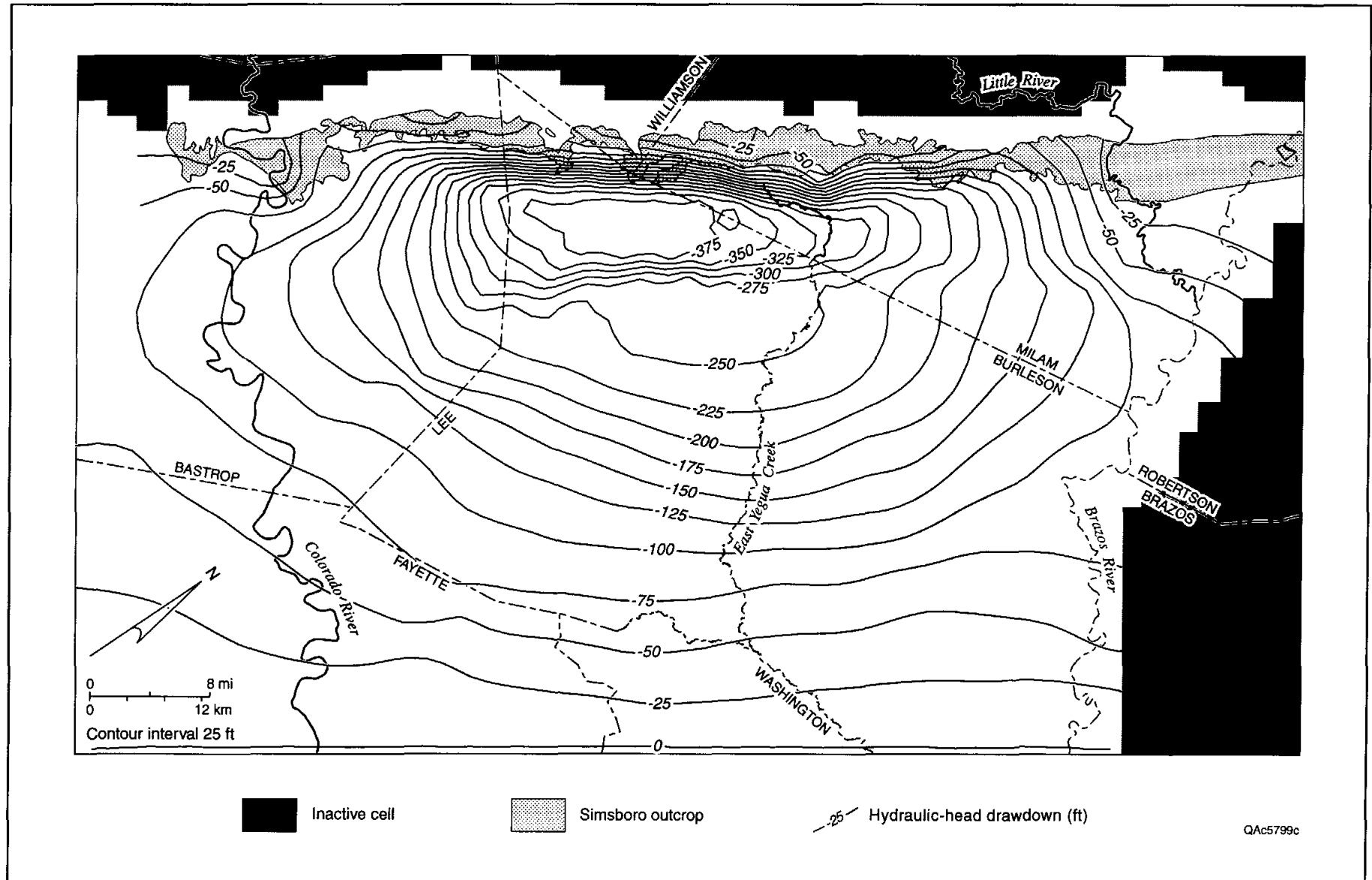


Figure B4. Projected 1996 through 2050 drawdown in the Simsboro for scenario 4, including cumulative effects of pumping areas A, B, C, D, and F (table 1, fig. B1) superposed on the pumping rates of the TWDB (1997) State Water Plan.

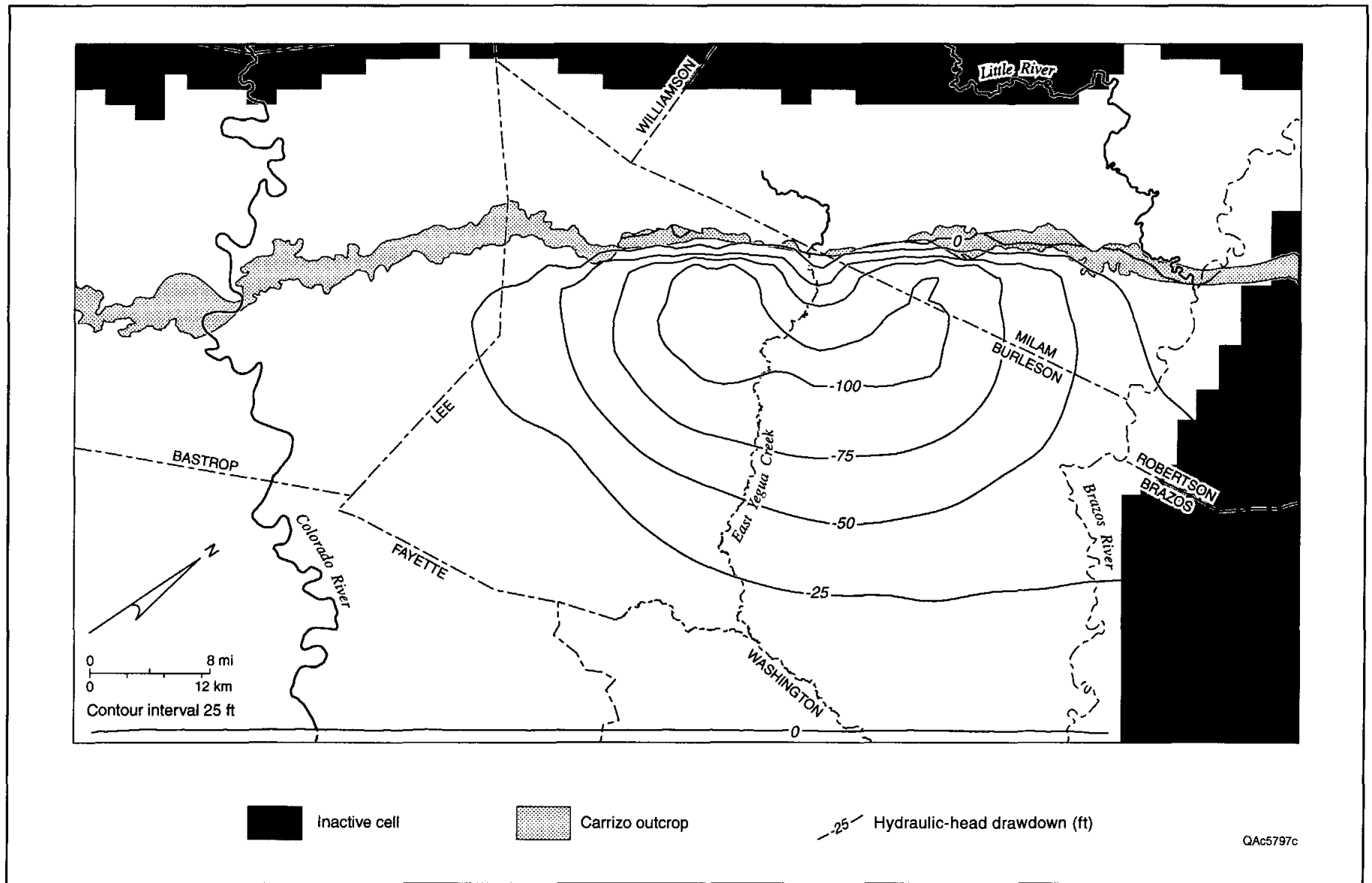


Figure B5. Projected 1996 through 2050 drawdown in the Carrizo for scenario 4, including cumulative effects of pumping areas A, B, C, D, and F (table 1, fig. B1) superposed on the pumping rates of the TWDB (1997) State Water Plan.

Technical Report

**Transmissivity, Hydraulic Conductivity,
and Storativity of the Carrizo-Wilcox Aquifer
in Texas**

by
**Robert E. Mace
Rebecca C. Smyth
Liyang Xu
Jinhua Liang**

RECEIVED

MAR 31 2000

**TWDB R&PF
GRANTS MANAGEMENT**

**Robert E. Mace
Principal Investigator**

prepared for
**Texas Water Development Board
under TWDB Contract No. 99-483-279, Part 1**

**Bureau of Economic Geology
Scott W. Tinker, Director
The University of Texas at Austin
Austin, Texas 78713-8924**

March 2000

Contents

Abstract	1
Introduction	2
Study Area	5
HYDROGEOLOGY	5
Methods	13
LITERATURE REVIEW	14
DATA COMPILATION	14
EVALUATION OF HYDRAULIC PROPERTIES IN DATABASE	19
Estimating Transmissivity from Specific Capacity Data	19
STATISTICAL DESCRIPTION	24
Results and Discussion	27
GENERAL CHARACTERISTICS OF THE DATABASE	27
TRANSMISSIVITY AND HYDRAULIC CONDUCTIVITY VALUES	32
Variations in Values from Different Sources	36
Variations in Values Due to Different Testing Methods	40
SPATIAL DISTRIBUTION OF TRANSMISSIVITY AND HYDRAULIC CONDUCTIVITY	42
Vertical Variability of Transmissivity and Hydraulic Conductivity	43
Lateral Variability of Transmissivity and Hydraulic Conductivity	47
Relationship between Hydraulic Conductivity and Sand Thickness	62
STORATIVITY	63
Conclusions	68
Acknowledgements	69
Acronyms	70
References	70
Appendix A	75

Figures

1. Location of the outcrop and subcrop of the Carrizo-Wilcox aquifer in Texas	6
2. Lower Tertiary stratigraphy in South Texas, Central Texas, and Sabine Uplift, Texas. Modified from Kaiser (1974), Hamlin (1988), and Galloway and others (1994)	8
3. Structural elements that affected Tertiary sedimentation along the Texas Gulf Coast. Modified from Ayers and Lewis (1985)	10
4. Aquifer thickness and percent sand for (a) lower Claiborne-upper Wilcox aquifer and (b) middle Wilcox aquifer. Modified from Hosman and Weiss (1991)	11
5. State well-numbering system for (a) 1° quadrangles in Texas, (b) 7.5-minute quadrangles within 1-minute quadrangles, and (c) 2.5-minute quadrangles within 7.5-minute quadrangles. Modified from Follett, 1970	17
6. Relationship between specific capacity and transmissivity in the Carrizo-Wilcox aquifer	22
7. Comparison of the ratios of estimated transmissivity to measured transmissivity for transmissivity estimated by the analytical and empirical approaches	26
8. Example semivariogram showing the range, sill, and nugget	26
9. Distribution of aquifer-test wells in the Carrizo-Wilcox aquifer from TNRCC well files, (b) TWDB well database, and (c) well log information from the TWDB	28
10. Number of aquifer test wells in each county	29
11. General characteristics of wells and aquifer tests in the database	30
12. Histograms of all estimates of transmissivity and hydraulic conductivity from the Carrizo-Wilcox aquifer	33
13. Cumulative distribution functions of transmissivity and hydraulic conductivity for different data sources	37
14. Cumulative distribution functions of transmissivity and hydraulic conductivity for different test types	41
15. Cumulative distribution functions of transmissivity and hydraulic conductivity for the different geologic units using the data collected from TWDB files	44
16. Cumulative distribution functions of transmissivity and hydraulic conductivity for the northern, central, and southern areas of the aquifer	54
17. Experimental (dots) and theoretical (lines) semivariograms of transmissivity and hydraulic conductivity in the Carrizo Formation and Wilcox Group	55
18. Spatial distribution of transmissivity in the Carrizo Formation using kriging values from the TWDB database. Location of control points shown in upper left-hand corner	58

19. Spatial distribution of hydraulic conductivity in the Carrizo Formation using kriging values from the TWDB database. Location of control points shown in upper left-hand corner	59
20. Spatial distribution of transmissivity in the Wilcox Group using kriging values from the TWDB database. Location of control points shown in upper left-hand corner	60
21. Spatial distribution of hydraulic conductivity in the Wilcox Group using kriging values from the TWDB database. Location of control points shown in upper left-hand corner	61
22. Histograms of storativity and specific storage for the Carrizo-Wilcox aquifer	65
23. Variation of storativity and specific storage with depth	67

Tables

1. Thickness of Carrizo (E_c) and Wilcox (E_w) stratigraphic units in four structural settings	12
2. Characteristics of wells and tests in the database	31
3. Transmissivity values (ft^2d^{-1}) estimated from the tests	34
4. Hydraulic conductivity values ($ft d^{-1}$) estimated from the tests	35
5. Transmissivity and hydraulic conductivity values compiled from lignite mine permit reports on file at the TRRC	38
6. Hydraulic conductivity values ($ft d^{-1}$) reported by Prudic (1991)	48
7. Transmissivity values (ft^2d^{-1}) from the TWDB database for the different counties in the study area	49
8. Hydraulic conductivity values ($ft d^{-1}$) from the TWDB database for the different counties in the study area	51
9. General areal distribution of transmissivity and hydraulic conductivity values	53
10. Fitting parameters for the theoretical semivariograms	56
11. Storativity and specific storage (ft^{-1}) values for the Carrizo-Wilcox aquifer	66

Abstract

Transmissivity, hydraulic conductivity, and storativity are important parameters for developing local and regional water plans and developing numerical ground-water flow models to predict the future availability of the water resource. To support this effort, we compiled and analyzed transmissivity, hydraulic conductivity, and storativity values from numerous sources for the entire Carrizo-Wilcox aquifer in Texas, resulting in a database of 7,402 estimates of hydraulic properties in 4,456 wells. Transmissivity and hydraulic conductivity results for all tests in the Carrizo-Wilcox aquifer are log-normally distributed. Transmissivity ranges from about 0.1 to 10,000 ft^2d^{-1} and has a geometric mean value of about 300 ft^2d^{-1} , and hydraulic conductivity ranges from about 0.01 to 4,000 ft d^{-1} and has a geometric mean value of about 6 ft d^{-1} . Transmissivity and hydraulic conductivity vary spatially, both vertically and areally, in the Carrizo-Wilcox aquifer. The Simsboro Formation and Carrizo Sand portions of the Carrizo-Wilcox aquifer have transmissivity and hydraulic-conductivity values that are 2.5 to 11 times higher and 2 to 6 times higher, respectively, than that of the Cypress aquifer, Calvert Bluff Formation, and undivided Wilcox Group.

Semivariograms show that transmissivity and hydraulic conductivity values in the Carrizo Sand and undivided Wilcox Group are spatially correlated over about 17 and 25 mi, respectively. Large nuggets in the semivariograms suggest local-scale heterogeneity and measurement errors. Kriged maps of transmissivity and hydraulic conductivity show the greatest values for the Carrizo Sand in the Winter Garden area and the greatest values for the Wilcox Group in the south-central and northeast parts of the aquifer. Storativity and specific storage values approximate log-normal distributions. Storativity ranges from about 10^{-6} to 10^{-1} with a geometric mean of 3.0×10^{-4} . Specific storage ranges from about 10^{-7} to 10^{-3} with a geometric mean of 4.5×10^{-6} . Lower values of storativity and specific storage tend to occur at shallow depths where the aquifer is unconfined.

Introduction

The purpose of this report is to present a database and analysis of a compilation of transmissivity, hydraulic conductivity, and storativity data in the Carrizo-Wilcox aquifer of Texas. These data are needed to address a host of regional ground-water management issues as part of long-term regional water plans involving aquifers. State-mandated programs call for the development of regional water plans that address near- and long-term water needs that consider surface- and ground-water interaction. Those responsible for developing regional water plans require permeability and storativity data to make accurate predictions of ground-water availability and potential water-level declines.

Transmissivity and hydraulic conductivity describe the general ability of an aquifer to transmit water (over the entire saturated thickness for transmissivity and over a unit thickness for hydraulic conductivity), and are among the most important hydrogeologic data needed for managing ground-water resources. Representative transmissivity and hydraulic conductivity data are required to ensure that the hydrologic assumptions and interpretations used in regional water plans are valid. Storativity describes the change in volume of water for a unit change in water level per unit area. Transmissivity, hydraulic conductivity, and storativity data are needed in tasks such as (1) numerical modeling of ground-water flow, (2) prediction of well performance, (3) evaluation of how site-specific test results compare with the variability of the regional aquifer, (4) assessing the transport of solutes and contaminants, and (5) selection of areas where additional hydrologic tests are needed.

It is important to have a transmissivity, hydraulic conductivity, and storativity database that is readily available for developing local and regional water plans and numerical ground-water flow models to predict future ground-water availability. Aquifer tests are expensive to run, and historical test data, although available, are labor-intensive to compile and evaluate. The

standard reference for aquifer hydraulic properties in Texas is Myers (1969), which includes many high-quality examples of time-drawdown curves and estimates of transmissivity, hydraulic conductivity, and storativity. Although useful, this database is not extensive, does not have good spatial coverage, does not include more recent aquifer tests, and does not take advantage of new techniques for estimating aquifer properties (see for example, Razack and Huntley, 1991; Huntley and others, 1992; Mace, 1997).

Previous investigators measured and compiled transmissivity, hydraulic conductivity, and storativity data for parts of the Carrizo-Wilcox aquifer in Texas, but none compiled this information for the entire aquifer. Myers (1969) included results of 102 aquifer tests for the Carrizo-Wilcox aquifer, but the tests are located in only half of the counties underlain by the aquifer. Kier and Larkin (1998) reviewed available aquifer tests for Bastrop, Caldwell, Fayette, Lee, Travis, and Williamson Counties.

As part of numerical ground-water flow modeling exercises, several authors (Klemt and others, 1976; Thorkildsen and others, 1989; Prudic, 1991; Guyton and Associates, 1998; Dutton, 1999) have compiled hydraulic properties of the Carrizo-Wilcox aquifer. Klemt and others (1976) developed a numerical ground-water flow model of the southwest part of the Carrizo aquifer. They analyzed pumping test and performance test data to estimate hydraulic conductivity of the aquifer's total thickness (Klemt and others, 1976, their figs. 15, 16). Thorkildsen and others (1989) developed a ground-water flow model for the central part of the aquifer in the vicinity of the Colorado River. They used electrical logs and existing studies to define hydraulic conductivity for the formations of the Carrizo-Wilcox aquifer (Thorkildsen and others, 1989, their figs. 8 through 11 in appendix 5). Prudic (1991), as part of the USGS regional aquifer-system analysis program, estimated hydraulic conductivity for the Gulf Coast regional aquifer system and developed a finite-difference numerical ground-water flow model of the aquifer. His

test results for Texas source from Myers (1969). He also used limited specific-capacity data to estimate transmissivity in the aquifer.

Guyton and Associates (1998) developed a ground-water flow model to investigate the interaction between surface water and ground water in the Winter Garden area in the Guadalupe, San Antonio, Nueces, and Rio Grande River Basins on the basis of the model by Klemt and others (1976). They used the same hydraulic properties as used by Klemt and others (1976) for the Carrizo aquifer, and estimated properties for the Wilcox aquifer from published reports. Dutton (1999) developed a ground-water flow model for the Carrizo-Wilcox aquifer approximately between the Colorado and Brazos Rivers and distributed test results according to the distribution of major-sand thickness in the Calvert Bluff and Simsboro formations. His aquifer test results were taken from permit reports for the Sandow lignite mine, well log interpretation, and preliminary results of this study.

To date, no one has comprehensively compiled aquifer and specific-capacity data for the entire Carrizo-Wilcox aquifer or investigated the spatial continuity of transmissivity and hydraulic conductivity in the aquifer. Therefore, the purpose of this study was to (1) review the literature for the hydraulic properties; (2) compile transmissivity, hydraulic conductivity, storativity, and specific-capacity data from publicly available sources; (3) estimate hydraulic properties from the compiled data; and (4) geostatistically describe the hydraulic properties of the aquifer.

This report is divided into three major sections: (1) study area, (2) methods, and (3) results. The study area section presents the basic hydrogeology of the aquifer in Texas. The methods section discusses the techniques used to review the literature and compile and analyze the hydrologic data. The results section presents results of the literature review and the data compilation and analysis. Some results, as they relate to the methodology, are presented in the methods section.

Study Area

The Carrizo-Wilcox aquifer extends from South Texas northeastward into East Texas, Arkansas, and Louisiana. In Texas the Carrizo-Wilcox aquifer provides water to all or part of 60 counties along a belt that parallels the Gulf Coast between the Rio Grande and the Sabine River (fig. 1). Water-bearing sediments that make up the Carrizo-Wilcox aquifer are utilized in outcrop and, more commonly, in the subsurface. Pumpage is mainly for irrigation, which accounts for 51 percent of production, and municipal, which accounts for 35 percent (Ashworth and Hopkins, 1995). Bryan-College Station, Lufkin-Nacogdoches, and Tyler are the major municipalities that rely on ground water from the Carrizo-Wilcox aquifer. The Winter Garden region of South Texas is a major irrigation area that relies on the aquifer. Nearly half of all fresh water drawn from the aquifer in 1985 was produced from Zavala, Frio, Atascosa, and Dimmit Counties (Ryder, 1996).

Numerous rivers cross the Carrizo-Wilcox outcrop belt flowing southeastward toward the coast, providing mechanisms for surface drainage, ground-water discharge, and less commonly ground-water recharge. Precipitation ranges between 21 to 30 inches/year in the southwest and 30 to 56 inches/year in the central and northeastern parts of the outcrop area (Ryder, 1988).

HYDROGEOLOGY

Between approximately 50 and 60 million yr before present (Ma), sediments of the Wilcox and Clairborne Groups were deposited along the edge of the Gulf of Mexico. At that time the coastline was approximately 100 to 150 mi farther inland than it is today (Galloway and others, 1994). South of the Trinity River and north of the Colorado River the Paleocene-Eocene Wilcox Group is divided into, from oldest to youngest, the (1) Hooper Formation, (2) Simsboro Formation, and (3) Calvert Bluff Formation (Barnes, 1970; 1974). The Wilcox Group is undifferentiated north of the Trinity River and south of the Colorado River because there the

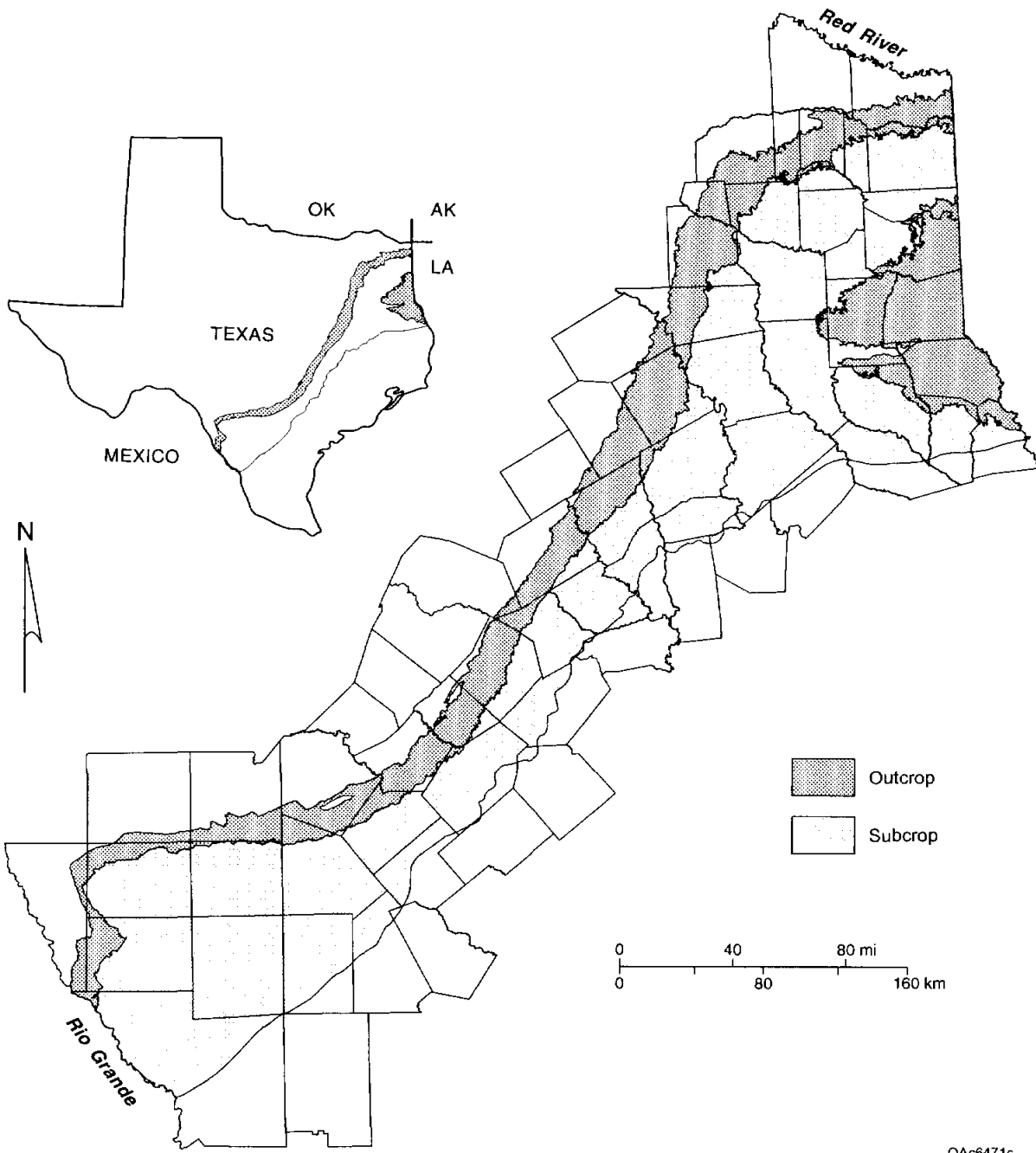


Figure 1. Location of the outcrop and subcrop of the Carrizo-Wilcox aquifer in Texas.

Simsboro Formation is absent as a distinct unit. The oldest unit of the overlying Eocene Clairborne Group is the Carrizo Sand (fig. 2). These geologic units crop out in a northeast-trending band between 150 and 200 mi inland from the Gulf of Mexico, dip south to southeast, and thicken toward the gulf, except near the Sabine Uplift in northeastern Texas. There the units thin or pinch out over the top of the structural dome and dip outward in a radial pattern (Ayers and others, 1985).

Geologic units composing the Carrizo-Wilcox aquifer are (1) the Simsboro and Calvert Bluff Formations of the Wilcox Group and (2) the unconformably overlying Carrizo Sand. Sediments of the Wilcox Group and Carrizo Sand form one of seven temporally distinct episodes of deposition in the Gulf Coast Basin during Paleogene time (65 to 25 Ma) (Galloway and others, 1994). Each of the seven episodes is represented in the rock record by sand, silt, and clay that eroded from the Rocky Mountains to the northwest, and less commonly from the Ouachita Mountains to the north, to feed fluvial-deltaic systems discharging into the Gulf of Mexico.

Marine flooding surfaces that contain shale with localized glauconite or carbonate chemical precipitates separate each of the seven terrigenous sedimentary packages. The marine deposits bound each of the terrigenous units above and below, effectively creating hydraulic barriers (Galloway and others, 1994). Shales of the lower Paleocene Midway Formation and the lower Wilcox Group Hooper Formation form the lower boundary for middle Wilcox terrigenous sediments. Shales of the Eocene Reklaw Formation bound the upper surface of Upper Wilcox-Carrizo terrigenous sediments (fig. 2). Thinner and less extensive marine flooding sequences, present within the middle and upper Wilcox and lower Carrizo sediments, form less complete hydrologic barriers between the laterally connected water-bearing sands of the composite Carrizo-Wilcox aquifer (Galloway and others, 1994).

TERTIARY	Series		South Texas		Central Texas		Sabine Uplift	
	Eocene	U	Jackson Group		Jackson Group		Jackson Group	
		M	Claiborne Group	Yegua Fm.	Yegua Fm.	Yegua Fm.		
				Cook Mountain Fm.	Cook Mountain Fm.	Cook Mountain Fm.		
				Sparta Sand	Sparta Sand	Sparta Sand		
				Weches Fm.	Weches Fm.	Weches Fm.		
				Queen City Sand	Queen City Sand	Queen City Sand		
		L	Wilcox Group	Reklaw Fm.	Reklaw Fm.	Reklaw Fm.		
				Carrizo sand	Carrizo Sand	Carrizo Sand		
	Paleocene	U	Wilcox Group	Upper Wilcox	Calvert Bluff Fm.	Upper Wilcox		
		L		Middle Wilcox	Simsboro Fm.	Middle Wilcox		
				Lower Wilcox	Hooper Fm.	Lower Wilcox		
			Midway Formation	Midway Formation	Midway Formation			

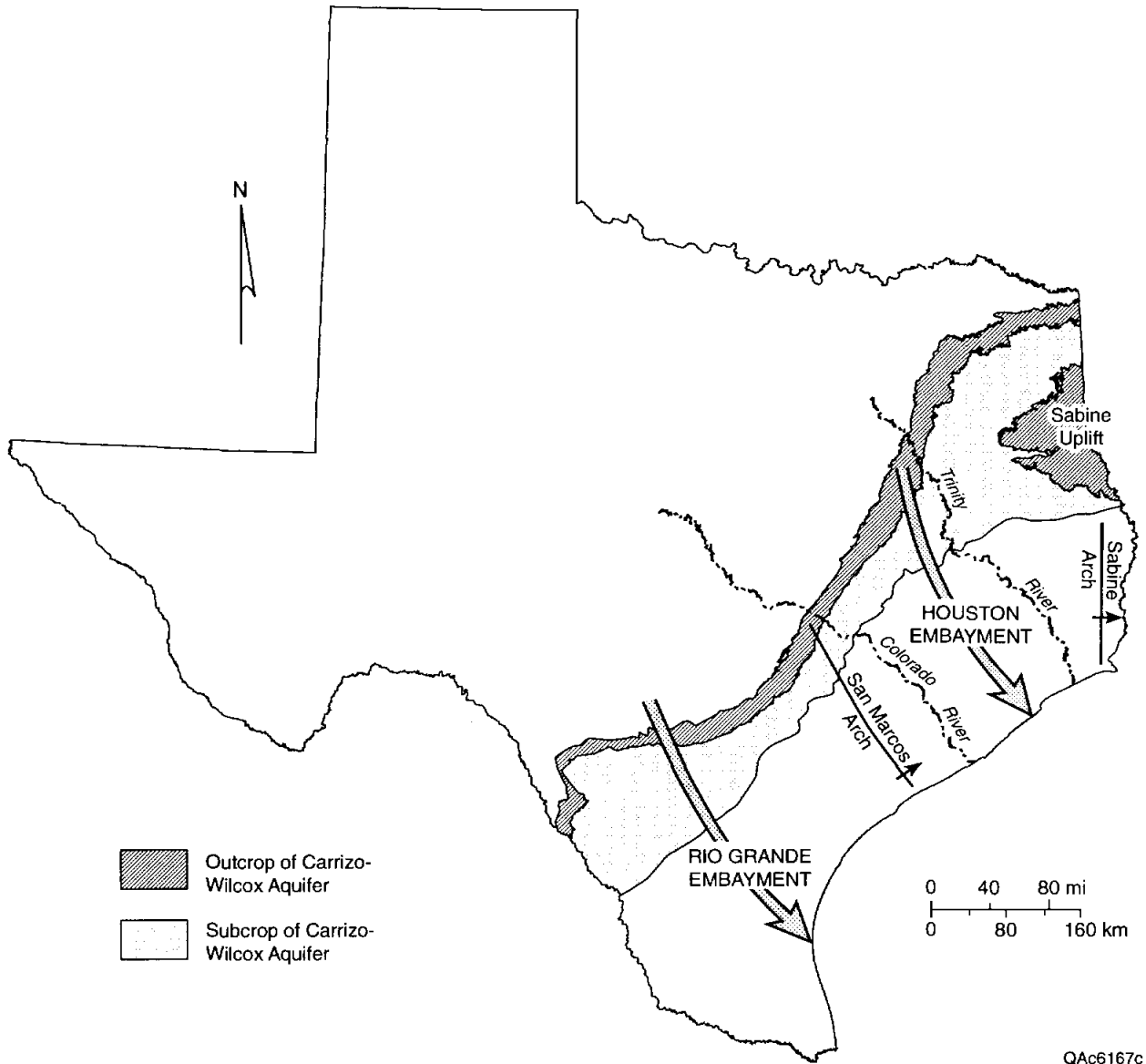
QAc6170c

Figure 2. Lower Tertiary stratigraphy in South Texas, Central Texas, and Sabine Uplift, Texas. Modified from Kaiser (1974), Hamlin (1988), and Galloway and others (1994).

Two foci of sedimentation active intermittently throughout the Paleocene in Texas were the Houston and Rio Grande embayments. The San Marcos Arch separates the embayments. The Sabine Arch lies northeastward of the Houston Embayment or East Texas Basin (fig. 3). The presence of structurally high and low areas along the prograding coastline, and the effects on delta location, allowed the contemporaneous deposition of both streamplain/shorezone and fluvial-deltaic sediments. Mexia-Talco faulting, movement in a compound graben system rooted in Jurassic or Triassic sediments, continued through Eocene time (Jackson, 1982). Faulting also influenced thickness and distribution of Wilcox and Carrizo sediments across the state.

During late Paleocene time, the Houston embayment was the principal drainage axis along which middle Wilcox fluvial-deltaic sediments were deposited. Carrizo Sand and upper Wilcox deposits were primarily focused along the Rio Grande Embayment drainage axis during early Eocene time (Galloway and others, 1994). Because of this shift in regional deposition through time, the older parts of the Carrizo-Wilcox aquifer are thicker between the Colorado and Trinity rivers (including the Simsboro Sand). Younger parts of the Carrizo-Wilcox aquifer are thicker to the south of the Colorado River (fig. 4, table 1).

Paleogene sediments of the Texas Gulf Coast are either (1) heterogeneous accumulations of sand, silt, and clay deposited primarily in lagoonal, delta-plain, delta-front, and shorezone environments or (2) more uniform sands deposited in upper coastal plain channel-fill, crevasse splay, or overbank settings. Middle Wilcox sediments are primarily type 1, have a mean sand content of approximately 55 percent and crop out in a belt 1 to 25 mi wide. The widest point of the outcrop belt and the thickest sediment accumulation is where the fluviially deposited Simsboro Sand Formation is present in the central part of the state (near Lee County). The Simsboro Sand is the only significant fluvial deposit in the Middle Wilcox. Upper Wilcox and Carrizo sediments, primarily type 2, have a mean sand content of 85 percent and crop out in a



QA6167c

Figure 3. Structural elements that affected Tertiary sedimentation along the Texas Gulf Coast. Modified from Ayers and Lewis (1985).

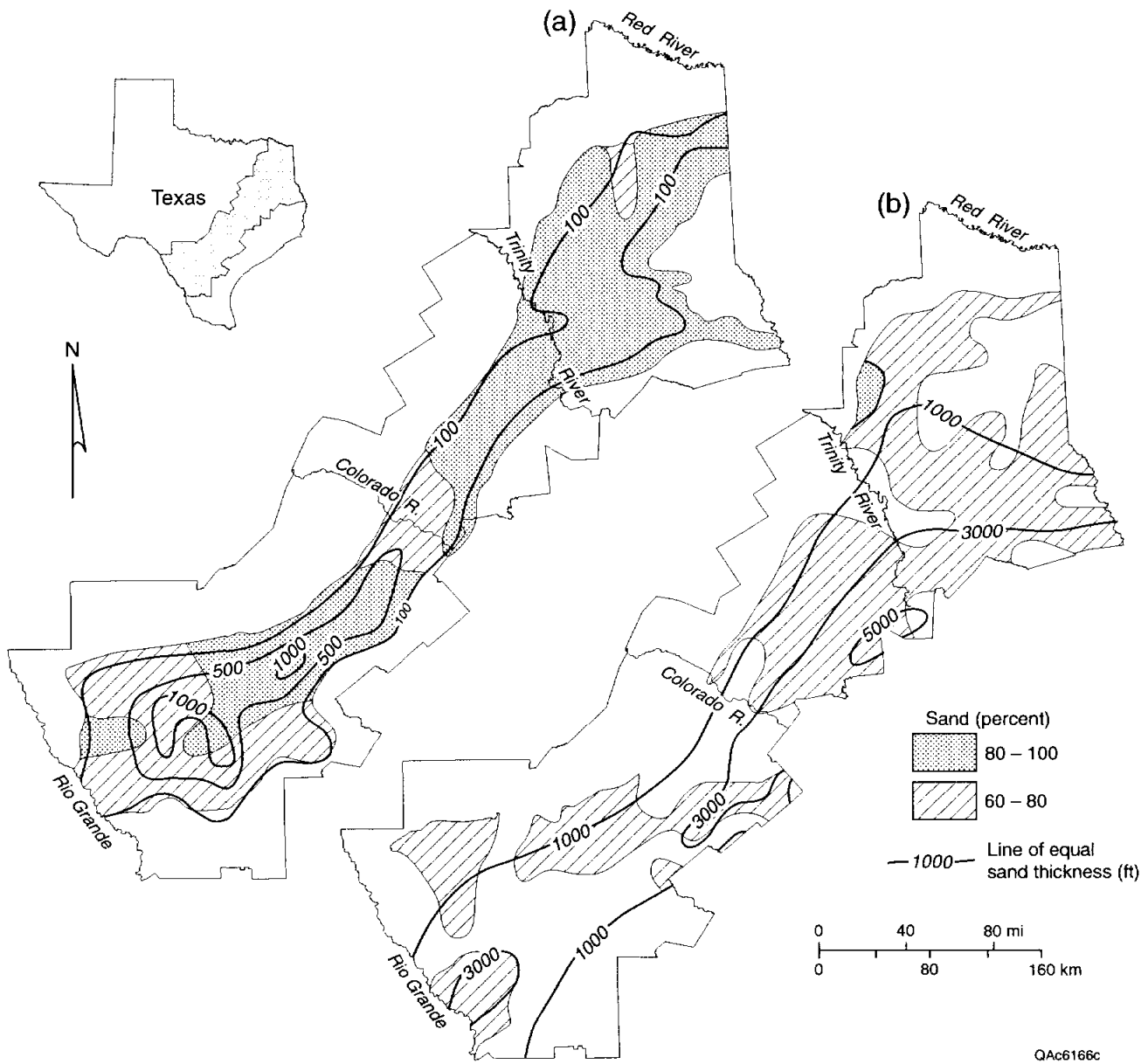


Figure 4. Aquifer thickness and percent sand for (a) lower Claiborne-upper Wilcox aquifer and (b) middle Wilcox aquifer. Modified from Hosman and Weiss (1991).

Table 1. Thickness of Carrizo (Ec) and Wilcox (Ew) stratigraphic units in four structural settings.

Structural setting	County	Thickness of Ec-upper Ew	Thickness of Ec-upper Ew	Thickness of middle Ew	Thickness of middle Ew
		fluvial deposits	section	fluvial deposits	section
		ft (m)	ft (m)	ft (m)	ft (m)
Rio Grande Embayment	Zavala	590 (184) ^a			
		725 (226)	783 (244)	0	248 (77)
	Dimmit	516 (161)	859 (268)	0	306 (95)
	La Salle	172 (54)	1,203 (375)	0	573 (179)
San Marcos Arch	Gonzales	726 (226)	802 (250)	0	344 (107)
	Karnes	1,088 (339)	1,088 (339)	0	649 (202)
	De Witt	173 (54) ^b			0
		382 (119)	1,088 (339)	0	687 (214)
Houston Embayment	Lee	477 (149)	477 (149)	0	229 (71)
	Fayette			1,566 (488) ^c	
		0 (0)	707 (220)	0	573 (179)
Sabine Arch	San Augustine	363 (113)	287 (89)	726 (226)	2,731 (851)

a - sand above Carrizo-Upper Wilcox

b - Winter Garden beach sand

c - Simsboro

belt that reaches up to 15 ft in width in outcrop in South Texas. In the vicinity of Karnes and Atascosa Counties, fluvial sands are overlain by approximately 50 ft of well-bedded, marine shelf sand (Ryder, 1988; Galloway and others, 1994).

Lignite, present throughout the Paleogene of Texas, is concentrated in economically significant amounts most commonly in middle and upper Wilcox lagoonal and deltaic interdistributary deposits (Ayers and Lewis, 1985, Kaiser, 1974). Carrizo-Wilcox ground-water resources are utilized for lignite development at mine-mouth power plants (Henry and others, 1979). However, ground water also hinders lignite-mining operations. For example, extensive dewatering of Calvert Bluff overburden is required in many of the mines to keep open pits from flooding during lignite extraction. Large lakes are often left at the surface after mining has ceased. In Milam and Lee Counties, Simsboro Sand is depressurized to prevent catastrophic buckling of mine pit floors; the depressurization water is discharged to East Yegua Creek and eventually flows to the Brazos River.

The Wilcox Group and the Carrizo Sand, Reklaw Formation, and Queen City Sand of the Claiborne Group are sometimes considered one hydrostratigraphic unit in northeast Texas called the “Cypress aquifer” (i.e., Broom and others, 1965).

Methods

Our methodology included (1) a review of the literature relating to transmissivity, hydraulic conductivity, and storativity measurements in the Carrizo-Wilcox aquifer; (2) a compilation of transmissivity, hydraulic conductivity, and storativity data; (3) analysis of the data; and (4) geostatistical description of transmissivity and hydraulic conductivity.

LITERATURE REVIEW

Our literature review involved using the American Geological Institute's GEOREF database of bibliographic information on the geosciences (last updated in June 1998). We used GEOREF to search for documents related to the Carrizo Sand and the Wilcox Group. The initial list of documents was organized into categories concerning (1) chemistry, (2) lignite, (3) contamination, (4) faulting, (5) geology, (6) hydrogeology, and (7) oil and gas. References in the hydrogeology and geology categories were acquired from the Geology Library at The University of Texas at Austin and reviewed for any information on permeability and storativity. Bibliographies and reference lists from these documents were used to supplement the initial GEOREF list.

DATA COMPILATION

Our compilation of transmissivity, hydraulic conductivity, and storativity data included publicly available published and unpublished data from the following sources:

- documents inspected during the literature review;
- well records at the Texas Water Development Board (TWDB);
- well records from Central Records of Municipal Solid Waste at the Texas Natural Resources Conservation Commission (TNRCC);
- published and open-file reports of the TWDB, Bureau of Economic Geology (BEG) and the U.S. Geological Survey (USGS);
- lignite mine permit reports on file at the Texas Railroad Commission (TRRC); and
- files from municipal and industrial ground-water users and water-supply companies.

Besides compiling existing transmissivity, hydraulic conductivity, and storativity data, we also compiled specific-capacity and step-drawdown test data (pumping rate, pumping time, and

resulting drawdown) because transmissivity can be determined from specific capacity and step-drawdown data (for example, Theis and others, 1963; Mace, in review; Mace and others, 1997).

We downloaded digital files from the TWDB ground-water database and compiled specific-capacity data from the remarks data file. We inspected paper files and compiled specific capacity data at the TNRCC. From these files, we compiled only information for wells that were pumped or jetted. Jetted and pumped wells provide much more accurate specific capacity data than did bailed wells. In data-poor areas of the aquifer, we compiled information on selected wells that were bailed. Well files at the TNRCC did not indicate the formation in which the well was completed. Therefore, we compared depth to the top of the screen and the bottom of the well as reported in TNRCC files with those reported for wells from the TWDB database for each corresponding 7.5-minute quadrangle to ensure that the TNRCC wells were completed in the Carrizo-Wilcox aquifer. For TNRCC wells with no corresponding well location in the TWDB database, we used the geologic cross-sections from Galloway and others (1994) in order to ensure completion within Carrizo-Wilcox aquifer sediments.

We reviewed lignite mine permit files at the TRRC Surface Mining Division file room for lignite mines in Wilcox Group sediments. TRRC requires mining companies to establish baseline ground-water conditions prior to mining through installation and hydraulic testing of numerous wells. In addition, mine operators frequently install and test additional wells as part of overburden dewatering and underburden depressurization activities. The geologic and hydraulic data from these lignite mine investigations tend to be the most detailed available for the aquifer.

In December of 1998, we coordinated with the TWDB a mass mailing to 467 water utilities requesting any available well-test information for the Carrizo-Wilcox aquifer. We sent another request in early February of 1999. A total of 42 entities responded to the request, 33 of which had well-test information. Data from the BEG and USGS came from published reports and previous studies.

If possible, the following information was collected for each test and entered into a Microsoft Excel spreadsheet:

- well identification number,
- data source
- county name,
- latitude and longitude,
- well depth,
- screened interval of well,
- depth to water,
- well diameter,
- well yield (production or discharge rate),
- drawdown in well due to well yield,
- pumping time of test,
- test method,
- specific capacity,
- transmissivity, hydraulic conductivity, and
- storativity.

Pumping rate, pumping duration, well diameter, and water-level drawdown were compiled to calculate specific capacity and help analytically estimate transmissivity from specific-capacity data. Screen intervals were compiled to calculate hydraulic conductivity (transmissivity divided by the aquifer thickness).

Wells that did not have any identification number are numbered according to the data source. Wells compiled from the TNRCC water-well files often did not have a unique identification number. In this case, the wells were named according to an abbreviated State well numbering system using an array of 1°, 7.5-minute, and 2.5-minute quadrangles (fig. 5). Although, several wells may have the same number, such as 33-59-1, to designate a position inside a 2.5-minute quadrangle, they are not precisely located within the quadrangle (i.e., not assigned the last two digits of the well number as shown in fig. 5). We retained this convention to

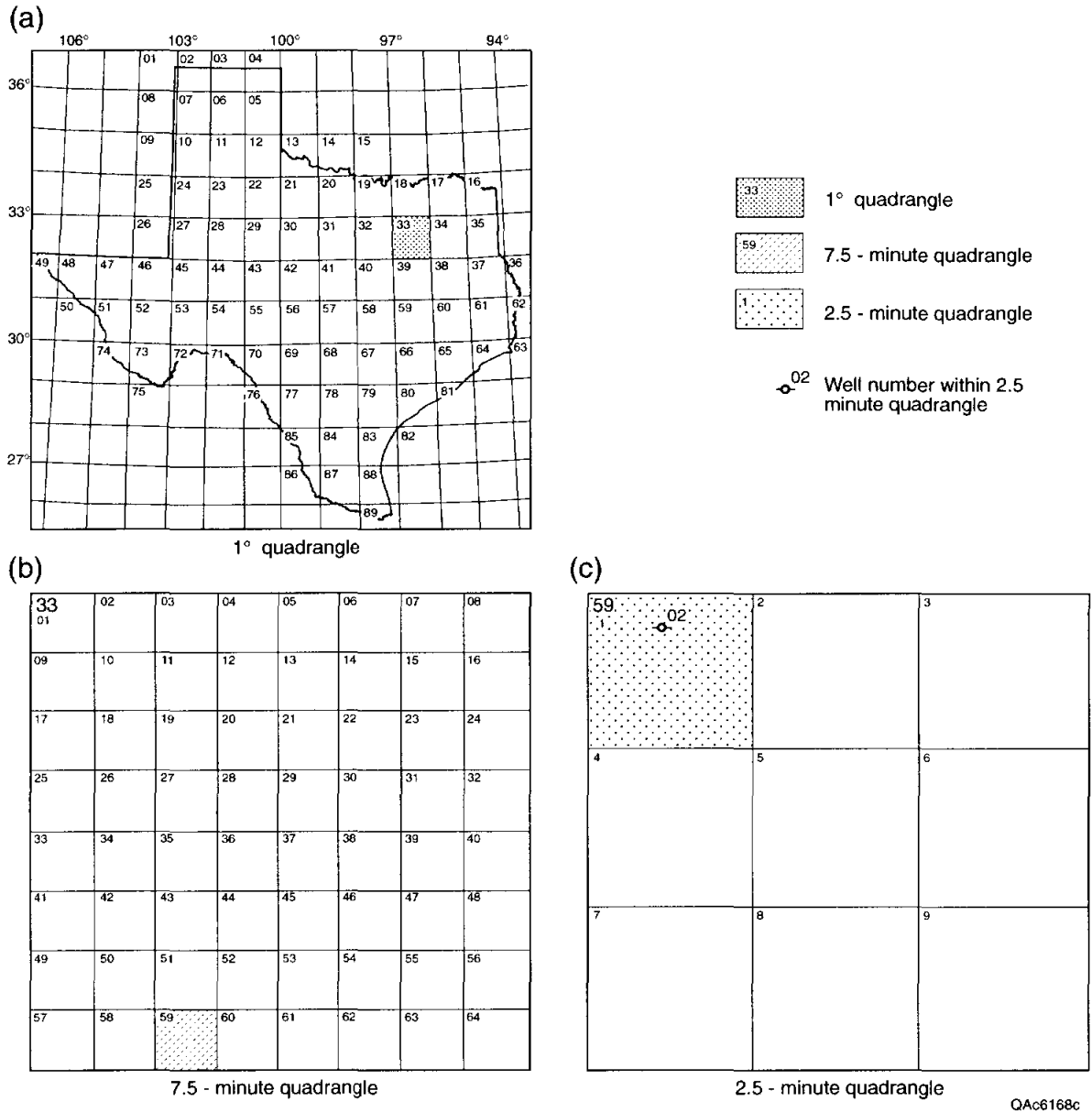


Figure 5. State well-numbering system for (a) 1° quadrangles in Texas, (b) 7.5-minute quadrangles within 1-minute quadrangles, and (c) 2.5-minute quadrangles within 7.5-minute quadrangles. Modified from Follett, 1970.

honor the existing naming scheme of the state and that in the original file. Other well data, such as depth, diameter, and pumping rate, can be used to locate the original file at the TNRCC. However, either the TNRCC or the TWDB may give wells a more specific name at a later date. For each test entry, we assigned a unique BEG test number.

Locational coordinates were reported for many wells. Wells with coordinates not in latitude and longitude were converted from their reported projection into latitude and longitude. Wells from the TNRCC files did not have coordinates assigned to them. Oftentimes, well reports contain only approximate map locations. Therefore, we assigned the center coordinates of the 2.5-minute quadrangle in which the well was located as the approximate well coordinates. Whereas these wells were not used to define the local distribution of permeability in the aquifer, they are useful for quantifying nonspatial statistics and the regional distribution of permeability in the aquifer.

Thorkildsen and others (1989) estimated hydraulic conductivity of the Carrizo Sand and Wilcox Group using electrical logs to define shale, channel, and interchannel deposits and assigning assumed hydraulic conductivities to the mapped deposits. They assumed a value of 1 gpd/ft² for shales, 25 to 50 gpd/ft² for interchannel deposits, and 140 to 500 gpd/ft² for channel deposits. They then calculated vertical averages for each formation. We attained copies of the original datasheets from the TWDB and entered the values into our digital database.

Data were organized in both Microsoft Excel spreadsheets and in ArcInfo geographic information system coverages. A companion browser-driven CD-ROM includes all the data files from this study.

EVALUATION OF HYDRAULIC PROPERTIES FROM THE TEST DATA

If needed, we analyzed aquifer test data for transmissivity and hydraulic conductivity and, in some cases, storativity. The parties that conducted many of the higher quality pumping tests had already analyzed the test data. In these cases, we reviewed the analyses for accuracy. For unanalyzed aquifer tests, we used standard techniques such as the Theis (1935) type curve analysis or the Cooper and Jacob (1946) straight line method (for example, Kruseman and de Ridder, 1990) to determine transmissivity. Hydraulic conductivity, K , was calculated by dividing the transmissivity, T , by the aquifer thickness, b :

$$K = \frac{T}{b} \quad (1)$$

Note that we defined aquifer thickness as the total length of the screened interval in the well. Water wells in the Carrizo-Wilcox are generally screened only in the most productive intervals of the aquifer. Larger wells will often be separately screened in a few different intervals. Therefore, many aquifer tests in the Carrizo-Wilcox aquifer measure the hydraulic properties of the most permeable sands.

Estimating Transmissivity from Specific Capacity

Many of the transmissivity and hydraulic conductivity values that we compiled were based on specific-capacity data. Although estimates of transmissivity and hydraulic conductivity derived from specific-capacity and step-drawdown data are generally not as accurate as estimates from time-drawdown data, relating specific capacity to transmissivity dramatically increased the number of transmissivity values in our database.

There are robust analytical and empirical methods that can be used to estimate transmissivity from specific-capacity data (for example, Thomasson and others, 1960; Theis, 1963; Brown, 1963; Razack and Huntley, 1991; Huntley and others, 1992; El-Naqa, 1994;

Mace, 1997). These techniques have been successfully used in the Cretaceous sandstone aquifers of North Central Texas (Mace and others, 1994), the Edwards aquifer (Hovorka and others, 1995, 1998; Mace, 1995), the Ogallala aquifer (Myers, 1969; Mullican and others, 1997), and the Hill Country Trinity aquifer (Mace, in prep). Prudic (1991) used specific-capacity data in his regional study of the Gulf Coast regional aquifer systems.

Water-well drillers often conduct a well-performance test after well completion to determine the specific capacity. During a well-performance test, the well is pumped at a constant rate, and the amount of drawdown is noted. Specific capacity, S_c , is then defined as the pumping rate, Q , divided by the amount of drawdown, s_w :

$$S_c = \frac{Q}{s_w} \quad (2)$$

Specific capacity is generally reported as discharge per unit of drawdown. For example, a well pumped at 100 gallons per minute (gpm) with 20 ft of drawdown would have specific capacity of 5 gpm/ft. Note that although specific capacity is generally reported in units of volume per length, it has the same units as transmissivity: length squared per time.

A total of 217 wells in the Carrizo-Wilcox aquifer had time-drawdown data and other information necessary to (1) calculate transmissivity using standard pumping-test analysis techniques and (2) estimate transmissivity using specific-capacity data. We evaluated two approaches for estimating transmissivity from specific capacity: an empirical approach and an analytical approach.

We developed an empirical relationship by linearly relating log-transformed transmissivity to log-transformed specific capacity calculated for the same well. To define an empirical relationship between transmissivity and specific capacity, we log-transformed values

of each parameter, plotted them against each other, and fit a line through the data using least squares regression (fig. 6). The best-fit line through the data is:

$$T = 1.99 S_c^{0.84}, \quad (3)$$

where the units of T and S_c are in ft^2d^{-1} , and the correlation coefficient, R^2 , is 0.91. The relationship has a 90 percent prediction interval that spans a little less than about an order of magnitude. The prediction interval means that we are 90 percent confident that an estimate of transmissivity for any given value of specific capacity is within an order of magnitude of the estimate.

We evaluated the analytical relationship between transmissivity and specific capacity by Theis and others (1963) for the Carrizo-Wilcox aquifer. Their relationship is based on the Theis (1935) nonequilibrium equation:

$$S_c = \frac{4\pi T}{\left[\ln \left(\frac{2.25 T t_p}{r_w^2 S} \right) \right]} \quad (4)$$

where S is the storativity of the aquifer, t_p is the time of production (that is, pumping) when the drawdown was measured, and r_w is the radius of the well in the screened interval. This equation assumes (1) a fully-penetrating well; (2) a homogeneous, isotropic porous media; (3) negligible well loss; (4) and an effective radius equal to the radius of the production well (Walton, 1970). Because equation 3 cannot be explicitly solved for transmissivity, it must be solved graphically or iteratively; we solved it iteratively in a spreadsheet.

To evaluate the relative accuracy of transmissivity estimated using the empirical relationship (equation 3) against transmissivity estimated using the analytical relationship

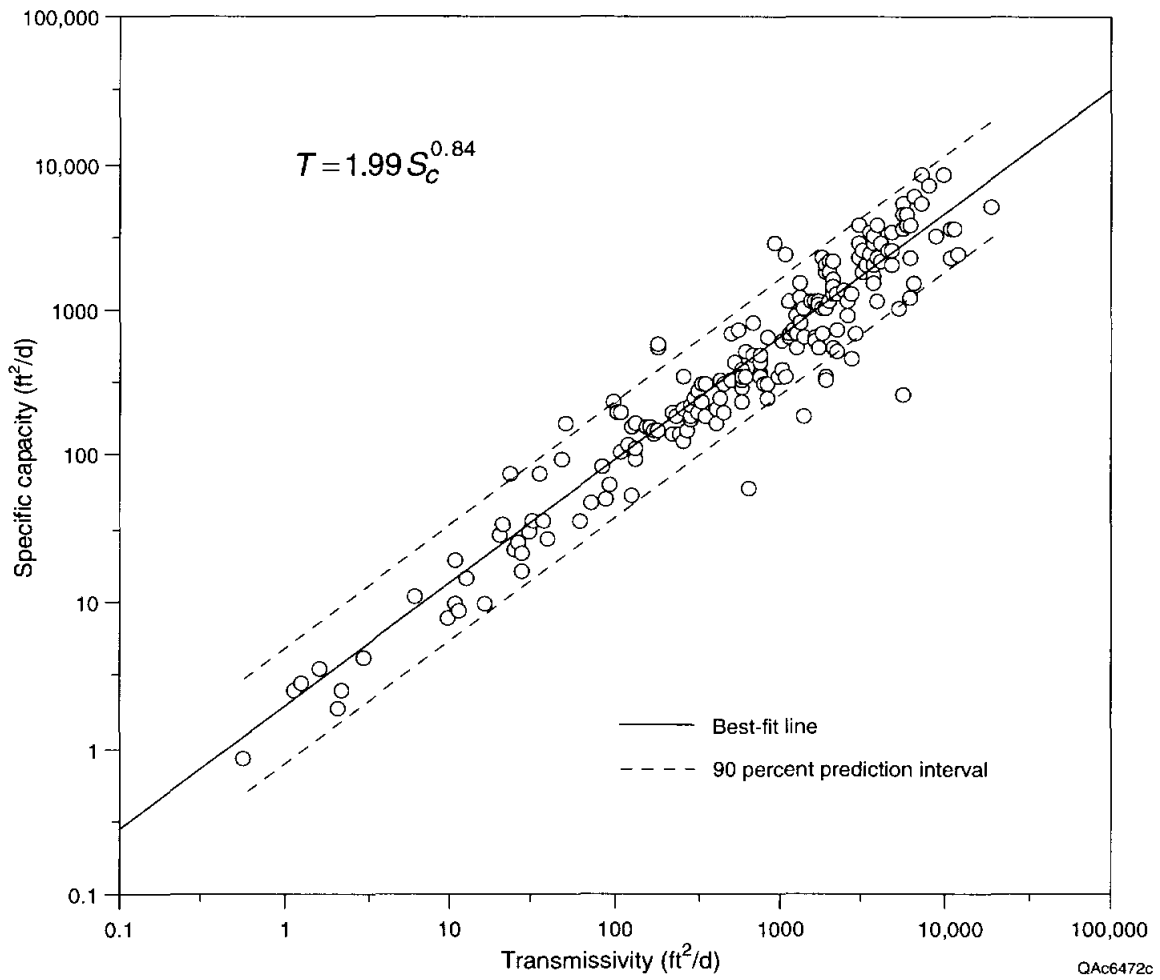


Figure 6. Relationship between specific capacity and transmissivity in the Carrizo-Wilcox aquifer.

(equation 4), we determined the mean absolute error and mean error. Mean absolute error, $|\bar{\varepsilon}|$, is defined by

$$|\bar{\varepsilon}| = \frac{1}{n} \sum_{i=1}^n \left| \log(T_m) - \log(T_e) \right| \quad (5)$$

where n is the number of values, T_m is the transmissivity determined from the pumping test, and T_e is the estimated value of transmissivity. Mean error, $\bar{\varepsilon}$, is defined by

$$\bar{\varepsilon} = \frac{1}{n} \sum_{i=1}^n \left[\log(T_m) - \log(T_e) \right] \quad (6)$$

Of the 217 tests used to define the empirical relationship between transmissivity and specific capacity, 57 tests had the appropriate information (discharge rate, drawdown, pumping time, and well radius) for estimating transmissivity with the analytical solution. Therefore, we were only initially able to use these 57 tests to determine the mean absolute error and mean error between calculated transmissivity (using time-drawdown data) and transmissivity estimated using the two specific capacity methods.

The mean absolute error and mean error for transmissivity estimated using the empirical relationship are 0.33 and 0.17, respectively. A mean absolute error of 0.33 means that, on average, the estimated value of transmissivity is within a factor of 2.1 of the measured value (determined by taking the inverse log of 0.33). The positive mean error indicates a bias toward over predicting transmissivity.

The mean absolute error and mean error for transmissivity estimated using the analytical approach are 0.17 and -0.002, respectively. A mean absolute error of 0.17 means that, on average, the estimated value of transmissivity is within a factor of 1.5 of the measured value (determined by taking the inverse log of 0.17). Because the mean error is close to zero, estimates of transmissivity made with the analytical approach are collectively unbiased and do not have a systematic error toward underestimating or overestimating transmissivity.

Based on the mean absolute errors calculated using data from 57 wells, the analytical approach provides slightly more accurate estimates of transmissivity than does the empirical approach. The limiting variables for analytically estimating transmissivity from specific-capacity data are pumping time and well radius. By using mean values of these variables from all other wells, we were able to increase the number of analytical estimates from 57 to 107. Using this approach slightly increases the mean absolute error and mean error for the analytical approach to 0.173 and -0.02, respectively. Therefore, even with assumed values, the analytical approach is more accurate. The empirical relationship may still be useful for (1) field applications where iterative solutions are unwieldy to solve and (2) where nonideal conditions such as partial penetration of the aquifer, turbulent well losses, or fracture flow conditions need to be considered (Mace, in review). Both methods of estimating transmissivity from specific capacity data can result in errors as much as a factor of 5 (fig. 7).

STATISTICAL DESCRIPTION

We statistically summarized transmissivity, hydraulic conductivity, and storativity data using standard statistics, graphical plots, and geostatistics. Standard statistics include arithmetic and geometric mean (average), median, variance, and standard deviation. A geometric mean is the mean value of log-transformed values. Graphical plots include histograms and cumulative distribution functions. A cumulative distribution function (CDF) is a way to display a probability distribution and represents the probability of observing a value less than or equal to another value. In this study we constructed CDFs using log-transformed values of transmissivity and hydraulic conductivity to more readily compare different categories of the data.

The geostatistical methods we used are semivariograms and kriging. Semivariograms statistically quantify spatial relationships of the data. If the values of a parameter such as hydraulic conductivity depend on spatial position, the values of that parameter measured at two

points are more likely similar if the two points are close together than if the points are far apart. This measure of similarity (or semivariance) can be quantified with a semivariogram, which is a plot of semivariance versus separation distance of the points (Clark, 1979; McCuen and Snyder, 1986). For discrete data, the semi-variance, γ , for a given separation distance, λ , is defined as

$$\gamma(\lambda) = \frac{1}{2n} \sum \{X(z_i) - X(z_i + \lambda)\}^2 \quad (7)$$

where n is the number of data pairs at a distance λ apart, and $X(z_i)$ and $X(z_i + \lambda)$ are the values of the data for the given pairs.

A range, sill, and nugget generally characterize semivariograms (fig. 8). The range generally represents the distance over which a parameter is spatially correlated. Graphically, this is usually the distance to where the semivariogram plateaus, which is called the sill. The separation distance at which the sill occurs is usually the same as the variance of the entire dataset. Theoretically, the semivariance at a separation distance of zero is zero. However, this may not occur because of measurement error, existence of microstructures (Matheron, 1979), or other characteristics of the data (Villaescusa and Brown, 1990). A nonzero value of semivariance at a separation distance of zero is termed the nugget. If the semivariogram is a flat line, it is termed a pure nugget and the data are not spatially correlated. Experimental semivariograms are simply plots of calculated semivariance versus separation distance using measured datapoints – transmissivity and hydraulic conductivity in this study. Theoretical semivariograms are models of the experimental semivariance and are used for kriging. In this study, spherical theoretical semivariograms were visually fit to the experimental semivariograms. We used Surfer to kriging transmissivity and hydraulic conductivity data.

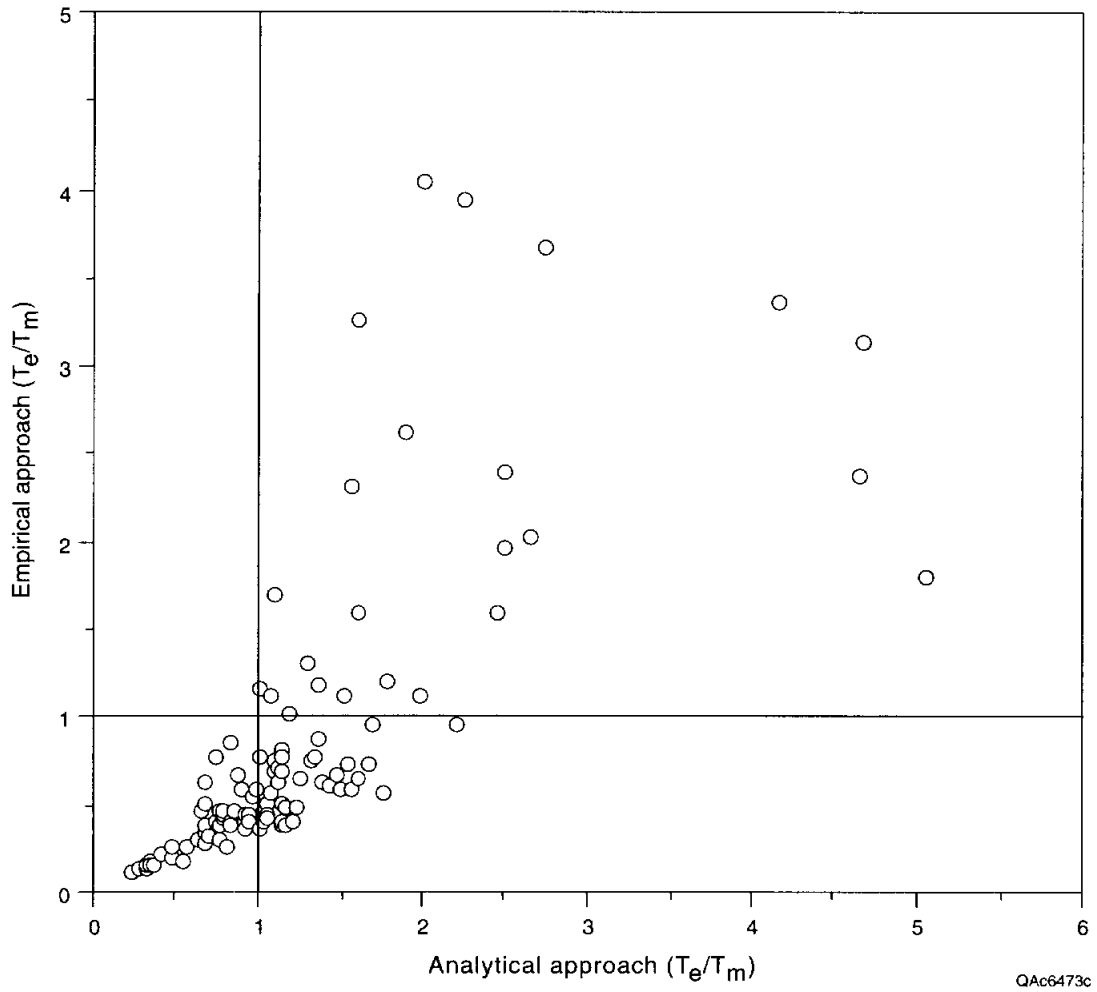


Figure 7. Comparison of the ratios of estimated transmissivity to measured transmissivity for transmissivity estimated by the analytical and empirical approaches.

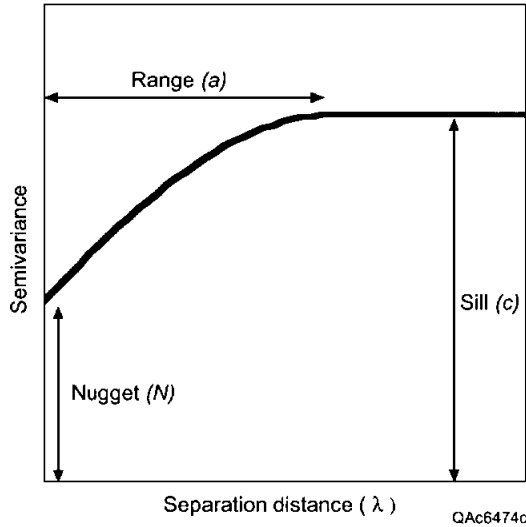


Figure 8. Example semivariogram showing the range, sill, and nugget.

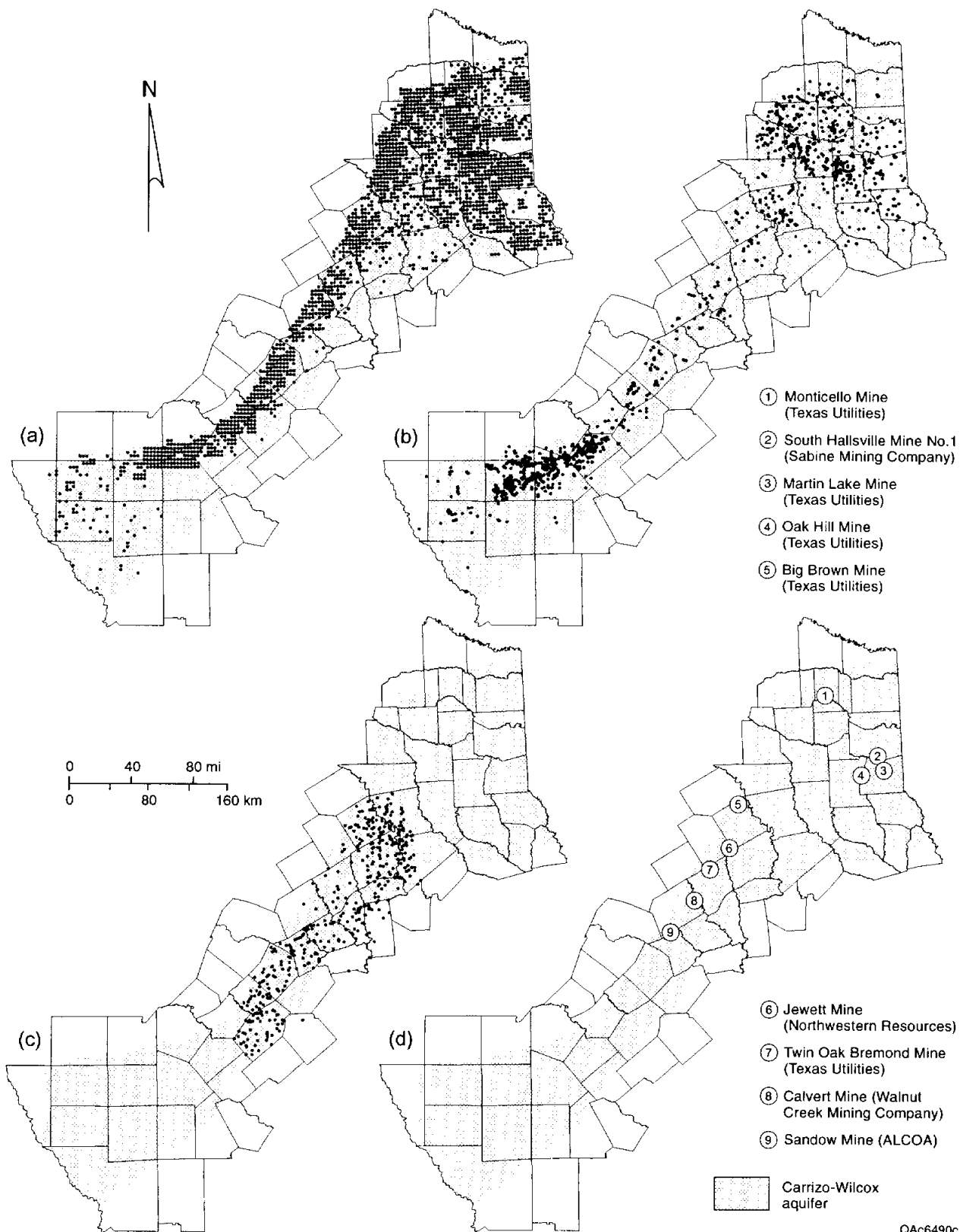
Results and Discussion

This section presents results and discussion on (1) the general characteristics of our compiled database, (2) a statistical description of transmissivity and hydraulic conductivity including analyses of differences between data sources and aquifer testing techniques, (3) the vertical and spatial distribution of transmissivity and hydraulic conductivity, and (4) storativity. Throughout this section we include results of other studies of the Carrizo-Wilcox aquifer for comparison.

GENERAL CHARACTERISTICS OF THE DATABASE

The entire Carrizo-Wilcox database includes 7,402 estimates of hydraulic properties in 4,462 wells. Of the total number of tests, 3,735 were compiled from TNRCC files, 1,671 from an unpublished study by the TWDB on the Carrizo-Wilcox aquifer in Central Texas, 1,394 from the TWDB digital database, 296 from published reports, 179 from TRRC files, and 127 from water utilities. Published reports used in the data compilation include Guyton (1942), Broom and others (1965), Broom (1966), Follett (1966), Tarver (1966), Broom (1968, 1969), Myers (1969), Gaylord and others (1985), Guyton and Associates (1972), Marquardt and Rodriguez (1977), Elder and Duffin (1980), McCoy (1991), and Fisher and others (1996). Test wells from which data are derived are located throughout the outcrop and subcrop of the Carrizo-Wilcox aquifer (fig. 9) and in most counties in the area (fig. 10). Wells become less abundant downdip of the outcrop probably because of drilling costs or because the shallower water-bearing units usually provide adequate yield.

General characteristics of tested wells include: (1) mean diameter of 4.7 inches (fig. 11a, table 2), (2) geometric mean depth of 398 ft (fig. 11b, table 2), and (3) geometric mean screen length of 50 ft (fig. 11c, table 2). Wells in the Carrizo-Wilcox aquifer are generally not screened



QAc6490c

Figure 9. Distribution of aquifer-test wells in the Carrizo-Wilcox aquifer from TNRCC well files, (b) TWDB well database, and (c) well log information from the TWDB.

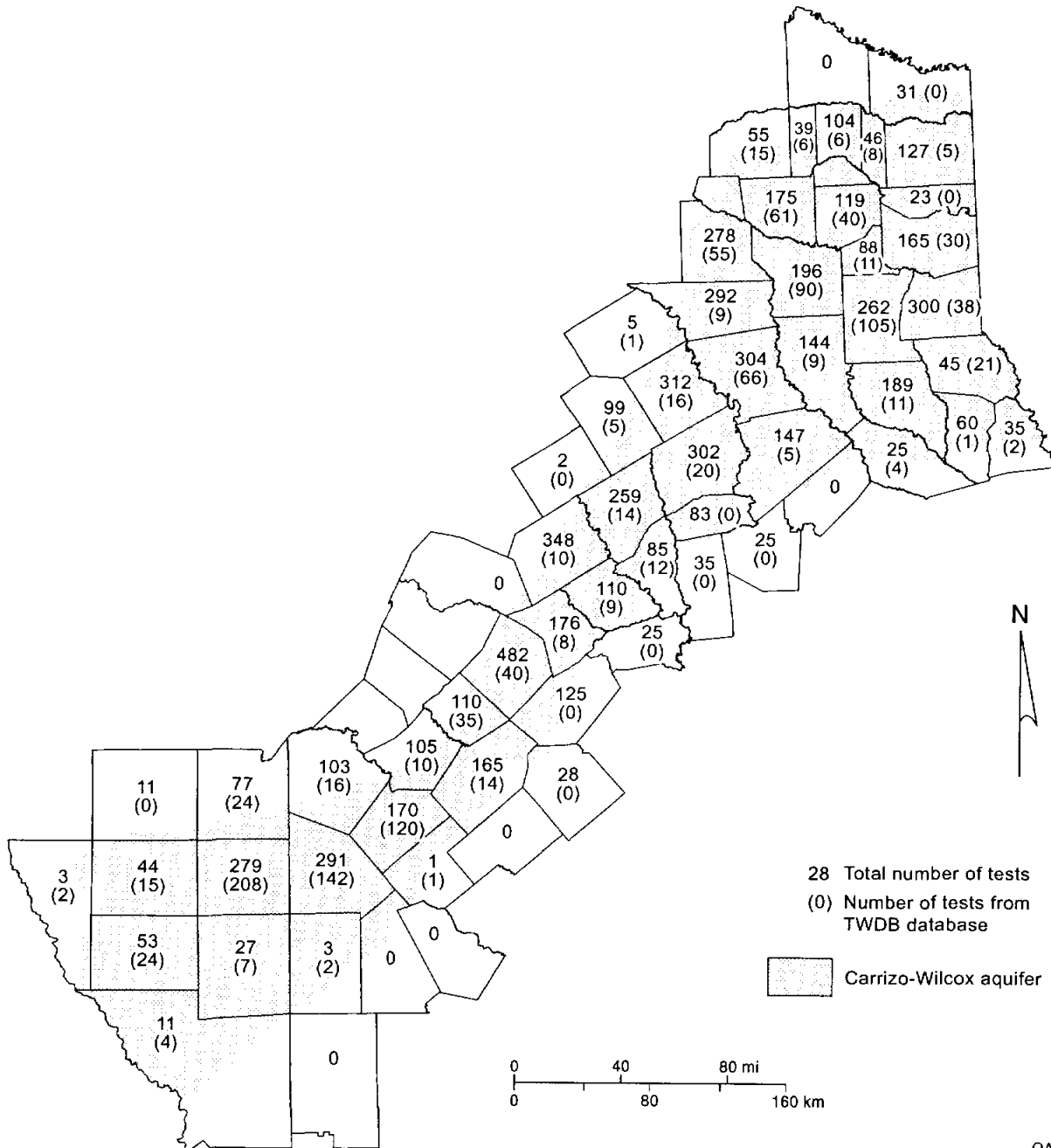


Figure 10. Number of aquifer test wells in each county.

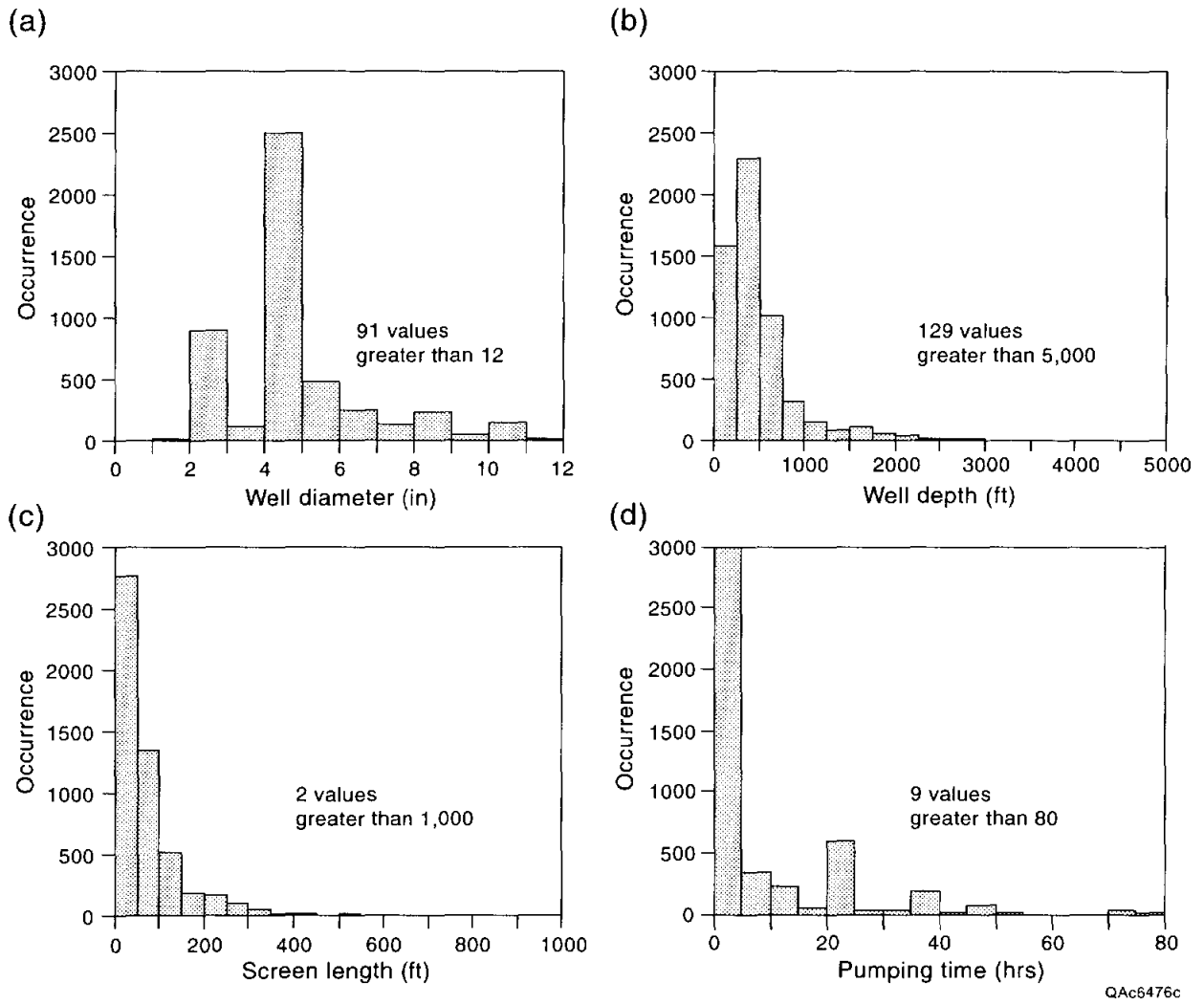


Figure 11. General characteristics of wells and aquifer tests in the database.

Table 2. Characteristics of wells and tests in the database.

Parameter	units	n	25th	50th	75th	90th	\bar{x}	s
Diameter	in	5,014	4.0	4.0	5.0	8.0	4.7	2.64
Depth	ft	5,772	240	388	600	1,074	398 ^a	0.38 ^b
Screen length	ft	5,219	25	41	81	158	50 ^a	0.37 ^b
Pumping time	hr	4,795	1	2	12	24	4.0 ^a	0.56 ^b

n number of values

25th 25th percentile

50th 50th percentile (median)

75th 75th percentile

90th 90th percentile

\bar{x} mean

s standard deviation

^a Geometric mean

^b Log-transformed standard deviation

Table 3. Transmissivity values (ft²d⁻¹) estimated from the tests.

	n	25th	50th	75th	90th	\bar{x} ^a	<i>s</i> ^b
All tests	5,734	86	240	910	4,600	300	0.79
<i>Source</i>							
TNRCC	3,735	64	150	340	860	150	0.60
TRRC	179	17	130	670	2,700	100	1.09
TWDB	1,397	360	1,400	5,500	11,000	1,300	0.73
Water utilities	127	410	930	2,400	6,900	1,000	0.59
References	296	440	1,600	4,000	9,300	1,300	0.65
<i>Test method</i>							
Pumping test	362	260	950	2,900	5,300	730	0.81
Specific capacity, all	5,300	85	230	810	4,500	290	0.77
Spec. cap., TWDB	1,394	400	1,300	5,000	10,000	1,300	0.73
Spec. cap., bailed	41	28	75	220	470	74	0.69
Spec. cap., jetted	1,481	54	140	370	900	150	0.62
Spec. cap., pumped	2,140	72	150	340	820	170	0.59
Slug tests	72	8	40	150	360	26	0.94
<i>Formation (only TWDB data except where noted)</i>							
Cypress aquifer	18	150	310	550	850	310	0.39
Carrizo	726	1,800	4,900	9,200	15,000	3,500	0.61
Calvert Bluff	13	85	420	800	1,400	310	0.62
Calvert Bluff, w/mine	138	19	110	410	940	79	0.96
Simsboro	56	1,300	2,800	4,500	7,300	2,400	0.42
Simsboro, w/mine	73	1,900	3,200	5,200	7,100	2,700	0.39
Carrizo-Wilcox	220	360	870	2,500	7,500	900	0.67
Wilcox	727	180	440	1,000	2,100	420	0.60

^a Based on log transformation of original data

^b Log-transformed standard deviation

- n** number of values
- 25th** 25th percentile
- 50th** 50th percentile (median)
- 75th** 75th percentile
- 90th** 90th percentile
- \bar{x} mean
- s* standard deviation

Table 4. Hydraulic conductivity values (ft d⁻¹) estimated from the tests.

	n	25th	50th	75th	90th	\bar{x} ^a	s ^b
All tests	5,963	2.3	6.6	21.	46.	6.6	0.67
<i>Source</i>							
TNRCC	3,700	1.8	3.8	9.5	25.	4.1	0.61
TRRC	179	1.2	4.9	16.	32.	3.7	0.84
TWDB	1,235	4.6	13.	36.	78.	12.	0.64
TWDB (log)	622	20.	26.	45.	54.	28.	0.21
Water utilities	103	6.1	11.	31.	50.	12.	0.51
References	127	8.0	16.	31.	89.	15.	0.59
<i>Test method</i>							
Pumping test	235	4.6	14.	28.	62.	11.	0.69
Specific capacity, all	5,037	2.1	5.0	15.	39.	5.6	0.65
Spec. cap., TWDB	1,233	5.0	13.	40.	79.	13.	0.64
Spec. cap., bailed	37	0.33	1.9	5.4	16.	1.6	0.79
Spec. cap., jetted	1,463	1.6	3.8	11.	27.	4.0	0.65
Spec. cap., pumped	2,129	1.9	3.8	8.8	23.	4.2	0.58
Slug tests	72	0.53	2.0	5.7	9.7	1.5	0.79
TWDB (log)	622	20.	26.	45.	54.	28.	0.21
<i>Formation (only TWDB data except where noted)</i>							
Cypress aquifer	7	3.0	4.9	9.6	13.	5.6	0.33
Carrizo	602	12.	30.	58.	120.	26.	0.58
Calvert Bluff	11	2.3	4.2	5.1	15.	4.2	0.48
Calvert Bluff, w/mine	136	1.2	4.5	10.	21.	3.2	0.75
Simsboro	56	11.	20.	31.	53.	18.	0.43
Simsboro, w/mine	73	13.	23.	33.	52.	20.	0.39
Carrizo-Wilcox	187	5.2	11.	31.	62.	11.	0.59
Wilcox	615	2.8	6.6	14.	31.	6.0	0.59

^a Based on log transformation of original data

^b Log-transformed standard deviation

n number of values

25th 25th percentile

50th 50th percentile (median)

75th 75th percentile

90th 90th percentile

\bar{x} mean

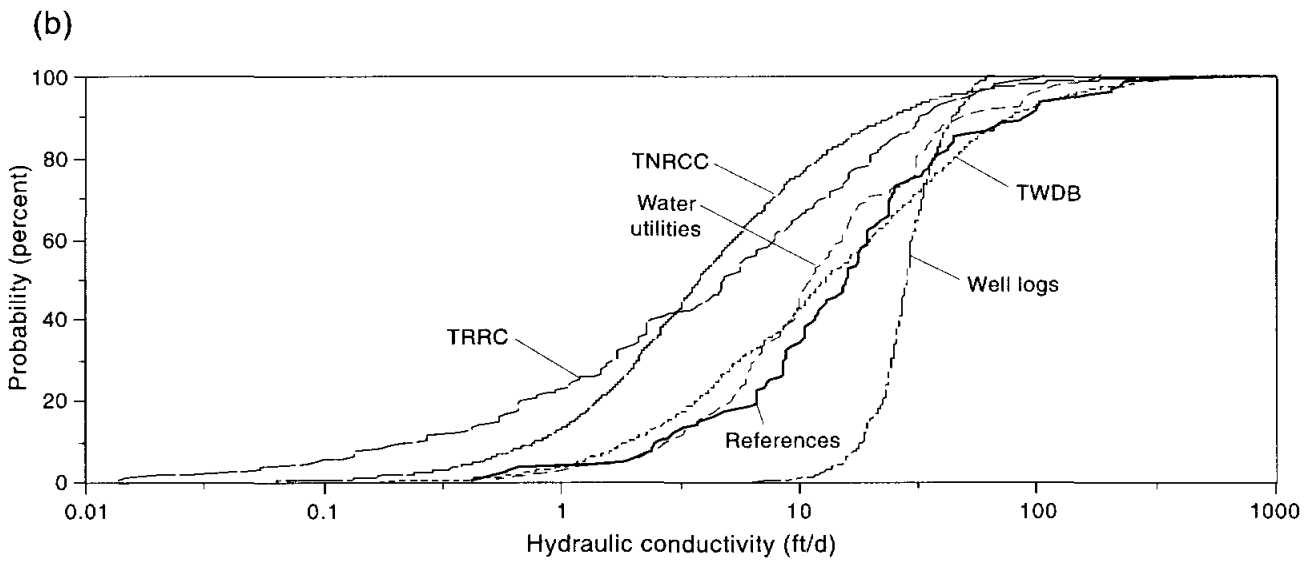
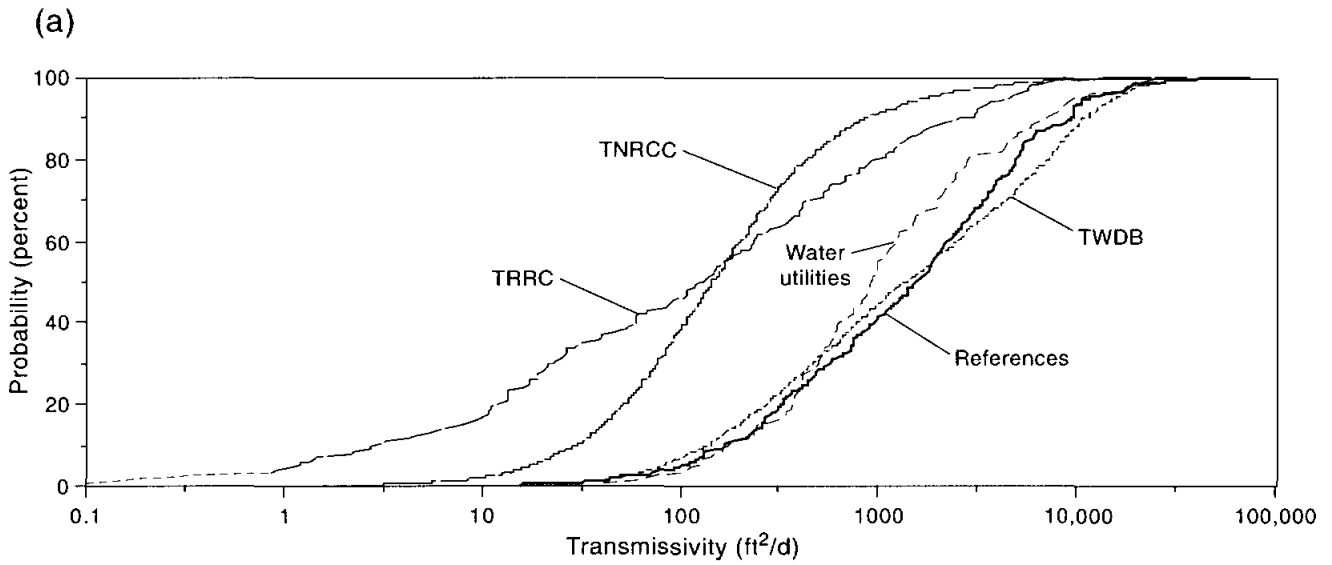
s standard deviation

Variations in Values from Different Sources

There are differences for geometric mean transmissivity and hydraulic-conductivity values between the different data sources. Tests from TNRCC and TRRC files have geometric mean transmissivity values that are about 10 times lower than tests from the TWDB database, water utilities, and reference sources (table 3, fig. 13a). Tests from TNRCC and TRRC files have geometric mean hydraulic-conductivity values that are about three to four times lower than tests from the TWDB database, water utilities, and reference sources (table 4, fig. 13b).

Most of the data from the TNRCC files are for private wells whereas most (at least 70 percent) of the data compiled for the TWDB database are from municipal public supply or industrial wells. Private wells do not require large yields to supply a household and are usually completed when the desired yield is reached during drilling. Consequently, private wells are usually screened in shallower water-bearing zones and rarely penetrate the entire aquifer unit. Municipal public supply and industrial wells are designed and constructed to maximize water yield.

Transmissivity and hydraulic conductivity values from TRRC lignite mine permit reports are lower than TWDB data because the TRRC data are biased toward lower permeability geologic units. This is because most of the TRRC-reported wells are completed in either Calvert Bluff Formation or undivided Wilcox Group deposits. For example, 87 percent of the TRRC wells are completed in Calvert Bluff Formation or undivided Wilcox Group and only 13 percent of the wells are completed in the Carrizo Sand and Simsboro Formation (table 5). The Calvert Bluff Formation and equivalent horizons of the undivided Wilcox Group are the main economically viable, lignite-bearing units in Texas. These heterogeneous units are characterized by higher permeability channel and overbank sands in deposits of low-permeability deltaic-mud and organic-rich swamp deposits (peat that later turned to lignite). The higher permeability



QA6478c

Figure 13. Cumulative distribution functions of transmissivity and hydraulic conductivity for different data sources.

Table 5. Transmissivity and hydraulic conductivity values compiled from lignite mine permit reports on file at the TRRC.

Results of Pumping Tests

Mine	Carrizo Sand			Calvert Bluff Formation		
	n	\overline{T}_g (ft ² d ⁻¹)	\overline{K}_g (ft d ⁻¹)	n	\overline{T}_g (ft ² d ⁻¹)	\overline{K}_g (ft d ⁻¹)
Big Brown	-	-	-	14	4.47	89.13
Calvert	-	-	-	-	-	-
Jewett	2	5.37	102.33	20	10.72	288.4
Sadow	-	-	-	7	8.91	97.72
Twin Oak	-	-	-	6	8.51	467.74
Martin Lake	1	64.57	1995.26	-	-	-
Monticello	-	-	-	-	-	-
Oak Hill	-	-	-	-	-	-
South Hallsville	2	15.49	588.84	-	-	-

Mine	Wilcox Group			Simsboro Formation		
	n	\overline{T}_g (ft ² d ⁻¹)	\overline{K}_g (ft d ⁻¹)	n	\overline{T}_g (ft ² d ⁻¹)	\overline{K}_g (ft d ⁻¹)
Big Brown	-	-	-	-	-	-
Calvert	-	-	-	7	21.38	3801.89
Jewett	-	-	-	-	-	-
Sadow	-	-	-	10	32.36	4,897.8
Twin Oak	-	-	-	-	-	-
Martin Lake	3	2.14	67.61	-	-	-
Monticello	25	2.14	69.18	-	-	-
Oak Hill	9	13.18	389.05	-	-	-
South Hallsville	1	0.05	2.24	-	-	-

n number of values

\overline{T}_g geometric mean of transmissivity

\overline{K}_g geometric mean of hydraulic conductivity

Table 5. continued

Results of Slug Tests

Mine	Carrizo Sand			Calvert Bluff Formation		
	n	\bar{T}_g (ft ² d ⁻¹)	\bar{K}_g (ft d ⁻¹)	n	\bar{T}_g (ft ² d ⁻¹)	\bar{K}_g (ft d ⁻¹)
Big Brown	-	-	-	12	1.05	10.47
Calvert	-	-	-	-	-	-
Jewett	-	-	-	1	57.54	3090.3
Sadow	-	-	-	2	0.62	7.59
Twin Oak	-	-	-	4	6.17	229.1
Martin Lake	1	0.47	15.85	-	-	-
Monticello	-	-	-	-	-	-
Oak Hill	-	-	-	-	-	-
South Hallsville	1	1.11	134.89	-	-	-

Mine	Wilcox Group			Simsboro Formation		
	n	\bar{T}_g (ft ² d ⁻¹)	\bar{K}_g (ft d ⁻¹)	n	\bar{T}_g (ft ² d ⁻¹)	\bar{K}_g (ft d ⁻¹)
Big Brown	-	-	-	-	-	-
Calvert	-	-	-	-	-	-
Jewett	-	-	-	-	-	-
Sadow	-	-	-	-	-	-
Twin Oak	-	-	-	-	-	-
Martin Lake	6	1.86	40.74	-	-	-
Monticello	27	2	38.02	-	-	-
Oak Hill	7	0.3	3.89	-	-	-
South Hallsville	11	1.59	31.62	-	-	-

n number of values

\bar{T}_g geometric mean of transmissivity

\bar{K}_g geometric mean of hydraulic conductivity

Carrizo Sand and Simsboro Formation were deposited in more fluvially dominant environments. The wide range of depositional environments represented by the TRRC tests also explains the greater variance of tests compiled from TRRC files (tables 2, 3; figure 12; note the wide distribution). Because of the bias toward lower permeability values (table 5), we did not use the TRRC data to analyze spatial statistics.

Hydraulic conductivity estimated by the TWDB on the basis of well logs are two to seven times higher than other values and have a much lower standard deviation (table 4, fig. 13b). Because this method may overestimate actual hydraulic conductivity and not give a realistic representation of the hydraulic properties of the aquifer, we excluded these data from our analysis of spatial statistics.

Variations in Values Due to Different Testing Methods

Values of transmissivity and hydraulic conductivity vary between the different test methods. Values of transmissivity estimated from pumping tests are about twice as high as those estimated from specific-capacity data (only those specific-capacity data compiled from the TNRCC) and almost 30 times higher than those estimated from slug tests (table 3, fig. 14a). Values of hydraulic conductivity estimated from pumping tests are about twice as high as those estimated from specific-capacity data and about seven times higher than those estimated from slug tests (table 4, fig. 14b). The highest estimates of hydraulic conductivity are from the well log interpretation (fig. 14b), which resulted in values 2.5 times higher than values estimated from pumping tests.

The difference is probably due largely to the type and purpose of the well tested. Pumping tests are generally performed in the higher yielding municipal wells. Slug tests are generally performed in formations with low permeability. In this case, the slug test data are

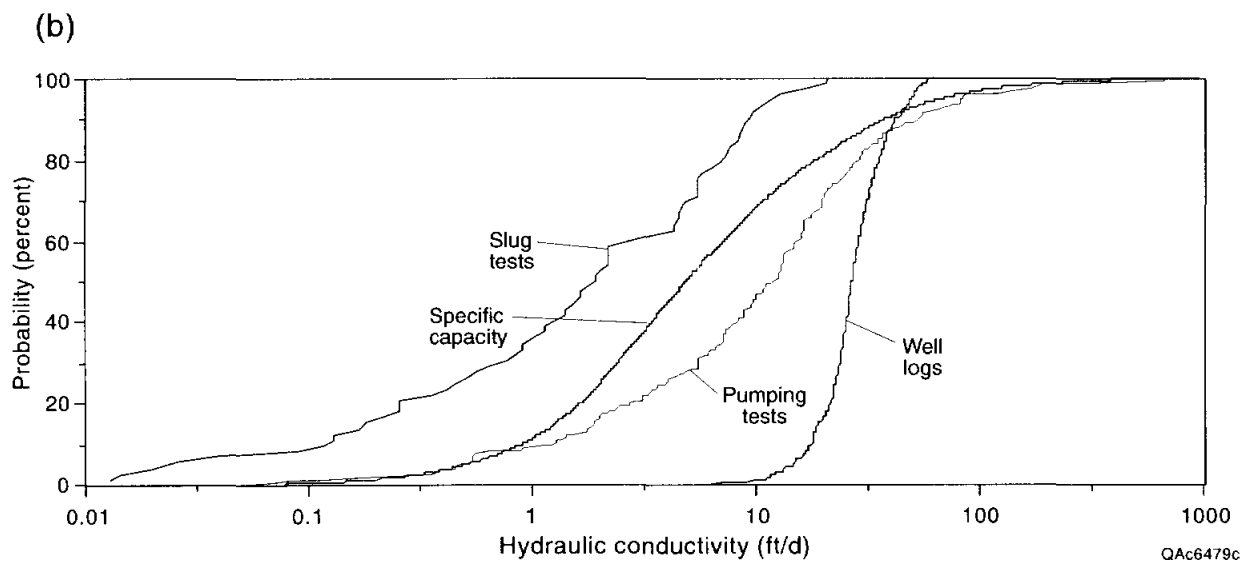
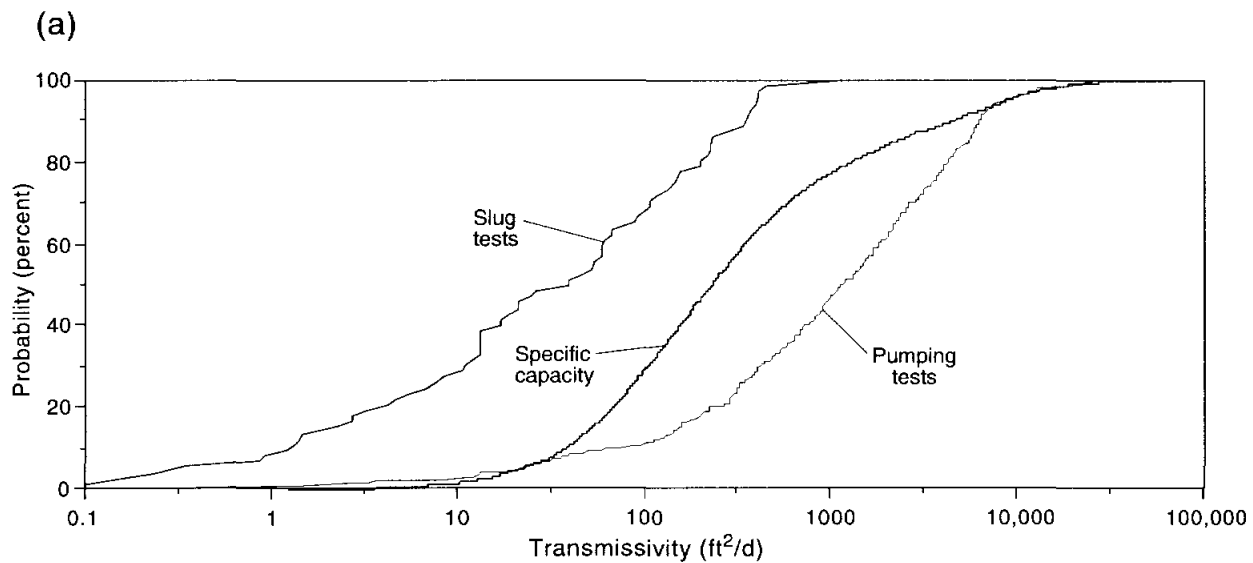


Figure 14. Cumulative distribution functions of transmissivity and hydraulic conductivity for different test types.

exclusively from TRRC-permitted lignite mines where tested wells are most frequently completed in lower permeability Calvert Bluff and Wilcox Group deposits (table 5).

Among tests where we estimated transmissivity from specific-capacity data, wells that were bailed had transmissivity values 100 times lower than wells that were jetted or pumped. Although we compiled substantially fewer specific-capacity data from tests in which wells were bailed, this difference in hydraulic properties supports our decision to forego compiling tests involving bailing. Note that tests for which we were able to determine the method of production used to collect specific capacity data are exclusively from TNRCC files. However, transmissivity values determined from TWDB specific-capacity data are about the same as those determined from pumping tests (table 3). Because of this close correlation, we believe that the method of production for the majority of specific-capacity tests compiled from the TWDB database was pumping.

Another method used to determine hydraulic conductivity is by laboratory analysis of aquifer materials. Klemt and others (1976, p. 12) hydraulically tested core samples from the aquifer and used grain size analysis on drill cuttings to estimate hydraulic conductivity of the Carrizo Sand in the southwestern part of the aquifer. They found county-averaged hydraulic conductivity values that ranged from 5 to 126 ft^2d^{-1} for values estimated from core and 72 to 91 ft^2d^{-1} for values estimated from cuttings. They noted that these values were greater than those determined from pumping tests.

SPATIAL DISTRIBUTION OF TRANSMISSIVITY AND HYDRAULIC CONDUCTIVITY

Spatial distribution refers to how transmissivity and hydraulic conductivity vary vertically and laterally within the aquifer. We first investigated how transmissivity and hydraulic conductivity vary between the different formations. Based on that analysis, we then investigated

how transmissivity and hydraulic conductivity vary laterally within the aquifer, both regionally and locally, using regional binning and geostatistics. Finally, we investigated if the geology, specifically regional net sand thickness, could help explain some of the lateral variability we observed. Where appropriate, we also include results of other studies that relate to vertical and lateral variability, such as the work of Prudic (1991) on the relationship between depth and hydraulic conductivity. All of the results we present in this section are based on analyses we performed with data sourced from the TWDB well database.

Vertical Variability of Transmissivity and Hydraulic Conductivity

We observe vertical variations in transmissivity and hydraulic conductivity among the different formations and aquifers. The Simsboro Formation and Carrizo Sand portions of the aquifer have transmissivity and hydraulic-conductivity values that are higher (2.5 to eleven times higher for transmissivity and two to six times higher for hydraulic conductivity) than those of the Cypress aquifer, Calvert Bluff Formation, and Wilcox Group as a whole (fig. 15, tables 3 and 4). This is geologically reasonable because the Carrizo Sand and Simsboro Formation tend to have a greater percentage of sand than do other hydrogeologic units within the Carrizo-Wilcox aquifer.

Values of hydraulic conductivity and transmissivity that we compiled are similar to values compiled and summarized by previous researchers (compare to values presented in table 4). Thorkildsen and Price (1991) reported the following hydraulic conductivity values for Carrizo-Wilcox sediments based on the analysis of well logs:

- (1) Carrizo Sand ranges from 26 to 140 ft d⁻¹, with an average value of 75 ft d⁻¹;
- (2) Undifferentiated Wilcox ranges from 2 to 204 ft d⁻¹, with an average of 31 ft d⁻¹;
- (3) Calvert Bluff ranges from 4 to 18 ft d⁻¹, with an average of 11 ft d⁻¹;
- (4) Simsboro ranges from 2 to 84 ft d⁻¹, with an average of 24 ft d⁻¹ ; and
- (5) the Carrizo-Wilcox Aquifer as a whole ranges from 7 to 21 ft d⁻¹, with an average of 12 ft d⁻¹

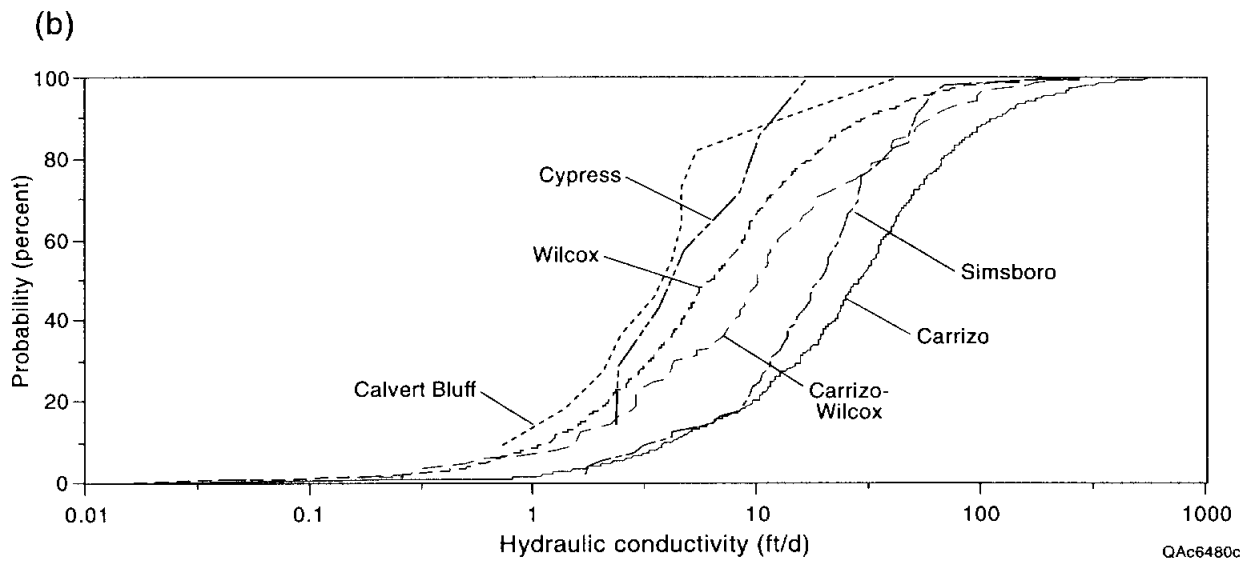
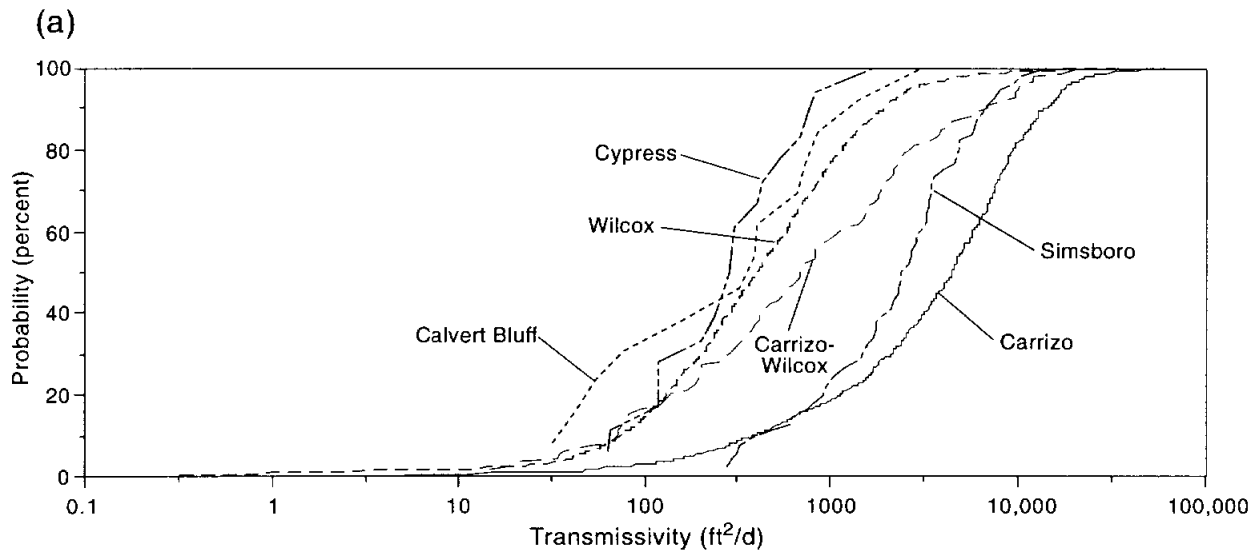


Figure 15. Cumulative distribution functions of transmissivity and hydraulic conductivity for the different geologic units using the data collected from TWDB files.

Thorkildsen and Price (1991) state that the Carrizo Sand is more lithologically uniform than the Wilcox Group. They note that the Carrizo is composed primarily of sand whereas the Wilcox Group is composed of both higher permeability sands and lower permeability clays. The range of hydraulic conductivity they give for Wilcox channel sands is 20 to 60 ft d⁻¹. They also present results from a previous study by Henry and others (1980), which gives hydraulic conductivity values from 3 to 7 ft d⁻¹ for Wilcox Group interchannel sands and muds.

Thorkildsen and Price (1991) spoke conceptually on the similarities and differences between the water-bearing units and suggest that the channel sands of the Wilcox Group have hydraulic conductivities similar to the Carrizo Sand. Our analysis of the entire aquifer finds the standard deviations of hydraulic conductivity of the Carrizo Sand and Wilcox Group to be nearly identical (0.58 ft d⁻¹ and 0.59 ft d⁻¹, respectively) (table 4). Because water wells in the TWDB database tend to be biased toward sandier intervals of the aquifer, we believe that our results are in agreement with the conceptual ideas presented by Thorkildsen and Price (1991).

Based on aquifer tests, Dutton (1999) finds the Carrizo Sand between the Colorado and Brazos Rivers to have a higher variance than the Simsboro and Calvert Bluff Formations of the Wilcox Group and notes that this observation is in contrast to the findings of Thorkildsen and Price (1991).

Prudic (1991) investigated the relationship between hydraulic conductivity and depth and found that hydraulic conductivity generally decreased with increasing depth. However, due to data scatter and poor regression, his equations, presented below, provide only a general description of the relationship. For the upper Wilcox-lower Claiborne in northeastern Texas, hydraulic conductivity increases slightly with depth.

For the Winter Garden area, the relationship for the middle Wilcox is

$$K = \frac{8.7}{10^{0.00022D}} \quad (7)$$

for a depth range of 34 to 3,536 ft and for the upper Wilcox-lower Claiborne is

$$K = \frac{110}{10^{0.00030D}} \quad (8)$$

for a depth range of 105 to 3,890 where D is depth below land surface in feet and K is in ft d^{-1} .

For the northeast area, the relationship for the middle Wilcox is

$$K = \frac{9.1}{10^{0.00010D}} \quad (9)$$

for a depth range of 67 to 2,200 ft and for the upper Wilcox-lower Claiborne is

$$K = 15 \left(10^{0.00044D} \right) \quad (10)$$

for a depth range of 91 to 1,370 ft where D is in feet and K is in ft d^{-1} .

Kier and Larkin (1998) questioned whether there is hydraulic connection between the Carrizo Sand and Simsboro Formation in the central part of the aquifer. Ryder (1988) and Hosman and Weiss (1991) separate the Carrizo-Wilcox into two distinct aquifers: the Lower Claiborne-Upper Wilcox Aquifer and the Middle Wilcox Aquifer. Although some workers have used very low vertical hydraulic conductivity values for confining units in ground-water flow models of the Carrizo-Wilcox aquifer (e.g., Dutton, 1999), it is unclear whether there is significant hydraulic connection between these two aquifer units throughout the state. For example, Dutton (1999) assumed the horizontal and vertical hydraulic conductivity of the clays in the Calvert Bluff and Hooper Formations to be $10^{-3.5}$ and $10^{-5.5}$ ft d^{-1} , respectively, for a numerical model in the central part of the aquifer.

Lateral Variability of Transmissivity and Hydraulic Conductivity

Areally, transmissivity and hydraulic conductivity in the Carrizo-Wilcox aquifer increases from north to south (tables 6 through 9). Counties north of and including Henderson, Anderson, and Houston have geometric mean transmissivity and hydraulic-conductivity values of $450 \text{ ft}^2\text{d}^{-1}$ and 6.7 ft d^{-1} , respectively (table 9; fig. 16). In comparison, counties south of and including Caldwell and Gonzales have geometric mean transmissivity and hydraulic-conductivity values of $4,200 \text{ ft}^2\text{d}^{-1}$ and 29 ft d^{-1} , respectively (table 9; fig. 16). This difference is partially due to geology because more water is produced solely from the sandier Carrizo Sand (fig. 4) in the south part of the aquifer (85 percent of the wells) than in the north part (15 percent of the wells).

Prudic (1991) noted greater values of hydraulic conductivity in the southwestern part of the aquifer than in the northeastern part (table 6). As part of a greater study of the Gulf Coast aquifers, he noted values of 43 ft d^{-1} for hydraulic conductivity of the aquifer in all the states in the coastal region, 14 ft d^{-1} for the northeastern part of the Carrizo-Wilcox aquifer in Texas, and 22 ft d^{-1} for the southwestern part of the Carrizo-Wilcox aquifer in Texas (Prudic, 1991)

Carrizo Sand and Wilcox Group transmissivity and hydraulic conductivity values from the TWDB database are spatially correlated (fig. 17). Semivariograms show a decrease in semivariance for smaller separation distances indicating spatial continuity. However, the semivariograms also have relatively large nuggets, especially the semivariograms for transmissivity and hydraulic conductivity in the Wilcox Group, suggesting a large amount of randomness due to local-scale heterogeneity and/or measurement errors.

The range, or the distance within which a parameter is spatially correlated, is about 80,000 to 100,000 ft for transmissivity and hydraulic conductivity in the Carrizo Sand and about 130,000 for transmissivity and hydraulic conductivity in the Wilcox Group (table 10, fig. 17). This means that transmissivity and hydraulic conductivity values measured in the Carrizo Sand

Table 6. Hydraulic conductivity values (ft d⁻¹) reported by Prudic (1991).

<i>Test</i>	<i>#</i>	<i>s</i>	\bar{x}_a	\bar{x}_h	\bar{x}_g	$P_{0.01}$	$P_{0.25}$	$P_{0.5}$	$P_{0.75}$	$P_{0.99}$
<i>upper Wilcox-lower Clairborne (all states)</i>										
AQ	104	67	70	16	39	0.69	20	43	83	390
SC	151	82	112	16	46	.69	26	47	88	800
COMB	255	76	97	16	43	.84	23	45	84	580
<i>middle Wilcox (all states)</i>										
AQ	213	43	94	5.2	14	.52	5.6	13	40	710
SC	569	48	75	7.4	22	.47	9.9	24	54	430
COMB	782	47	81	6.6	20	.50	8.5	20	51	440
<i>lower Wilcox (all states)</i>										
AQ	58	158	181	32	95	1.0	60	91	170	720
SC	78	129	149	4.2	65	.06	34	77	190	710
COMB	136	141	164	6.6	76	.43	44	84	180	720
<i>Texas Coastal Uplands Aquifer (Texas, Winter Garden area)</i>										
AQ	23	46	59	5.6	18	.61	7.8	17	84	220
SC	43	47	49	7.2	25	.39	13	33	50	180
COMB	66	47	52	6.5	22	.39	9.8	28	54	220
<i>Texas Coastal Uplands Aquifer (Northeast Texas area)</i>										
AQ	185	19	25	5.0	10	.57	5.3	10	23	170
SC	177	27	27	10	18	.79	9.6	17	37	140
COMB	362	23	26	6.6	14	.58	6.9	14	29	140

AQ = T from aquifer tests

SC = T from specific capacity datas

COMB = both together

number of tests

s standard deviation

\bar{x}_a arithmetic mean

\bar{x}_h harmonic mean

\bar{x}_g geometric mean

$P_{0.01}$ 1st percentile

$P_{0.25}$ 25th percentile

$P_{0.5}$ 50th percentile (median)

$P_{0.75}$ 75th percentile

$P_{0.99}$ 99th percentile

Statistical analysis excludes values above 1,000 ft d⁻¹

Table 7. Transmissivity values (ft²d⁻¹) from the TWDB database for the different counties in the study area.

	n	25 th	50 th	75 th	90 th	\bar{x} ^a	s ^b
Anderson	66	360	860	2,300	3,900	850	0.54
Angelina	4	2,400	2,600	2,900	3,200	2,700	0.09
Atascosa	140	3,500	6,300	9,300	15,000	5,200	0.42
Bastrop	40	670	1,800	3,300	5,500	1,300	0.59
Bexar	16	430	980	2,700	10,000	1,200	0.74
Brazos	12	3,900	6,600	8,400	10,000	4,600	0.40
Burleson	9	930	1,100	2,300	2,400	1,200	0.25
Caldwell	35	140	910	1,700	3,000	560	0.63
Camp	25	210	340	680	980	330	0.45
Cass	5	190	510	610	650	230	0.68
Cherokee	9	220	300	1,300	3,200	410	0.75
Dimmit	24	940	1,200	2,500	3,600	1,400	0.34
Franklin	6	140	650	1,800	3,000	550	0.72
Freestone	16	170	180	260	410	210	0.29
Frio	208	5,400	8,700	13,000	19,000	8,100	0.33
Gonzales	14	820	4,600	6,800	7,900	2,400	0.71
Gregg	11	190	220	370	790	270	0.31
Guadalupe	10	450	1,400	2,700	31,000	1,700	0.79
Harrison	30	150	320	710	1,300	310	0.52
Henderson	9	100	350	370	420	170	0.46
Hopkins	15	150	330	590	680	270	0.40
Houston	5	830	1,400	2,500	3,800	1,500	0.42
Karnes	1	-	-	-	-	-	-
La Salle	7	1,600	2,400	3,100	4,200	2,400	0.23
Lee	8	140	790	2,700	3,700	620	0.73
Leon	20	300	510	1,000	2,500	550	0.46
Limestone	5	650	860	1,100	1,100	620	0.37
Maverick	2	-	-	-	-	120	-
McMullen	2	-	-	-	-	1,400	-
Medina	24	400	1,700	4,600	13,000	1,600	0.66
Milam	10	420	2,100	3,100	3,800	950	0.76
Morris	8	100	180	330	640	210	0.51
Nacogdoches	11	200	450	660	810	380	0.30
Navarro	1	-	-	-	-	1,300	-
Panola	38	160	600	1,000	1,400	440	0.51
Rains	12	160	210	300	640	240	0.28
Robertson	14	440	1,400	2,000	3,500	1,000	0.52
Rusk	105	280	570	1,100	1,900	530	0.45
Sabine	2	-	-	-	-	21	-
San Augustine	1	-	-	-	-	980	-

Table 7. continued

Parameter	n	25 th	50 th	75 th	90 th	\bar{x} ^a	s ^b
Shelby	21	170	460	760	1,500	390	0.42
Smith	90	240	990	3,000	5,000	900	0.64
Titus	6	180	330	830	1,000	310	0.52
Upshur	40	78	170	360	710	190	0.46
Van Zandt	55	150	290	510	690	280	0.39
Webb	4	19	33	120	920	69	1.20
Wilson	120	2,600	5,400	10,000	15,000	4,800	0.47
Wood	61	170	460	1,000	2,700	460	0.55
Zavala	15	4,500	7,500	9,300	12,000	6,000	0.31

^a Based on log transformation of original data

^b Log-transformed standard deviation

n number of values

25th 25th percentile

50th 50th percentile (median)

75th 75th percentile

90th 90th percentile

\bar{x} mean

s standard deviation

Table 8. Hydraulic conductivity values (ft d⁻¹) from the TWDB database for the different counties in the study area.

	n	25 th	50 th	75 th	90 th	\bar{x} ^a	s ^b
Anderson	66	5.1	11.	21.	47.	11.	0.54
Angelina	4	25.	26.	30.	34.	28.	0.10
Atascosa	123	16.	34.	58.	94.	27.	0.49
Bastrop	35	5.6	18.	28.	79.	15.	0.60
Bexar	12	8.7	14.	45.	57.	13.	0.83
Brazos	12	9.1	15.	26.	30.	12.	0.44
Burleson	9	8.0	13.	23.	28.	13.	0.35
Caldwell	30	4.3	14.	48.	80.	12.	0.68
Camp	25	2.8	5.4	9.0	11.	4.7	0.47
Cass	5	0.50	3.4	3.6	4.5	1.4	0.66
Cherokee	8	3.0	5.1	8.6	64.	7.7	0.74
Dimmit	12	3.6	4.0	12.	20.	6.3	0.35
Franklin	6	2.6	12.	28.	45.	8.5	0.76
Freestone	16	2.8	3.5	5.0	6.3	3.5	0.27
Frio	180	23.	37.	85.	170.	43.	0.41
Gonzales	14	24.	55.	230.	390.	60.	0.73
Gregg	11	3.0	4.2	8.4	11.	3.2	0.62
Guadalupe	8	20.	24.	49.	200.	32.	0.58
Harrison	30	2.3	4.3	10.	23.	4.6	0.51
Henderson	5	3.5	4.5	5.8	7.2	4.0	0.31
Hopkins	15	3.9	7.2	11.	15.	6.3	0.32
Houston	5	4.8	7.3	13.	26.	8.9	0.43
Karnes	1	-	-	-	-	9.4	-
La Salle	5	6.1	6.6	9.8	11.	7.5	0.14
Lee	6	1.8	4.7	170.	1300.	21.	1.47
Leon	20	3.5	6.9	10.	27.	6.7	0.44
Limestone	5	4.4	14.	23.	38.	11.	0.59
Maverick	1	-	-	-	-	0.62	-
McMullen	2	-	-	-	-	4.2	-
Medina	10	9.6	17.	44.	70.	14.	0.75
Milam	8	5.5	12.	22.	51.	12.	0.50
Morris	8	1.2	2.2	5.1	13.	2.9	0.62
Nacogdoches	11	3.9	4.8	7.7	9.3	4.9	0.23
Panola	36	2.6	11.	20.	27.	8.1	0.59
Rains	12	3.4	3.9	6.2	11.	5.0	0.26
Robertson	9	4.3	7.0	12.	33.	8.1	0.47
Rusk	93	4.0	7.0	11.	24.	6.8	0.44
Sabine	2	-	-	-	-	0.85	-
San Augustine	1	-	-	-	-	19.	-
Shelby	17	2.9	9.5	24.	36.	9.2	0.52

Table 8. continued

	n	25th	50th	75th	90th	\bar{x} ^a	<i>s</i> ^b
Smith	79	4.7	11.	29.	51.	11.	0.56
Titus	6	4.3	9.5	13.	13.	5.9	0.49
Upshur	40	1.2	3.1	7.6	14.	3.1	0.51
Van Zandt	51	2.3	4.8	8.8	13.	4.5	0.45
Webb	3	0.13	1.6	1.7	1.8	0.31	1.28
Wilson	108	19.	37.	69.	150.	33.	0.54
Wood	60	3.0	9.0	19.	55.	8.6	0.60
Zavala	8	22.	48.	89.	150.	42.	0.56

^a Based on log transformation of original data

^b Log-transformed standard deviation

- n** number of values
- 25th** 25th percentile
- 50th** 50th percentile (median)
- 75th** 75th percentile
- 90th** 90th percentile
- \bar{x} mean
- s* standard deviation

Table 9. General areal distribution of transmissivity and hydraulic conductivity values.

	n	25th	50th	75th	90th	\bar{x} ^a	s ^b
<i>Transmissivity (ft²d⁻¹)</i>							
Northeastern area	635	190.	450.	1,000.	2,600.	450.	0.55
Central area	135	330.	1,000.	2,600.	5,300.	920.	0.61
Southwestern area	624	2,200.	5,800.	10,000.	17,000.	4,200.	0.58
<i>Hydraulic conductivity (ft d⁻¹)</i>							
Northeastern area	596	3.0	7.0	15.	33.	6.7	0.54
Central area	120	4.1	9.2	22.	44.	9.8	0.59
Southwestern area	517	15.	33.	68.	130.	29.	0.57

Counties north of and including Henderson, Anderson, and Houston Counties define the northeastern area. Counties south of and including Caldwell and Gonzales Counties define the southwestern area. The central area includes counties between the northeastern and southwestern areas.

^a Based on log transformation of original data

^b Log-transformed standard deviation.

- n** number of values
- 25th** 25th percentile
- 50th** 50th percentile (median)
- 75th** 75th percentile
- 90th** 90th percentile
- \bar{x} mean
- s** standard deviation

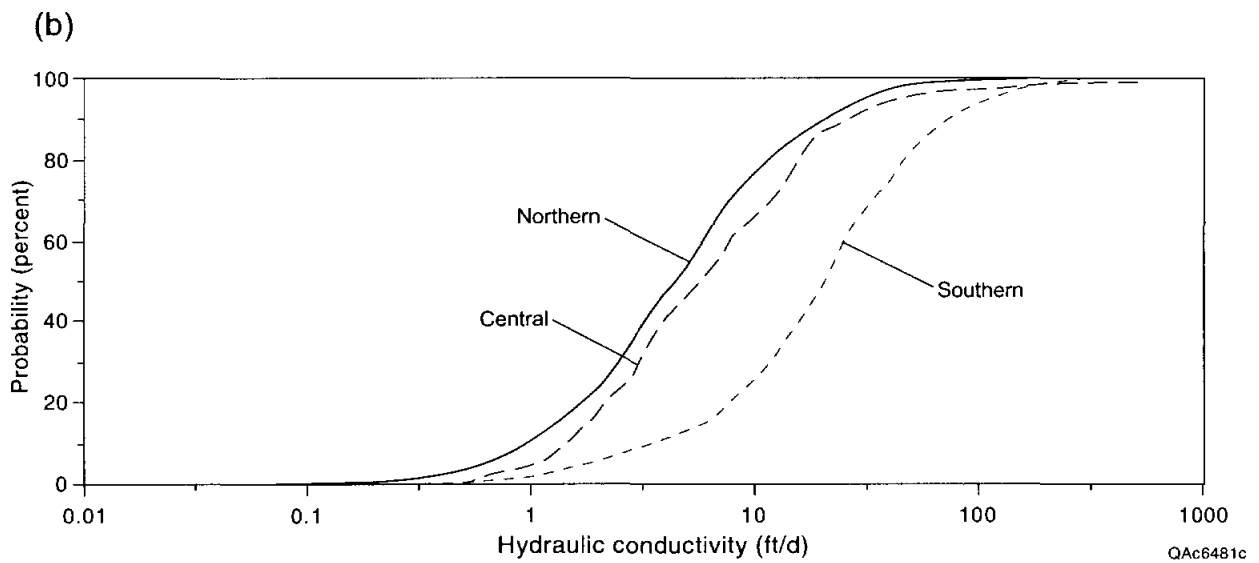
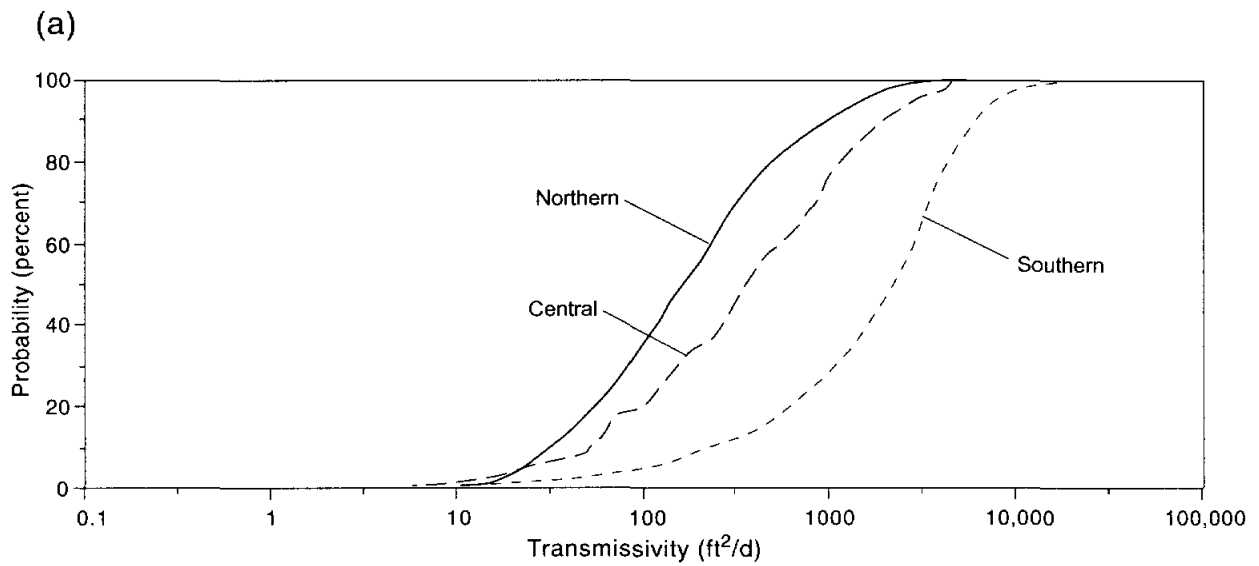
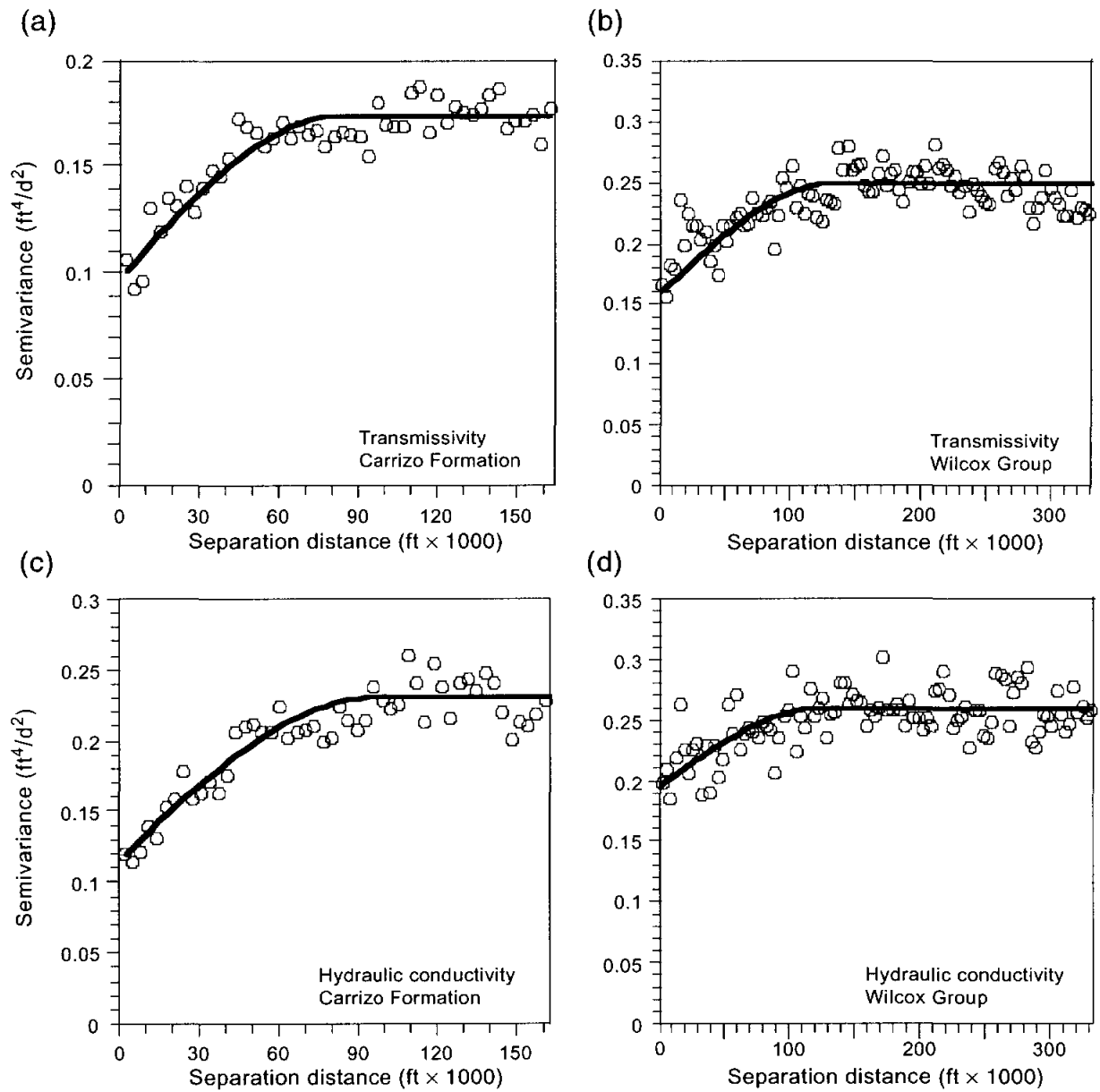


Figure 16. Cumulative distribution functions of transmissivity and hydraulic conductivity for the northern, central, and southern areas of the aquifer.



QA6482c

Figure 17. Experimental (dots) and theoretical (lines) semivariograms of transmissivity and hydraulic conductivity in the Carrizo Formation and Wilcox Group.

Table 10. Fitting parameters for the theoretical semivariograms.

	<i>N</i>	<i>C</i>	<i>a</i>
Transmissivity in Carrizo Sand	0.1	0.075	82,000
Transmissivity in Wilcox Group	0.16	0.09	130,000
Hydraulic conductivity in Carrizo Sand	0.11	0.12	98,000
Hydraulic conductivity in Wilcox Group	0.19	0.07	130,000

for semivariograms of transmissivity, *N* and *C* have units of ft^4d^{-2}
 for semivariograms of hydraulic conductivity, and have units of ft^2d^{-2}
a has units of ft

and the Wilcox Group are similar to other values within about 17 and 25 mi, respectively. Although the range is larger for the Wilcox Group than for the Carrizo Sand, the autocorrelation of transmissivity and hydraulic conductivity in the Carrizo Sand is stronger because there is less of a nugget effect (80 percent of the variance is represented by the nugget for hydraulic conductivity for the Wilcox Group compared with 50 percent for the Carrizo Sand). In other words, we quantify the more homogeneous nature of the Carrizo Sand relative to the Wilcox Group.

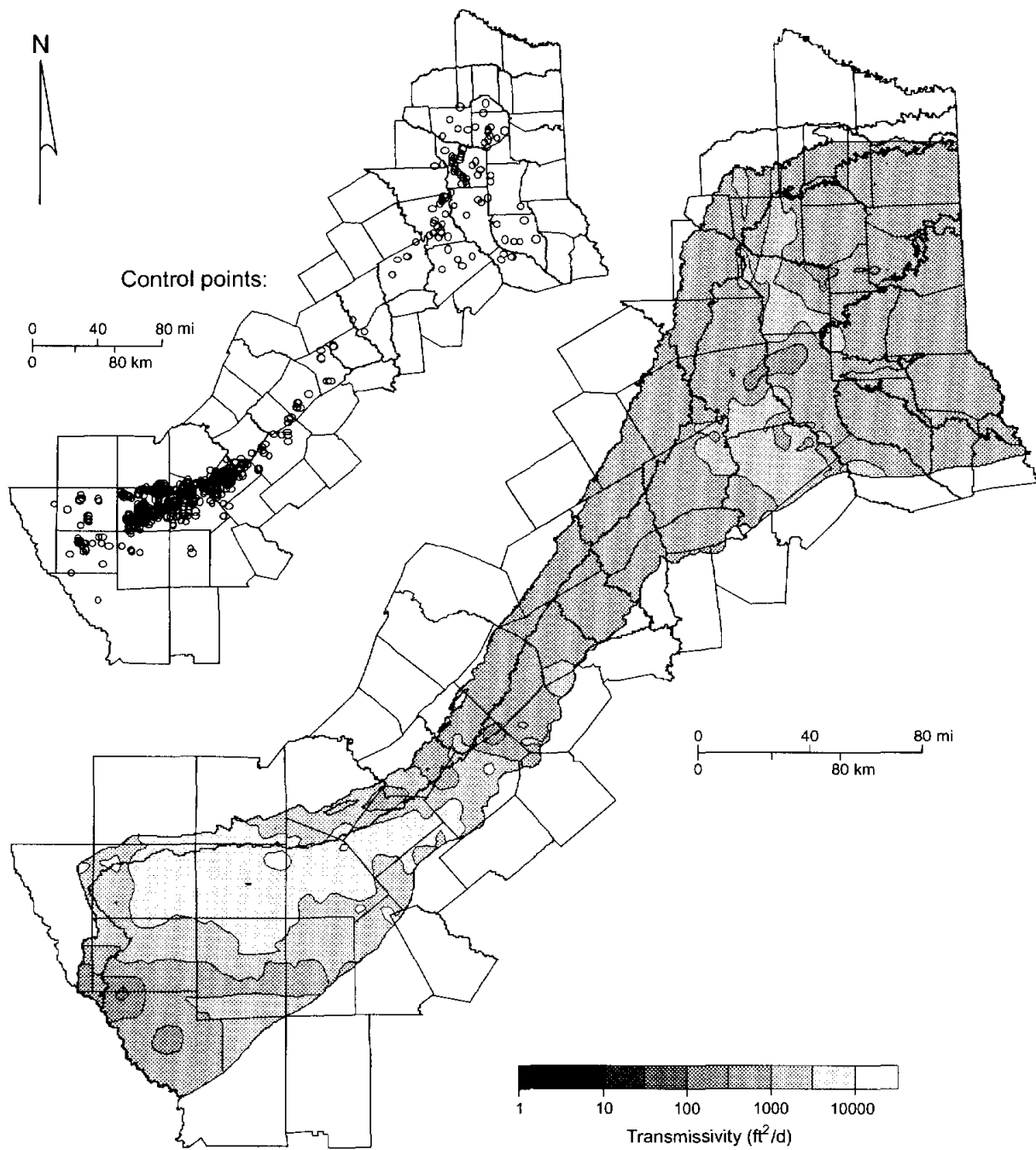
Theoretical semivariograms, spherical semivariograms with a nugget effect, were visually fit to the experimental data. The spherical semivariogram, γ is described by

$$\gamma(h) = N + C \left[\frac{3h}{3a} - \frac{h^3}{2a^3} \right] \quad (7)$$

where h is the separation distance, N is the nugget, C is the sill, and a is the range (see fig. 8). Parameters, N , C , and a for the four semivariograms shown in figure 17 are listed in table 10.

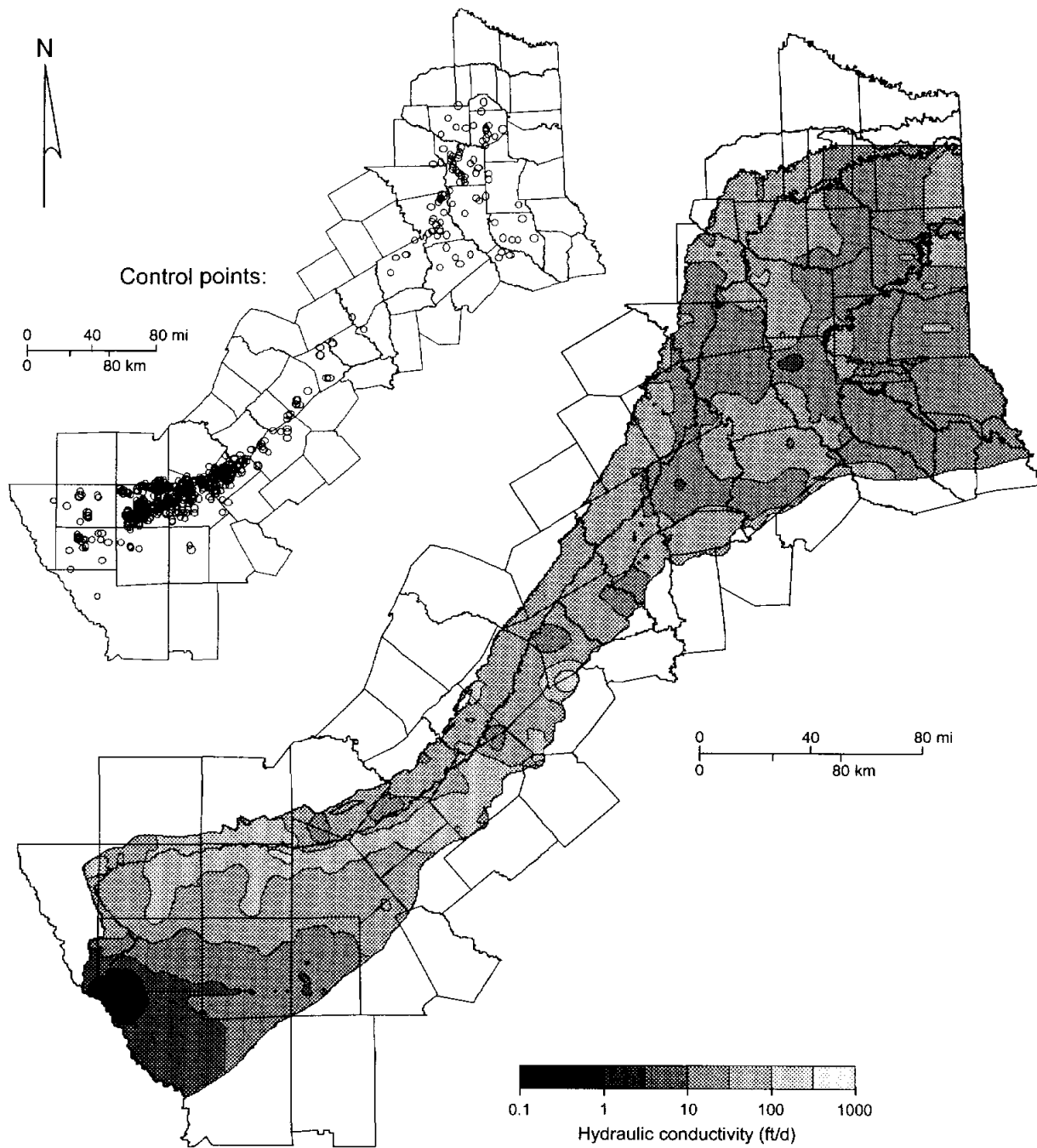
Using parameters for the fitted theoretical semivariograms, we used the kriging function in Surfer (GSI, 1995) to contour transmissivity and hydraulic conductivity of the Carrizo Sand and Wilcox Group for tests from the TWDB database. Note that although transmissivity and hydraulic conductivity are contoured for the entire extent of the aquifer, interpolated and extrapolated values are only valid near control points (figs. 18 through 21).

Transmissivity and hydraulic conductivity values for the Carrizo Sand are abundant in (1) the Winter Garden irrigation district area in the southwest part of the aquifer (south of the Nueces River) and (2) in the west part (Sabine Uplift) of the north part of the aquifer (north of the Trinity River) (figs. 18, 19). The Carrizo Sand has higher values of transmissivity and hydraulic conductivity in the southwest part of the aquifer than in the northeast and central parts (figs. 18, 19). The greatest transmissivities and hydraulic conductivities in the Carrizo Sand are



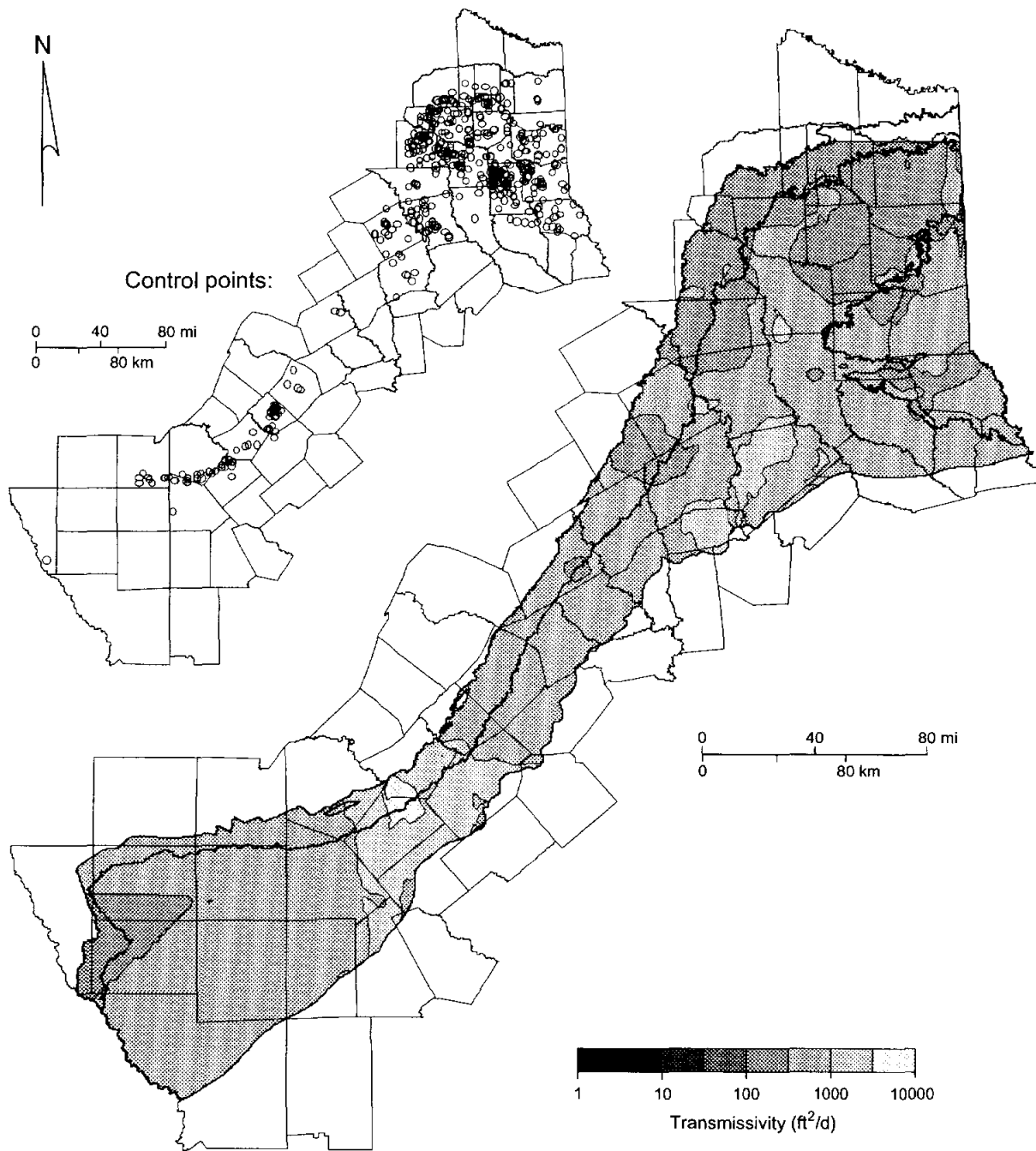
QA6483c

Figure 18. Spatial distribution of transmissivity in the Carrizo Formation using kriging values from the TWDB database. Location of control points shown in upper left-hand corner.



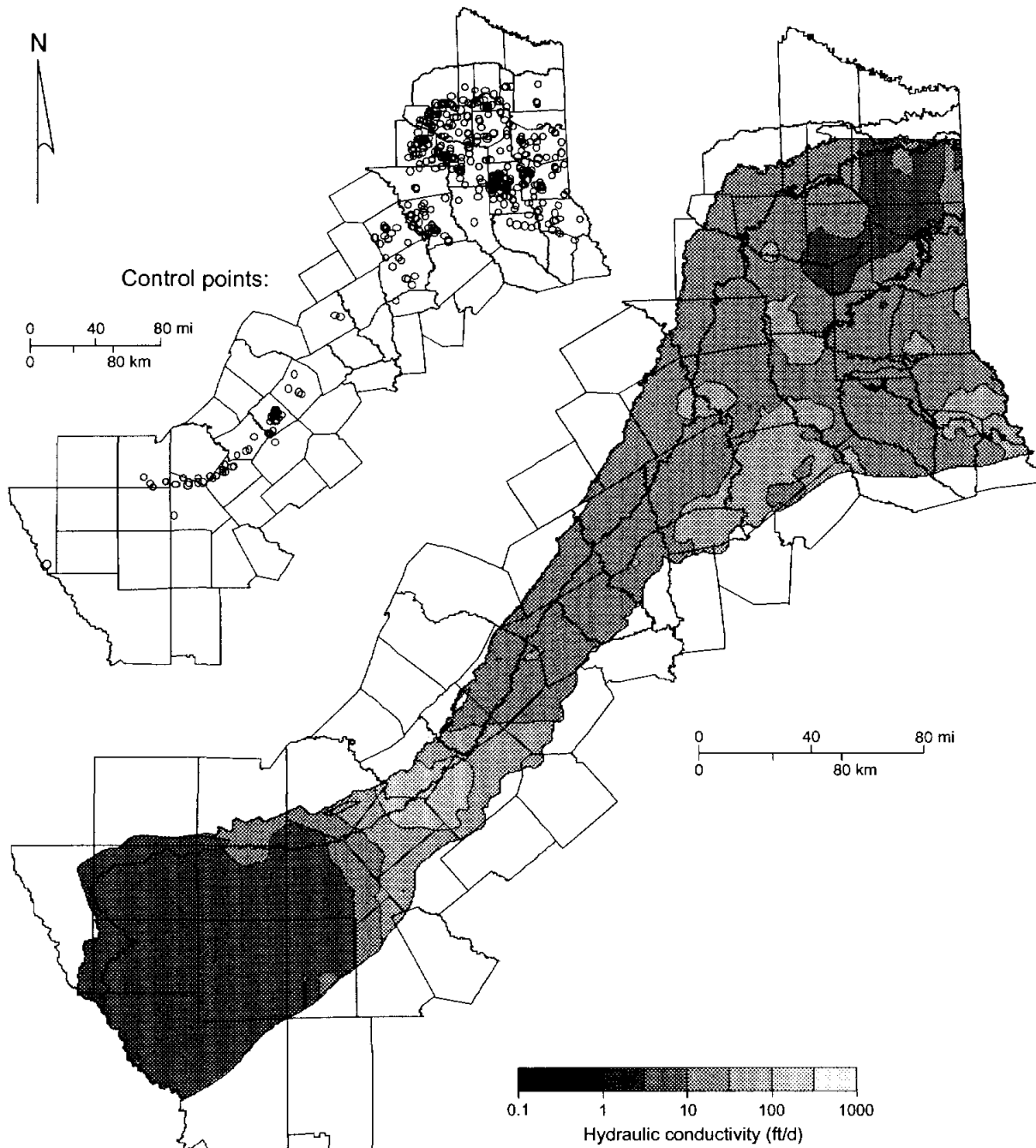
QA6484c

Figure 19. Spatial distribution of hydraulic conductivity in the Carrizo Formation using kriging values from the TWDB database. Location of control points shown in upper left-hand corner.



QA6485c

Figure 20. Spatial distribution of transmissivity in the Wilcox Group using kriging values from the TWDB database. Location of control points shown in upper left-hand corner.



QA6486c

Figure 21. Spatial distribution of hydraulic conductivity in the Wilcox Group using kriging values from the TWDB database. Location of control points shown in upper left-hand corner.

found in Atascosa, Frio, Gonzales, Wilson, and Zavala Counties (figs. 18, 19). This finding is consistent with the observation by Ashworth and Hopkins (1995) that some of the greatest yields are produced in the Carrizo sand in the south, or Winter Garden, area of the aquifer. This localization of higher transmissivity and hydraulic conductivity in the Winter Garden area is also consistent with observed increases in (1) percent sand and sand thickness of the Lower Claiborne-Upper Wilcox aquifer (fig. 4 and table 1) and (2) presence of a very high permeability beach sand deposit (table 1).

Transmissivity and hydraulic conductivity values for the Wilcox Group are abundant in the northeast part of the aquifer (Sabine Uplift) and in the outcrop of the Winter Garden irrigation district area in the southwest part of the aquifer (figs. 20, 21). The Wilcox Group has higher values of transmissivity and hydraulic conductivity in (1) the south-central part of the aquifer just south of the Guadalupe River and (2) the south part of the northeast part of the aquifer, adjacent to the Trinity River (figs. 20, 21). The greatest transmissivities and hydraulic conductivities in the Wilcox Group are found in Caldwell, Guadalupe, Wilson, and parts of Anderson, Leon, and Smith Counties (figs. 20, 21). We expected the Wilcox Group hydraulic values to be higher to the north of the Colorado and south of the Trinity Rivers because this is where the Simsboro Formation is present. The scarcity of control point wells in this area is probably influencing the lower than expected values of transmissivity and hydraulic conductivities of the Wilcox Group kriged data.

Relationship between Hydraulic Conductivity and Sand Thickness

To investigate the possible relationship between hydraulic conductivity and sand thickness, we digitized generalized net sand maps for the upper and lower Wilcox Group published in Bebout and others (1982). We then used the geographic information system to query the net sand map for the net sand in each well test from the TWDB database and tested for a

relationship between net sand thickness and hydraulic conductivity. However, of the 642 transmissivity values available for analysis, 41 percent of the well locations were in the outcrop where net-sand values are not available, and 58 percent of the remaining well locations had the same value for net sand. Therefore, we were not able to assess the relationship between regional net-sand thickness and hydraulic properties.

More detailed, local-scale analyses of the relationship between hydraulic conductivity and sand thickness were conducted by several other workers. Payne (1975) investigated the relationship between hydraulic conductivity and sand thickness. He found that for sands deposited in stream channels, the hydraulic conductivity varied directly with the sand thickness. Henry and others (1979, 1980) reported hydraulic conductivities of 20 to 66 ft d⁻¹ (6 to 20 m d⁻¹) for the Simsboro and Calvert Bluff sands and 3 to 6 ft d⁻¹ (1 to 2 m d⁻¹) for interchannel muds in East Texas. Fogg (1986) found that thicker channel-fill sands in the Wilcox Group were more permeable and continuous than sands deposited in the adjacent floodplain and interchannel basins. Thorkildsen and Price (1991) reported hydraulic conductivities ranging from 20 to 60 ft d⁻¹ in the channel sand deposits and 3 to 7 ft d⁻¹ in the interchannel muds. Prudic (1991) did not find a conclusive relationship between hydraulic conductivity and sand thickness for the entire region.

STORATIVITY

We were able to compile 107 values of storativity and calculate 68 values of specific storage (storativity divided by the screen length) for the Carrizo-Wilcox aquifer. Of the storativity values, we compiled 64 percent from TRRC files of pumping and slug tests at lignite mines. Eleven of the values compiled from TRRC files were determined from slug tests.

Storativity and specific storage both approximate log-normal distributions (fig. 22). Storativity ranges from about 10^{-6} to 10^{-1} , with a geometric mean of 3.0×10^{-4} (fig. 22a; table 11). These results cover the range of expected unconfined, semiconfined, and confined values of storativity. Specific storage ranges from about 10^{-7} to 10^{-3} with a geometric mean of 4.5×10^{-6} (fig. 22b; table 11). Lower values of storativity and specific storage tend to occur at shallow depths, as would be expected with unconfined conditions (fig. 23). However, semiconfined to confined storativities (values less than 0.01) also occur at shallow depths (fig. 23). We did not see patterns in differences of geometric mean storage values for different data sources, test methods, or formations.

Several researchers have reported on the storage properties of the Carrizo-Wilcox aquifer. Follett (1970) reported storativities in the Carrizo-Wilcox aquifer that range from 0.0003 to 0.0006. Klemt and others (1976) reported an average unconfined storativity (specific yield) of 0.25 and an average confined storativity of 0.0005 for the Carrizo aquifer. Duffin and Elder (1979) used seismic refraction along 20 profiles to estimate specific yield in the Carrizo Sand in South Texas (west of Gonzales County) and found values that range between 0.05 and 0.35. They found higher values (0.26 to 0.32) east of the Frio River and lower values (0.16 to 0.24) west of the Frio River. Thorkildsen and others (1989) estimated confined storativity to range between 10^{-5} and 10^{-3} and unconfined storativity (specific yield) to range between 0.05 and 0.3. Prudic (1991) assumed that (1) the storativity was 0.15 for well depths or top of screened interval shallower than 150 ft, and (2) the specific storage was 4×10^{-6} ft⁻¹ for well depths greater than 150 ft. Thorkildsen and Price (1991) reported confined storativities to range between 10^{-2} and 10^{-5} and unconfined storativity to range from 0.1 to 0.3. Ryder (1996) estimated that the unconfined storativity ranges between 0.1 and 0.3 and the confined storativity ranges between 1.0×10^{-4} and 1.5×10^{-3} .

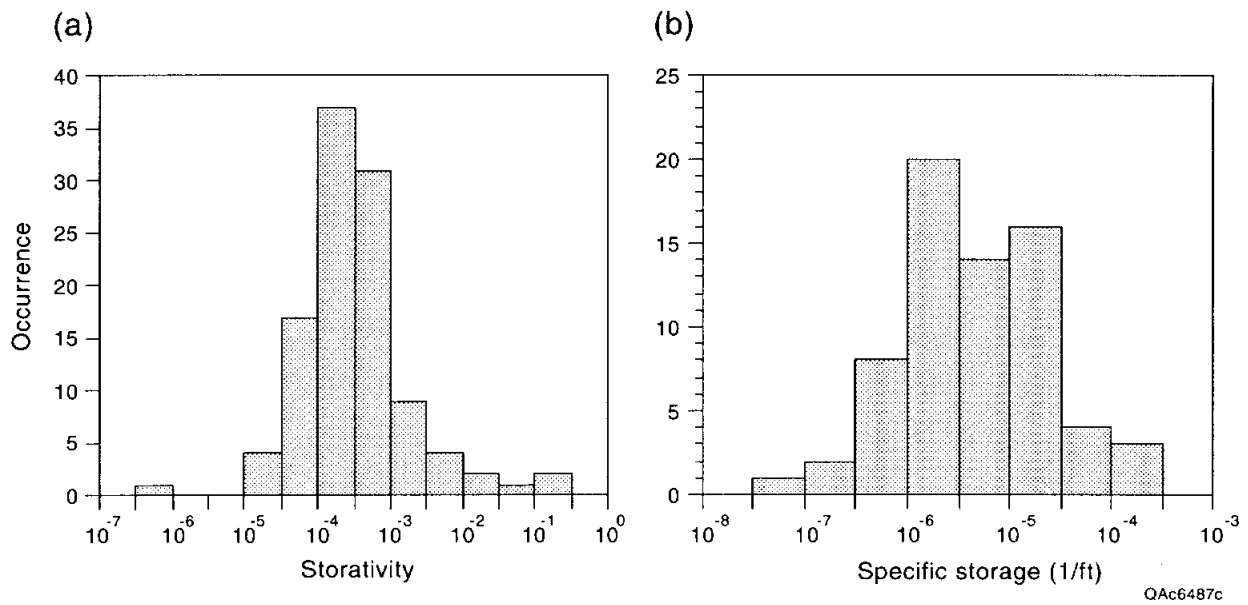


Figure 22. Histograms of storativity and specific storage for the Carrizo-Wilcox aquifer.

Table 11. Storativity and specific storage (ft⁻¹) values for the Carrizo-Wilcox aquifer.

	n	25th	50th	75th	90th	\bar{x} ^a	s^b
Storativity (-)	108	10 ^{-4.00}	10 ^{-3.52}	10 ^{-3.22}	10 ^{-2.60}	10 ^{-3.52}	0.78
Specific storage	68	10 ^{-5.83}	10 ^{-5.35}	10 ^{-4.81}	10 ^{-4.49}	10 ^{-5.34}	0.69

^a Based on log transformation of original data

^b Log-transformed standard deviation.

n number of values

25th 25th percentile

50th 50th percentile (median)

75th 75th percentile

90th 90th percentile

\bar{x} mean

s standard deviation

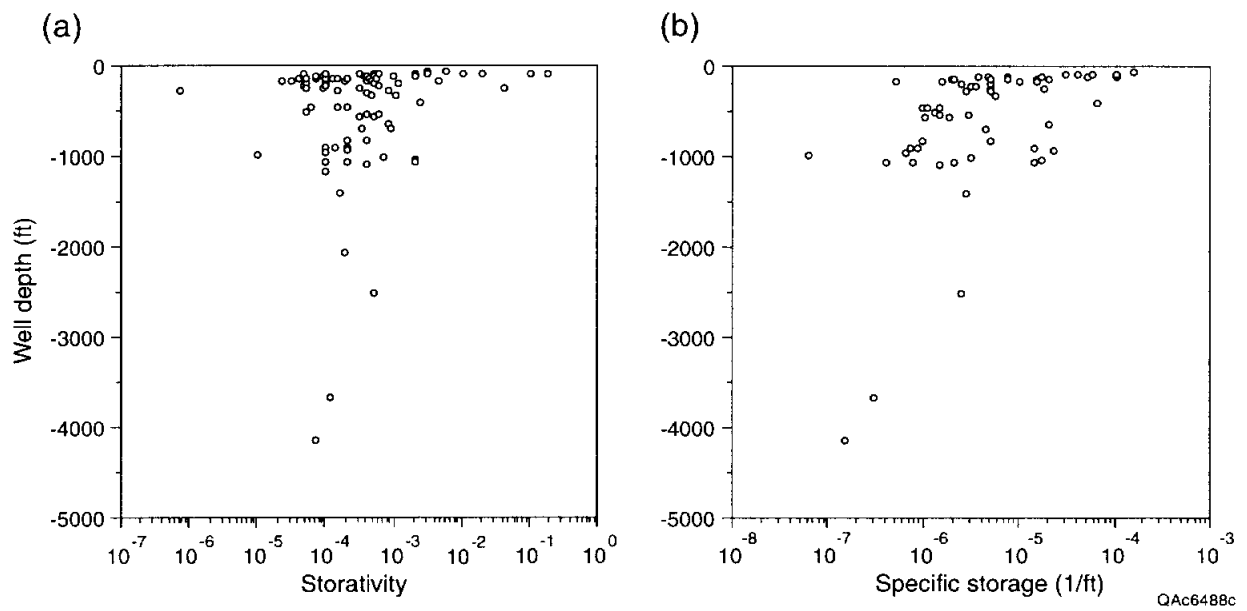


Figure 23. Variation of storativity and specific storage with depth.

Conclusions

In addition to compiling a large data base of hydraulic properties, this study quantifies the variability and spatial distribution of transmissivity, hydraulic conductivity, and storativity and reviews previous hydrogeologic studies of the units that compose the Carrizo-Wilcox aquifer. We think the results of this study will be useful for developing local and regional water plans and developing numerical ground-water-flow models to predict the future availability of the water resource. The main conclusions of our analysis of the data base are:

1. Transmissivity, hydraulic conductivity, and storativity are log-normally distributed.

Transmissivity ranges from about 0.1 to 10,000 ft²d⁻¹ and has a geometric mean value of about 300 ft²d⁻¹, and hydraulic conductivity ranges from about 0.01 to 4,000 ft d⁻¹ and has a geometric mean value of about 6 ft d⁻¹. Storativity and specific storage both approximate log-normal distributions and range from about 10⁻⁶ to 10⁻¹ with a geometric mean of 3.0 × 10⁻⁴ and from about 10⁻⁷ to 10⁻³ with a geometric mean of 4.5 × 10⁻⁶, respectively. Lower values of storativity and specific storage tend to occur at shallow depths, as would be expected with unconfined conditions. We did not see differences of geometric mean storage values for different data sources, test methods, or geologic formations.

2. Different data sources and testing procedures may be biased and result in different statistical distributions of transmissivity and hydraulic conductivity. Tests from TNRCC and TRRC files have geometric mean transmissivity and hydraulic conductivity values that are about 10 and 4 times lower, respectively, than tests from the TWDB data base, water utilities, and reference sources. This difference is due in part to the wide range in geologic environments tested and the types of wells (municipal versus private) tested.

3. Transmissivity and hydraulic conductivity vary vertically among formations and laterally within formations. The Simsboro and Carrizo Sands have transmissivity and hydraulic-conductivity values that are 2.5 to 11 times higher and 2 to 6 times higher, respectively, than does the Cypress aquifer (Wilcox Group, Carrizo Sand, Reklaw Formation, and Queen City Sand in northeast Texas), Calvert Bluff Formation, and Wilcox Group.
4. Lateral variations of transmissivity and hydraulic conductivity have spatial continuity. Semivariograms show that transmissivity and hydraulic-conductivity values in the Carrizo Sand and Wilcox Group are spatially correlated over about 17 and 25 mi, respectively. However, the semivariograms also have relatively large nuggets, especially for tests from the Wilcox Group, suggesting a large amount of randomness due to local-scale heterogeneity and measurement errors. Kriged maps of transmissivity and hydraulic conductivity show the greatest values for the Carrizo Sand in the Winter Garden area and the greatest values for the Wilcox Group in the south-central and northeast parts of the study area.

Acknowledgments

The work described in this report was sponsored by the Texas Water Development Board. We thank the municipal and industrial ground-water users and water-supply companies that shared their data and thoughts with us. We thank Mr. David Thorkildsen of the TWDB for sharing the hydraulic-conductivity data estimated from well logs for the TWDB models of the Carrizo-Wilcox aquifer. We also thank the friendly staff at the TWDB, TRRC, and the TNRCC for their help in retrieving data from their files. Report illustrations were prepared by Jana Robinson under the direction of Joel L. Lardon, Graphics Manager. Word processing was done by Susan Lloyd, and Lana Dieterich edited the report under the supervision of Susan Doenges.

Acronyms

BEG	Bureau of Economic Geology
TNRCC	Texas Natural Resource Conservation Commission
TRRC	Texas Railroad Commission
TWDB	Texas Water Development Board
USGS	U.S. Geological Survey

References

- Ashworth, J. B., and Hopkins, Janie, 1995, Aquifers of Texas: Texas Water Development Board Report 345, 69 p.
- Ayers, W. B. and Lewis, A. H., 1985, The Wilcox Group and Carrizo Sand (Paleogene) in east-central Texas: depositional systems and deep-basin lignite: University of Texas at Austin, Bureau of Economic Geology Special Publication, 19 p., 30 pl.
- Barnes, V. E., 1970, Waco sheet: University of Texas at Austin, Bureau of Economic Geology, Geologic Atlas of Texas, scale 1:250,000.
- _____ 1974, Austin sheet: University of Texas at Austin, Bureau of Economic Geology, Geologic Atlas of Texas, scale 1:250,000.
- Bebout, D. G., Weise, B. R., Gregory, A. R., and Edwards, M. B., 1982, Wilcox Sandstone reservoirs in the deep subsurface along the Texas Gulf Coast; their potential for production of geopressured geothermal energy: University of Texas at Austin, Bureau of Economic Geology Report of Investigations No.117, 125 p.
- Broom, M. E., Alexander, W. H., and Myers, B. N., 1965, Ground-water resources of Camp, Franklin, Morris, and Titus Counties, Texas: Texas Water Commission Bulletin 6517, 153 p.
- Broom, M. E., 1966, Ground-water resources of Harrison County, Texas: Texas Water Development Board Report 27, 75 p.
- _____ 1968, Ground-water resources of Wood County, Texas: Texas Water Development Board Report 79, 89 p.
- _____ 1969, Ground-water resources of Gregg and Upshur Counties, Texas: Texas Water Development Board Report 101, 83 p.
- Brown, R. H., 1963, Estimating the transmissivity of an artesian aquifer from the specific capacity of a well: U.S. Geological Survey Water Supply Paper 1536-I, p. 336-338.
- Clark, Isobel, 1979, Practical geostatistics: Applied Science Publishers, Limited, London, 129 p.
- Cooper, H. H., Jr., and Jacob, C. E., 1946, A generalized graphical method for evaluating formation constants and summarizing well field history: American Geophysical Union Transactions, v. 27, p. 526-534.

- Duffin, G. L., and Elder, G. R., 1979, Variations in specific yield in the outcrop of the Carrizo Sand in South Texas as estimated by seismic refraction: Texas Department of Water Resources Report 229, 56 p.
- Dutton, A. R., 1999, Groundwater availability in the Carrizo-Wilcox aquifer in Central Texas- numerical simulations of 2000 through 2050 withdrawal projections: University of Texas at Austin, Bureau of Economic Geology Report of Investigations No. 256, 53 p.
- Elder, G. R., and Duffin, G. L., 1980, Records of wells, water levels, pumpage, and chemical analysis of water from the Carrizo aquifer in the Winter Garden area, Texas: Texas Department of Water Resources Report 254, 127 p.
- El-Naqa, A., 1994, Estimation of transmissivity from specific capacity data in fractured carbonate rock aquifer, central Jordan: *Environmental Geology*, v. 23, no. 1, p. 73-80.
- Fisher, R. S., Mace, R. E., and Boghici, Erika, 1996, Ground-water and surface-water hydrology of Camp Swift, Bastrop County, Texas: The University of Texas at Austin, Bureau of Economic Geology, final report for the Adjutant General's Department of Texas, Texas Army National Guard and the Nature Conservancy of Texas, 53 p.
- Fogg, G. E., 1986, Groundwater flow and sand body interconnectedness in a thick, multiple-aquifer system: *Water Resources Research*, v. 22, no. 5, p. 679-694.
- _____, 1980, Aquifer modeling of the Oakwood salt dome area, *in* *Geology and geohydrology of the East Texas Basin; a report on the progress of nuclear waste isolation feasibility studies*: University of Texas at Austin, Bureau of Economic Geology Geological Circular 81-7, p. 139-149.
- Follett, C. R., 1966, Ground-water resources of Caldwell County, Texas: Texas Water Development Board Report 12, 138 p. + 3 pl.
- _____, 1970, Ground-water resources of Bastrop County, Texas: Texas Water Development Board Report 109, 138 p.
- Galloway, W. E., Liu, Xijin, Travis-Neuberger, Deborah, and Xue, Liangqing, 1994, Reference high-resolution correlation cross sections, Paleogene section, Texas Coastal Plain: University of Texas at Austin, Bureau of Economic Geology, 19 p., 4 pl.
- Gaylord, J. L., Slade, R. M., Jr., Ruiz, L. M., Welborn, C. T., and Baker, E. T., Jr., 1985, Water resources appraisal of the Camp Swift lignite area, Central Texas: U.S. Geological Survey, Water-Resources Investigations Report 84-4333, 164 p.
- Grubb, H. F., and Carillo, J. J., 1988, Region 23, Gulf of Mexico coastal plain, *in* Back, W., Rosenshein, J. S., and Seaber, P. R., eds., *Hydrogeology*: Boulder, Colorado, Geological Society of America, *The Geology of North America* v. O-2, p. 219-228.
- GSI, 1995, Surfer (Win32) Version 6.01, Surface Mapping System: Golden, Colorado, Golden Software, Inc., software.
- Guyton, W. E., 1942, Results of pump tests in wells at Camp Swift, Texas: U.S. Geological Survey, Open File Report, 27 p.
- Guyton, W. F. & Associates, 1972, Ground-Water conditions in Andson, Cherokee, Freestone, and Henderson Counties, Texas: Texas Water Development Board Report 150, 250 p.
- Guyton and Associates, 1998, Interaction between ground water and surface water in the Carrizo-Wilcox aquifer: Final contract report prepared for the Texas Water Development Board by LBG-Guyton and Associates in association with HDR Engineering, Inc., variously paginated.

- Hamlin, H. S., 1988, Depositional and ground-water flow systems of the Carrizo-Upper Wilcox, South Texas: University of Texas at Austin, Bureau of Economic Geology Report of Investigations, No. 175, 61 p.
- Henry, C. D., Basciano, J. M., and Duex, T. W., 1979, Hydrology and water quality of the Eocene Wilcox Group; significance for lignite development in East Texas: Transactions - Gulf Coast Association of Geological Societies, v. 29, p. 127-135.
- _____ 1980, Hydrology and water quality of the Eocene Group- significance for lignite development in east Texas: The University of Texas at Austin, Bureau of Economic Geology Geological Circular 80-3, 9 p.
- Hosman, R. L. and Weiss, J. S., 1991, Geohydrologic units of the Mississippi embayment and Texas coastal uplands aquifer systems, south-central United States: U.S. Geological Survey Professional Paper 1416-B, variously paginated, 19 pl.
- Hovorka, S. D., Mace, R. E., and Collins, E. W., 1995, Regional distribution of permeability in the Edwards Aquifer: University of Texas at Austin, Bureau of Economic Geology, Final contract report to the Edwards Underground Water District under contract no. 93-17-FO, 126 p
- _____ 1998, Permeability structure of the Edwards aquifer, south Texas- Implications for aquifer management: University of Texas at Austin, Bureau of Economic Geology, Report of Investigations No. 250, 55 p.
- Huntley, David, Nommensen, Roger, and Steffey, Duane, 1992, The use of specific capacity to assess transmissivity in fractured-rock aquifers: *Ground Water*, v. 30, no. 3, p. 396-402.
- Jackson, M. P. A., 1982, Fault tectonics of the East Texas Basin: University of Texas at Austin, Bureau of Economic Geology Circular 82-4, 31p.
- Kaiser, W. R., 1974, Texas lignite: near-surface and deep basin resources: University of Texas at Austin, Bureau of Economic Geology Report of Investigations No. 79, 70 p.
- Kier, R. S., and Larkin, R. G., 1998, Hydrogeology of the Carrizo-Wilcox aquifer system- Bastrop, Caldwell, Fayette, Lee, Travis, and Williamson Counties: preliminary report prepared for the Aqua Water Supply Company, Bastrop, Texas: Robert S. Kier Consulting, variously paginated.
- Klemt, W. B., Duffin, G. L., and Elder, G. R., 1976, Ground-water resources of the Carrizo aquifer in the Winter Garden area of Texas, volume 1: Texas Water Development Board report 210, 30 p.
- Kruseman, G. P. and de Ridder, N. A., 1990, Analysis and evaluation of pumping test data, 2nd edition: Wageningen, The Netherlands, International Institute for Land Reclamation and Improvement, 377 p.
- Mace, R. E., 1995, Geostatistical description of hydraulic properties in karst aquifers, a case study in the Edwards Aquifer: in Charbeneau, R. J., ed., *Groundwater Management*, Proceedings of the International Symposium: Water Resources Engineering Division, American Society of Civil Engineers, American Society of Civil Engineers, p. 193-198.
- Mace, R. E., 1997, Determination of transmissivity from specific capacity data in a karst aquifer, *Ground Water*, v. 35 no. 5, p. 738-742.
- Mace, R. E., in review, Using specific-capacity data in hydrogeologic investigations: UT BEG.

- Mace, R. E., Nance, H. S., and Dutton, A. R., 1994, Geologic and hydrogeologic framework of regional aquifers in the Twin Mountains, Paluxy, and Woodbine Formations near the SSC site, North-Central Texas: Draft topical report submitted to the TNRLC under contract no. IAC(92-93)-0301 and no. IAC 94-0108, 48 p.
- Marquardt, G., and Rodriguez, E. Jr., 1977, Ground water resources of the Carrizo Aquifer in the Winter Garden area of Texas: Texas Water Development Board Report 210, 466 p.
- Matheron, G., 1979, Principles of geostatistics: *Economic Geology*, v. 58, p. 1246-1266.
- McCoy, T. W., 1991, Evaluation of the ground-water resources of the Western Portion of the Winter Garden area, Texas: Texas Water Development Board, Report 334, 64 p.
- McCuen, R. H., and Snyder, W. M., 1986, Hydrologic modeling: statistical methods and applications: Englewood Cliffs, New Jersey, Prentice Hall, 568 p.
- Mullican, W. F., III, Johns, N. D., and Fryar, A. E., 1997, Playas and recharge of the Ogallala aquifer on the southern High Plains of Texas- an examination using numerical techniques: University of Texas at Austin, Bureau of Economic Geology Report of Investigations No. 242, 72 p.
- Myers, B. N., 1969, Compilation of results of aquifer tests in Texas: Texas Water Development Board Report 98, 532 p.
- Payne, J. N., 1975, Geohydrologic significance of lithofacies of the Carrizo Sand of Arkansas, Louisiana, and Texas and the Meridian Sand of Mississippi: U.S. Geological Survey Professional Paper, P 0569-D, 11 p.
- Prudic, D. E., 1991, Estimates of hydraulic conductivity from aquifer-test analyses and specific-capacity data, Gulf Coast regional aquifer systems, south-central United States: U. S. Geological Survey, Water-Resources Investigations, WRI 90-4121, 38 p.
- Razack, M., and Huntley, David, 1991, Assessing transmissivity from specific capacity in a large and heterogeneous alluvial aquifer: *Ground Water*, v. 29, no. 6, p. 856-861.
- Ryder, Paul, 1996, Ground water atlas of the United States- Oklahoma, Texas: - U.S. Geological Survey, HA 730-E, variously paginated.
- Ryder, P. D., 1988, Hydrogeology and predevelopment flow in the Texas Gulf Coast Aquifer System, U.S. Geological Survey Water Resource Investigations Report 87-4248, 109 p.
- Tarver, G. E., 1966, Ground-water resources of Houston county, Texas: Texas Water Development Board Report 18, 86 p. + 2 pl.
- Theis, C. V., 1935, The relation between the lowering of the piezometric surface and the rate and duration of discharge of a well using groundwater storage: *American Geophysical Union Transactions*, v. 16, p. 519-524.
- _____ 1963, Estimating the transmissivity of a water-table aquifer from the specific capacity of a well: U.S. Geological Survey Water Supply Paper 1536-I, p. 332-336.
- Theis, C. V., Brown, R. H., and Myers, R. R., 1963, Estimating the transmissibility of aquifers from the specific capacity of wells. Methods of determining permeability, transmissivity, and drawdown: U.S. Geological Survey Water Supply Paper, 1536-I.
- Thomasson, H. J., Olmstead, F. H., and LeRoux, E. R., 1960, Geology, water resources, and usable ground water storage capacity of part of Solano County, CA: U.S. Geological Survey Water Supply Paper 1464, 693 p.
- Thorkildsen, D., and Price, R. D., 1991, Ground-water resources of the Carrizo-Wilcox aquifer in the Central Texas Region: Texas Water Development Board Report 332, variously paginated.

- Thorkildsen, D., Quincy, R., and Preston, R., 1989, A digital model of the Carrizo-Wilcox aquifer within the Colorado River basin of Texas: Texas Water Development Board Report LP-208, 59 p.
- Villaescusa, E., and Brown, E. T., 1990, Characterizing joint spatial correlation using geostatistical methods *in* Barton, Nick, and Stephansson, Ove, Rock joints, Brookfield, Vermont, Proceedings of the International Symposium on Rock Joints, Loen, Norway: A. A. Balkema Publishers, p. 115-122.
- Walton, W. C., 1970, Groundwater resource evaluation: New York, McGraw-Hill.

Appendix A:

List of Cities and water utilities responding to the survey

No.	City	Utility
1	College Station	City of College Station
2	Hallsville	City of Hallsville
3	Seguin	Springs Hill Water Supply Corporation
4	Caldwell	City of Caldwell
5	Carrizo Springs	City of Carrizo Springs
6	Hemphill	South Sabine Water Supply Corporation
7	Mt. Vernon	Cypress Springs Water Supply Corporation
8	Cauton	Crooked Creek Water Supply Corporation
9	Stockdale	Sunko Water Supply Corporation
10	Alba	Bright Star-Salem Water Supply Corporation
11	Kilgore	Liberty City Water Supply Corporation
12	Carrizo Springs	Carrizo Hill Water Supply Corporation
13	Marshall	Cypress Valley Water Supply Corporation
14	Cotulla	City of Cotulla
15	Teague	City of Teague
16	Brownsboro	Edom Water Supply Corporation
17	Stockdale	City of Stockdale
18	Eustace	Purtis Creek State Park
19	Waskom	City of Waskom
20	Waskom	Waskom Rural Water Supply Corporation
21	Carrison	City of Carrison
22	Nacogdoches	Lilly Grove Water Supply Corporation
23	Wills Point	MacBee Water Supply Corporation
24	Dale	Dale Water Supply Corporation
25	McDade	Bastrop County W.C.I.D
26	Yantis	City of Yantis
27	Gladewater	Union Grove Water Supply Corporation
28	New Summerfield	City of New Summerfield
29	San Antonio	Texas Department of Transportation
30	Mineola	City of Mineola
31	Centerville	Southeast Water Supply Corporation
32	Catarina	Catarina Water Supply Corporation
33	Henderson	Chalk Hill Special Utility District
34	Grapeland	City of Grapeland
35	-	TRI-County Supply Corporation
36	Lufkin	City of Lufkin Water Utilities Department
37	Lufkin	M & M Water Supply Corporation
38	Etoile	Etoile Water Supply Corporation

Appendix A (cont.)

No.	City	Utility
39	Athens	City of Athens
40	Jacksonville	City of Jacksonville
41	Huntsville	Texas Department of Criminal Justice Office of Environmental
42	Marlin	TRI-County SUDAppendix A: